UNIVERSIDAD DE CHILE
FACULTAD DE CIENCIAS FÍSICAS Y MATEMÁTICAS
DEPARTAMENTO DE INGENIERÍA DE MINAS

"MODEL PREDICTIVE CONTROL OF FROTH FLOTATION PROCESSES AIDED BY A DYNAMIC SIMULATOR"

TESIS PARA OPTAR AL GRADO DE MAGISTER EN
CIENCIAS DE LA INGENIERIA MENCION METALURGIA EXTRACTIVA

OCTAVIO FRANCISCO FUENZALIDA GONZALEZ

PROFESOR GUIA:
WILLY KRACHT GAJARDO
PROFESOR CO-GUIA:
LEANDRO VOISIN ARAVENA

MIEMBROS DE LA COMISION:
CLAUDIO ACUÑA PEREZ
CHRISTIAN IHLE BASCUÑAN

SANTIAGO DE CHILE
2018

ABSTRACT

A model and simulation based methodology is used to implement a multi-layer model predictive control (MPC) strategy for a rougher row of mechanical flotation cells. Pilot-scale tests are done to calibrate and validate both the process simulation models and the predictive simulation models. The hierarchical control strategy considers three layers: orchestrator, advanced control and basic control; is deployed, in a commercial control system and, tested in a pilot row.

The orchestrator is divided in two: the row supervisor and the row optimizer. The row supervisor monitors and manages all the other components of the control structure. The optimizer is a MPC-based controller which optimal criterion is separation efficiency (SE) and; according to recent developments, that happens with a balanced mass-pull profile along the row. The advanced control layer includes individual cell MPC in coordination with a symbolic MPC for all pulp levels along the row. The basic control layer consists of single loop proportional and integral (PI) controllers and their corresponding valves and instruments. After simulation, the control layers are successively downloaded in an industrial controller, starting from the basic control layer and ending with orchestrator's algorithms. Then, the control structure provides good disturbance rejection against feed variabilities. Regarding the orchestrator, it supports smooth and logical transitions between control modes as well as good abnormal situation management.

This work shows promising results of the power of integrated process control design and model based methodologies; allowing earlier and better selection and validation of: flotation machine technology, cutting edge instrumentation and, advanced control structure and strategies. Given pre-defined economic assumptions, estimated results are obtained for the simulated industrial scenario: almost 40 percent reduction of capital expenditure (Capex), with almost the same operational expenditure (Opex). From the total Capex reduction, almost 80% is due to integrated process and control design (IPCD), being the other 20% a consequence of advanced process control and optimization structure and strategies. MPC-based control algorithms show their potential to have a main role in mineral processing processes' feasibility and optimality.

Keywords: control strategy, flotation, MPC, simulations.

RESUMEN

Se utiliza una metodología basada en modelos y simulaciones para implementar una estrategia de control predictivo basado en modelos (MPC) de varias capas para una fila de celdas de flotación mecánica Rougher. Las pruebas a escala piloto se realizan para calibrar y validar los modelos de simulación tanto de procesos como de predicciones. La estrategia de control jerárquico considera tres capas: orquestador, control avanzado y control básico; se implementa, en un sistema de control comercial y se prueba en una fila de piloto.

El orquestador se divide en supervisor y optimizador de fila. El supervisor de fila supervisa y administra todos los demás componentes de la estructura de control. El optimizador está basado en MPC y su criterio óptimo es la eficiencia de separación (SE) con un perfil de recuperación en peso equilibrado a lo largo de la fila. La capa de control avanzado incluye un MPC de celda individual en coordinación con un MPC simbólico para todos los niveles de pulpa a lo largo de la fila. La capa de control básica consiste en controladores proporcionales e integrales (PI) y sus válvulas e instrumentos correspondientes. Después de la simulación, las capas de control se descargan sucesivamente en un controlador industrial, desde la capa de control básica hasta el orquestador. La estructura de control logra un buen rechazo de perturbaciones de alimentación. En cuanto al orquestador, admite transiciones suaves y lógicas entre los modos de control, así como una buena gestión de situación anormal.

Este trabajo muestra resultados prometedores del poder del diseño de control de procesos integrado y de las metodologías basadas en modelos; permitiendo una mejor y más temprana selección y validación de: tecnología de máquina de flotación, instrumentación y estructura de control avanzada. Dados los supuestos económicos predefinidos, se obtienen resultados estimados para el escenario industrial simulado: casi 40 por ciento de reducción del gasto de capital (Capex), con casi el mismo gasto operacional (Opex). De la reducción total de Capex, casi el 80% se debe al diseño integrado de procesos y control (IPCD), siendo el otro 20% una consecuencia del control avanzado del proceso y la estructura y estrategias de optimización. Los algoritmos de control basados en MPC muestran su gran potencial.

Palabras clave: estrategia de control, flotación, MPC, simulaciones.

DEDICATORY

To God

To Miriam, my ambassador in heaven

To Valeria, my first minister on earth

ACKNOWLEDGEMENTS

I would like to express my gratitude to my advisor Professor Willy Kracht, for giving me the opportunity of working with him. His wise words and insightful opinions motivated me to bring out the best of me to accomplish this goal.

TABLE OF CONTENTS

LIST OF TABLES

LIST OF FIGURES

1. INTRODUCTION

This chapter is a concise presentation on the “why”, “what”, and “how” on the subject. They are presented in the context, relevance and outline sections.

1.1. CONTEXT AND WIDE PERSPECTIVE

Minerals are valuable natural resources being finite and non-renewable. The mining cluster is by no doubt the most important sector of Chilean economy. But, mineral yields that have fed Chilean society for a long time are decreasing both in quantity and quality. Further use of intelligence is needed in order to mitigate the exhaustion of natural resources. Intelligence, whether natural or synthetic, derives from a model of the world in which the system operates. Greater intelligence arises from powerful and “fit for purpose” models, capable of strike a balance between accuracy and interpretability of predictions. The software implementation of models is known as simulator or simulation framework. A specific realization of a certain scenario in the simulator is known as simulation. Model based design is well recognized as a systematic approach to design and implement industrial plants.

1.2. RELEVANCE

Modern metallurgical plants shall be high efficient and that implies operation near constraints with stronger attention to process dynamics and controls. In other words, to optimize, processes shall be under control which needs good measurements. Therefore, the role of process control systems has to be considered as an integrated element of business planning in order to simultaneously ensure feasibility and optimality of process operation. Model predictive control is a particular branch of model-based design: a dynamical model of the open-loop process is explicitly used to construct an optimization problem aimed at achieving prescribed system's performance under specified restrictions on input/output variables.

Many attempts have been made to improve the flotation process itself. An excellent review on the major developments up to the mid-1970 is compiled by Trahar and Warren (1976). Some of them are still being used or revisited. Two main lines have been followed; being the first one by reagents with the aim to enhance the agglomeration of fine particles, increasing the probability of collision. The second line is developing new cell machines with the aim to create more favorable hydrodynamic conditions for flotation (i.e. Gorain et al., 2000). For nearly a century mechanical cells have dominated the market. Faced with increasing demands to improve the processing of fine particles, cell suppliers have shown their resilience by increased cell size; the use of adjustable froth launders and; new agitation mechanisms (Yianatos, 2007a).

1.3. THESIS OUTLINE

Chapter 2 presents the literature review. As this work is related to more than one field of knowledge, a Venn methodology is considered appropriate as starting point. Then, references related to optimization, control design, modelling and MPC are shown. In chapter 3, objectives and scope of this thesis are set. Chapter 4 is related to an important part of the experimental work of this thesis; starting with the industrial context with its given definitions and assumptions and followed by exploratory and variability campaigns. Both campaigns are described and used to evaluate a non-conventional flotation machine. In addition to its intrinsic value, the work in chapter 4 is used afterwards to implement, calibrate and validate an important fraction of both process and prediction models; starting with the metallurgical modelling work at the end of the chapter and; following by the process simulation framework described in chapter 5. Chapter 6 explains the main specific application of this work: a hierarchical model predictive control of a row of rougher flotation cells. Chapter 7 is the ending chapter, where the discussion and conclusions of this thesis are presented.

2. LITERATURE REVIEW

2.1. REVIEW METHODOLOGY AND SIMILAR WORKS

Fit for purpose + self-explained: this review follows a fit for purpose approach and then is focused on this thesis' perspective. Nevertheless, appropriate context is given in order to be self-explained.

Literature review methodology: this work is related to more than one field of knowledge and therefore a Venn methodology is used and shown in figure 2.1. The universe is the subject which in this case is rougher froth flotation using rows of mechanical cells. Then, one set is the problem (optimization), the second set is methodology (modelling) and the third set is the focus (control). Following Venn methodology, the primary attention should be on similar works.

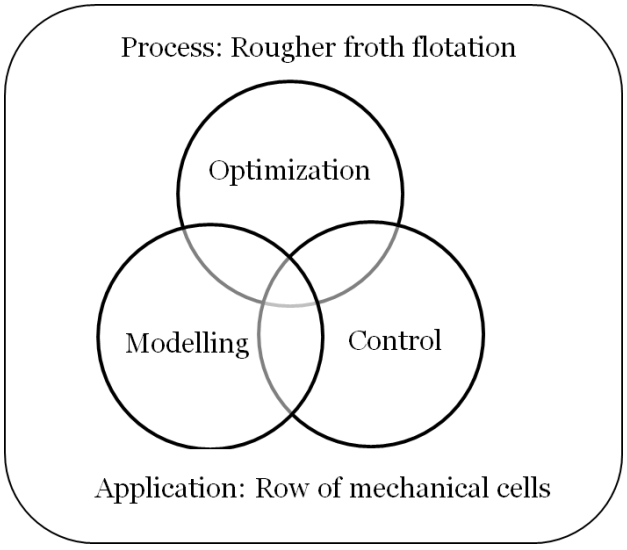

Figure 2.1: Literature review using Venn approach.

Optimization in mining, metal and mineral processing (Goodwin et al., 2008): Every decision making problem involves some form of optimization, often implicit rather than explicit. They state that making optimization explicit has many advantages including the integration between technical and commercial information, as a balanced approach to decision-making. Matching cost reporting areas to process areas greatly assist management. A reasonably close match makes it much easier to estimate the potential costs and benefits of process changes.

Goodwin et al. note that optimization can play a role at many levels in an enterprise including: data reconciliation; single feedback loops; coordination of feedback loops; interconnection of unit operations through the value chain(s); supply chain management and; long-term corporate investment strategies. By the exception of last two, all the other optimizations are under this thesis' scope. The role of process control has to be considered as an integrated element of business planning in order to support feasibility and optimality of process operation. Process control systems shall support asset management decision making through: dynamic optimization, abnormal situation support systems and asset integrated information at central control room. Dynamic optimization and abnormal situations are under the scope.

Optimization of a concentration operation According to Wills (2006), the purpose of mineral processing is to increase the economic value of the ore. Mineral processes move along a recovery-grade curve, with a trade-off between grade and recovery. The usage of concentrate grade and recovery is the most widely accepted method of assessing metallurgical performance. Then, any concentration operation can be expressed by figure 2.2. Regarding economic efficiency, the aim is to determine the best economic combination of recovery and grade. However, this combination may not promote the highest return if those conditions change.

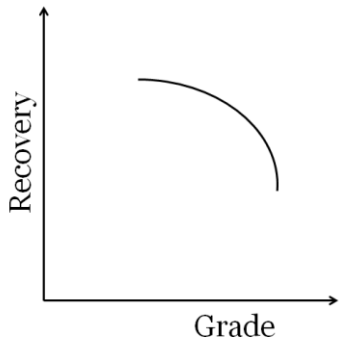

Figure 2.2: Typical grade versus recovery curve

Regarding technical efficiency, Schulze (1984) defines separation efficiency as the difference between the recoveries of valuable and gangue minerals. According to Wills (2006): “although the value of separation efficiency can be useful in comparing the performance of different operating conditions on selectivity, it takes no account of economic factors, and a high value of separation efficiency does not necessarily lead to the most economic return”. Therefore, neither economics nor technical approaches can define the optimum by themselves alone. This thesis considers separation efficiency (SE) as optimal criterion, but the simulation framework has the flexibility to incorporate and/or biases the optimal criterion based on economics.

Optimal control: Maldonado et al. (2007) study the optimal control of rougher flotation rows. The row optimization objective is the minimization of the Cu tailing grade given a desired final Cu concentrate grade. They conclude that their simulation results show good correlations between their optimization strategy and actual operating practices at the rougher flotation plant under study.

Profiling has been proposed as row dynamic optimizer (i.e. Seguel et al., 2015; Sing and Finch, 2014 and; Hadler & Cilliers, 2010). Maldonado et al. (2011) find that, if entrainment is neglected, the maximum SE is obtained when each of the cells along the row has the same recovery. Singh and Finch (2014) confirm that with simulations and industrial data and then, they use math and simulations to propose that, considering entrainment, a balanced mass-pull profile is optimum. Seguel et al. (2015) revisit row optimization through froth depth profiling and the following formulation of the optimization problem: maximization of copper Cu recovery while satisfying a minimum concentrate grade. Their conclusion is that optimal profile also provides a balanced mass-pull profile. A balanced mass-pull profile is considered as base scenario herein, but the simulation framework allows a balanced recovery profile.

In terms of control theory, profiling schemes are related to setpoint tracking. Traditional model predictive controllers are tuning around a particular operating point, fitting fairly well for fixed set-points but not necessarily for moving set-points. Asymptotic tracking performance and stability is crucial for profiling based optimizing applications and adaptive model predictive control (AMPC) family of algorithms is capable to ensure system asymptotic tracking performance and stability under large parametric, structural and parametric disturbance uncertainties (Tao, 2014). AMPC is considered in this thesis for advanced profiling controllers.

Model predictive control applied to froth flotation: Rojas and Cipriano (2011) use simulations to compare three control strategies, one conventional and two MPC-based ones. Their assumption is that the optimum is achieved maximizing the recovery and keeping the concentrate grade over a minimum. The first MPC strategy considers row tailings and concentrates grades and the other MPC strategy includes estimation of concentrate grade in intermediate cells. They conclude that even though both MPC strategies deliver high performance regardless disturbances, the economic benefits obtained with the second MPC strategy are greater, noting the importance of intermediate measurements. Consequently, in this thesis: virtual sensors are developed to estimate individual mass pulls and concentrate grades, including the intermediate cells; the row instrumentation is used incrementally for further characterization and; in other words, the instrumentation planned for the row is used for 1, 2, 3 and four cells.

Putz & Cipriano (2015) propose and simulate a hybrid model predictive control (H-MPC) for rougher flotation. They define three operating modes for each rougher flotation cell: no concentrate (sunken cell), normal operation and presence of pulp in overflow of concentrate (pulping cell). Their approach emphasizes the relevance of MPC algorithms, the modal nature of industrial froth flotation systems and the lack of abnormal situation integration to control strategies. In this thesis, virtual sensors are used for sunken and pulping cells.

Air recovery (Hadler & Cilliers, 2010): they add another component to mass pull and recovery profiles, stating that air flowrate and froth depth could affect froth structure and stability, which in turn could affect mass pull. They propose air recovery, or the fraction of air entering a cell that overflows the lip, as measure of froth stability. Air recovery, α, is determined using the over flowing froth velocity, V_f; the overflowing froth height above the cell lip, h, the over flowing length, w, and the inlet air flowrate, Q_a, as shown in equation (2.1). A high air recovery, therefore, indicates a more stable froth. The complement to the air recovery $(1-\alpha)$ gives the fraction of air that leaves through bursting. They mention that "when operating a cell at the air rate that yields the peak air recovery (PAR), an improvement in flotation performance, particularly mineral recovery, can be obtained". an increase in mass pull by means of a higher air flow, increase mineral recovery as far as air rate peak is still not achieved.

$$\alpha = \frac{V_f \cdot h \cdot w}{Q_a} \qquad (2.1)$$

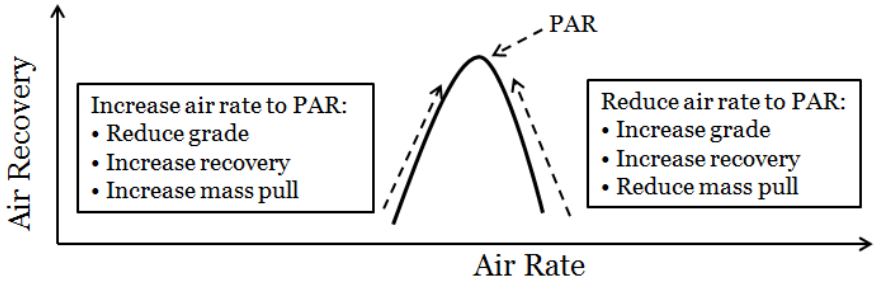

Figure 2.3: Air recovery optimization, from Hadler & Cilliers, 2010

Brief of profiling methods: As a main conclusion, the technical optimum is obtained by means of a balanced mass pull along the row. Then, a simple and practical criterion for row optimization is given: balanced mass pull profile along the row. In this thesis, air recovery is one of two froth stability indices. In addition, in almost all the articles two variables are considered for profiling but only one at a time; in process control words, setpoint tracking is needed for the "profiled variable" while setpoint regulation is needed for the others.

2.2. MODELING ESSENTIALS

As this thesis is model-based, models are its pillars. In its essence, process modelling is an exercise of translation of knowledge about the process into an abstract mathematical representation (Cameron & Hangos, 2001). The nature of knowledge is diverse and thus modelling methods can naturally be segmented accordingly: white box models represent a broad class of models based on physical or chemical laws; black box models represent a modelling framework based exclusively on process data and; grey box parametric models where the model structure is first-principle-based, but the model fitting is data driven. Here, both process and control simulation sub systems are built upon a selection and synthesis of white, black and grey box models.

As part of the modelling's synthesis work of this thesis; the following golden rules are almost everywhere a good modelling work has been done:

Golden Rule 1: Simple. According to Brooks (1991), there is little point in creating a model if it has all the complexity of the object it is modelled after. The best model of every system is itself. The single key component of a model is simplification.

Golden Rule 2: Incremental. According to Luyben (1990), the first design should be based on simple models with low number of estimated parameters and globally convergent and then further details should be incorporated as available and needed.

Golden Rule 3: Modular. A set of comprehensive models is better than single mega models. According to Brooks (1991), general purpose models that try to in incorporate practically everything shall be avoided. Such models are difficult to validate, to interpret, to calibrate statistically and, most importantly, to explain.

Golden Rule 4: Fit for purpose. Matzopoulos (2011) states that unneeded details increase calculation times and reduce model robustness. He also recommends to implement fit-for-purpose models that could be "parameterized" in order to easily include or exclude phenomena. In other words, the model has to be useful or otherwise there would be little point in creating the model.

Flotation modeling (Yianatos, 2007a): flotation is a solid–solid separation, where fine solid particles, suspended in water contact an air bubble in well-mixed air–pulp dispersion. Flotation separation is based on different mineral surface properties: hydrophobic particles can attach to air bubbles, while hydrophilic particles do not. Then, hydrophobic particles can be selectively separated by levitation against gravity in the aqueous medium. A generic flotation machine can be observed as a sequence of two operations, 'reaction' and 'separation', as shown in figure 2.4. The reactor is fed with: the pulp containing the solids to be separated; chemical reagents to produce selective aggregation of particles with air bubbles and; energy to keep the solids in suspension and to disperse the air into fine bubbles".

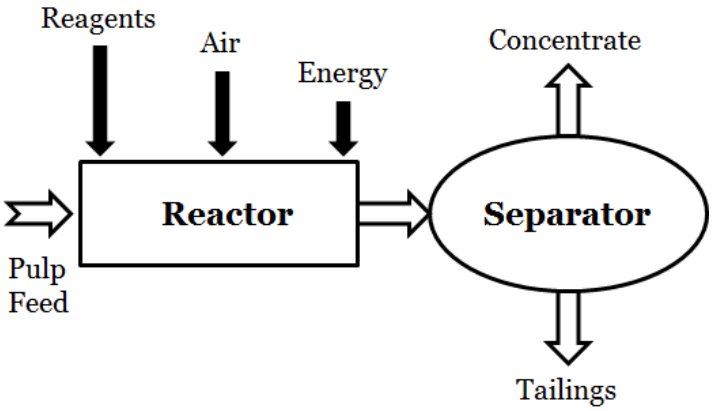

Figure 2.4: Generic flotation machine (from Yianatos, 2007a)

The collection process has been represented similar to a chemical reaction; being the 'reactants' hydrophobic mineral particles that collide with and adhere to air bubbles. The reaction 'product' is a particle-bubble aggregate that is less dense than the medium and moves upwards against gravity while hydrophilic particles are reported down to the tails. A necessary condition for mineral separation in a flotation process is the existence of a froth zone with a distinctive pulp-froth interface. The critical boundary conditions for industrial flotation equipment in terms of bubble size and superficial gas rate, regarding the loss of the pulp–froth interface, froth stability and limiting carrying capacity has been reported by Yianatos and Henríquez (2007b).

Compartmental models: the compartmental approach to model flotation involves the division of the flotation cell contents into two or more zones that combine to form a coherent system. The subprocesses occurring in each phase are collectively represented by an equivalent macroprocess.

For mechanical cells, Arbiter and Harris (1962) are among the first to take the froth phase into account. Their two-phase model of the flotation process is based on the assumption that both pulp and froth are well-mixed. Harris et al. (1963) and Harris & Rimmer (1966), carry out extensive testing of the two-phase model under steady state and transient conditions. As a theoretical improvement of the well-mixed hypothesis some authors describe froth behavior by applying plug-flow models as Cutting & Divinish (1975).

The first three compartment model for mechanical cells is proposed by Hanumanth and Williams (1992); including drainage of solids in the froth layer, and its dependence on froth height. They also outline procedures to estimate the parameters of the model, and validate the model comparing its predictions with experimental results.

Gorain & Franzidis & Manlapig (2000), describe mechanical cells as having three distinctive hydrodynamic zones. According to them, a mechanical flotation cell needs three hydrodynamic zones for effective flotation. They define the collection zone as the region close to the impeller that gives the turbulence needed for: solids suspension; gas dispersion and; bubble-particle interaction for minerals' collection. According to them, the quiescent zone is a relatively less turbulent region above the collection zone where the bubble-particle aggregates rise up. They note that the quiescent zone reduce the number of gangue minerals which may have been entrained mechanically or entrapped between bubbles for upgrading of valuable minerals. They remark that the froth zone above the quiescent zone serves as an additional cleaning step and improves the grade of the concentrate product. The three hydrodynamic zones in mechanical flotation cells are shown in next figure 2.5.

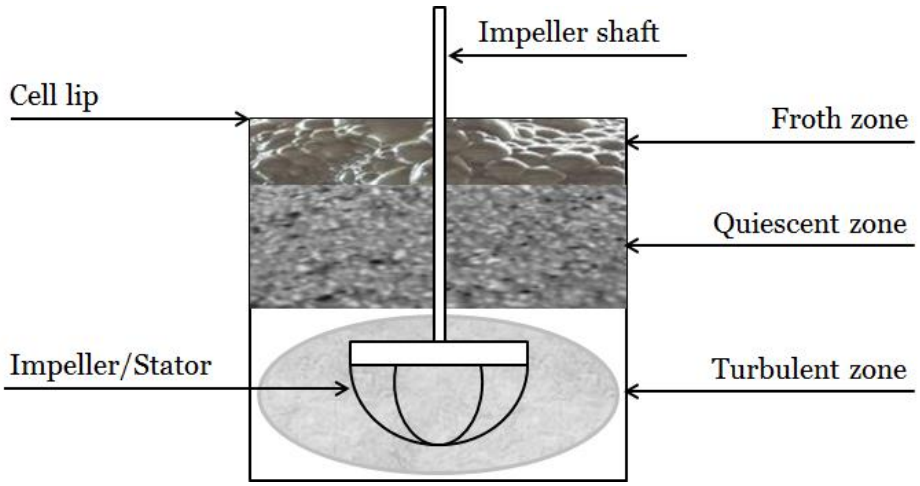

Figure 2.5: Hydrodynamic zones in mechanical cells (from Gorain et al., 2000)

2.3. STARTUP MODELS

Three models are considered herein as starting points in terms of froth flotation modeling synthesis: Savassi's (2005) compartmental model; Kämpjärvi & Jämsä-Jounela (2003) dynamic model and; Polat & Chandler (2000) collection zone model. In this sub-chapter, these three models are described using – almost - authors' own words.

Savassi´s model description (from Savassi, 2005): figure 2.6 shows Savassi's model for water (left) and suspended particles (right) in terms of the following flowrates: F, feed throughput; Y, suspension due to impeller action; I, influx to the froth; D, drainage from the froth; X, re-circulation by both impeller action and particle settling; C, concentrate; T, tail. The subscript "s" when applied to the pulp indicates suspended particles, but the same subscript when applied to the froth indicates particles that crossed the pulp–froth interface by entrainment (whether or not those particles remain suspended in water all the way to the concentrate launder).

The transfer of a target particle class by true flotation mechanism is illustrated in Fig. 2.7. The flowrate D represents the drop-back of attached particles from the froth due to detachment followed by drainage. Note that the subscript A when applied to the pulp indicates particles attached to air bubbles, but the same subscript when applied to the froth indicates particles originally attached to bubbles before entering the froth".

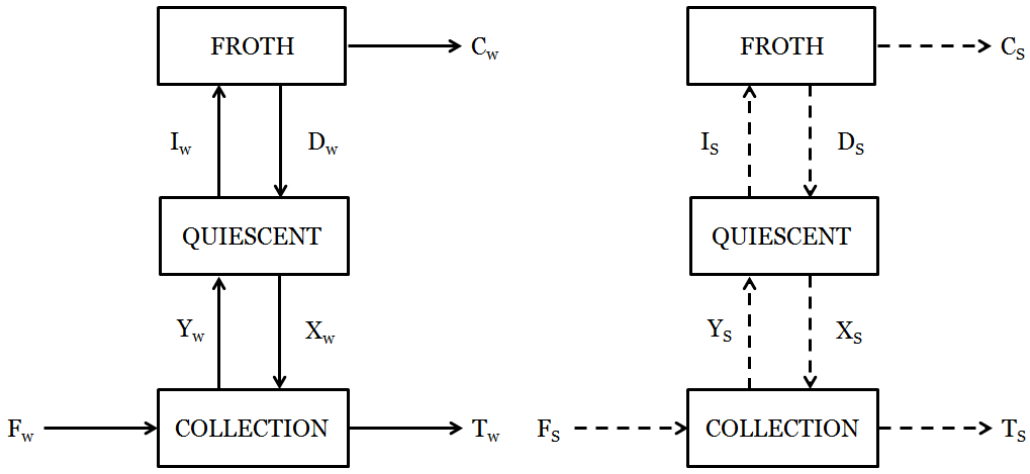

Figure 2.6: Transfer of water and suspended particles, from Savassi (2005)

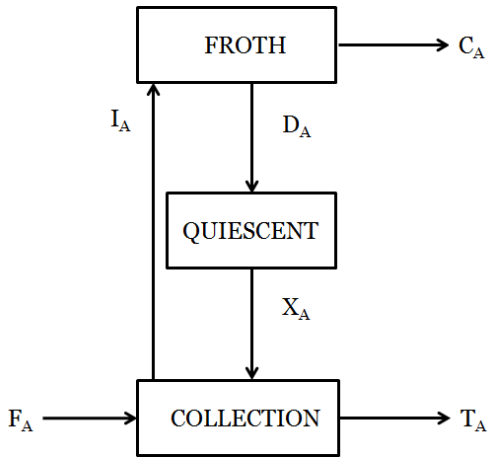

Figure 2.7: Transfer by true flotation mechanism, from Savassi (2005)

Then, for a particular valuable particle class, the total recovery by means of true flotation is given by:

$$R_{tot} = \frac{R_c \cdot R_f}{1 - R_c \cdot (1 - R_f)} \qquad (2.2)$$

Next figure 2.8 shows the mass transfer by true flotation and entrainment. Any particle suspended in the quiescent zone has three possible recent origins: rejection from the froth due to water drainage, D_S; rejection from the froth due to detachment followed by water drainage, D_A; and suspension from the bottom of the cell due to impeller action, Y_S.

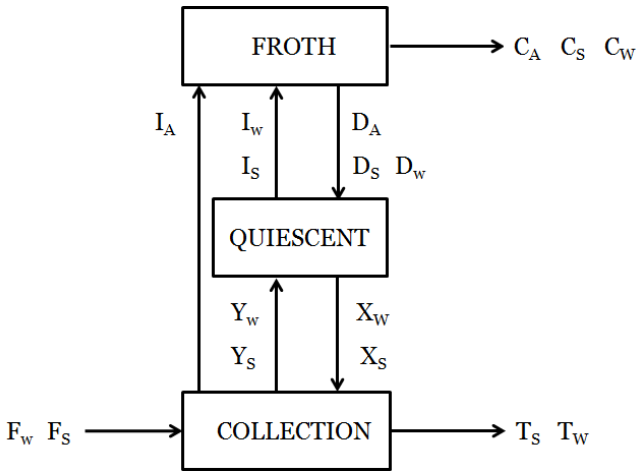

Figure 2.8: Mass transfer by true flotation and entrainment (Savassi, 2005)

Any particle suspended in the quiescent zone can be either transferred to the froth by entrainment, I_S, or to the collection zone for a chance of collision against an air bubble, X_S. If in addition to already stated assumptions, a single, non-distributed rate constant for the whole ore sample is considered, the overall steady state recovery is:

$$R = \frac{k_c \cdot \tau_c \cdot R_f \cdot (1 - R_w) + ENT \cdot R_w}{(1 + k_c \cdot \tau_c \cdot R_f) \cdot (1 - R_w) + ENT \cdot R_w} \qquad (2.3)$$

k_c : flotation rate exclusive for the collection zone

τ_c : residence time in the collection zone

R_f : froth recovery of attached particles

R_w : water recovery from the feed to the concentrate streams

ENT : degree of entrainment

Equation (2.3) is known as “the compartment model equation”. Since this model is semi-empirical, its parameters need to be determined through calibration tests, either by direct measurement or indirect methods. In turn, the parameters of the specific models that represent these phenomena should also be defined from the measurements performed. Once all parameters have been set, the model can be used for other conditions, within inherent limitations and extrapolation possibilities. Thus, the methodology for conducting the calibration tests depends on the requirements to determine each of the flotation phenomena according to each specific model to be used (Alves dos Santos et al, 2014).

Kämpjärvi & Jämsä-Jounela dynamic model: the simulation kernel for levels is a symbolic implementation based on the model for pulp-level published by Kämpjärvi & Jämsä-Jounela (2003) and represented by Figure 2.9 and equations (2.4) to (2.5) and (2.6):

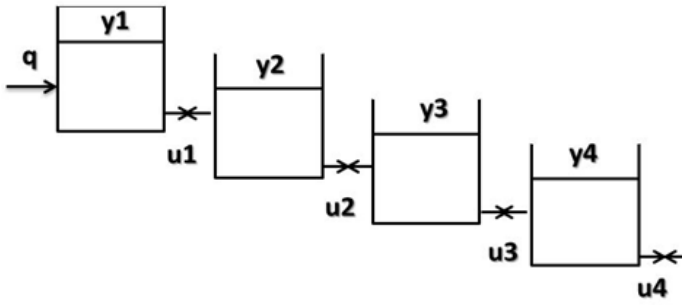

Figure 2.9: Diagram of flotation cells, Kämpjärvi & Jämsä-Jounela (2003)

Where y1, y2, y3 and, y4; are the pulp cell levels. u1, u2, u3 and, u4; are the valves' positions and; q is the volumetric feed to first cell. Then, for each cell along the row, the corresponding volumetric balance is done:

$$\frac{dV_i}{dt} = Q_{F,i} - Q_{C,i} - Q_{T,i} \qquad (2.4)$$

Q_{Fi}, Q_{Ci} and Q_{Ti} are the corresponding volumetric flows at feed, concentrate and, tailings. In addition, V_i is the pulp volume of cell i. Then, assuming that concentrate volumetric flows could be neglected, for four cells:

$$\frac{dV_1}{dt} = q - Q_{T,1} \qquad (2.5)$$

$$\frac{dV_2}{dt} = Q_{T,1} - Q_{T,2} \qquad (2.6)$$

$$\frac{dV_3}{dt} = Q_{T,2} - Q_{T,3} \qquad (2.7)$$

$$\frac{dV_4}{dt} = Q_{T,3} - Q_{T,4} \qquad (2.8)$$

Then, a constant transversal area "S" is assumed, together with a constant physical difference in height between the cells "a". In addition the same valves are assumed for all cell discharges and therefore, the valve coefficient "C_v"depends only on the control variable "u". Also, atmospheric discharge for cell 4 is assumed.

Using Bernoulli's equation:

$$S\cdot\frac{dY_1}{dt}=q-k\cdot C_V(u_1)\cdot\sqrt{\delta_1\cdot g\cdot y_1-\delta_2\cdot g\cdot(y_2-a)} \qquad (2.9)$$

$$S\cdot\frac{dY_2}{dt}=k\cdot C_V(u_1)\cdot\sqrt{\delta_1\cdot g\cdot y_1-\delta_2\cdot g\cdot(y_2-a)}-k\cdot C_V(u_2)\cdot\sqrt{\delta_2\cdot g\cdot y_2-\delta_3\cdot g\cdot(y_3-a)} \qquad (2.10)$$

$$S\cdot\frac{dY_3}{dt}=k\cdot C_V(u_2)\cdot\sqrt{\delta_2\cdot g\cdot y_2-\delta_3\cdot g\cdot(y_3-a)}-k\cdot C_V(u_3)\cdot\sqrt{\delta_3\cdot g\cdot y_3-\delta_4\cdot g\cdot(y_4-a)} \qquad (2.11)$$

$$S\cdot\frac{dY_4}{dt}=k\cdot C_V(u_3)\cdot\sqrt{\delta_3\cdot g\cdot y_3-\delta_4\cdot g\cdot(y_4-a)}-k\cdot C_V(u_4)\cdot\sqrt{\delta_4\cdot g\cdot y_4} \qquad (2.12)$$

Also, Jämsä-Jounela assumes constant densities along the row: δ1=δ2=δ3=δ4 and, extracts and group terms into K. Also, he doesn't differentiate among real pulp densities and apparent pulp densities (with gas holdup). Also, each level derivative could be considered as space state component:

$$\frac{dY_1}{dt}=(q/S)-K\cdot C_V(u_1)\cdot\sqrt{y_1-y_2+a}=f_1(Y,U) \qquad (2.13)$$

$$\frac{dY_2}{dt}=k\cdot C_V(u_1)\cdot\sqrt{y_1-y_2+a}-k\cdot C_V(u_2)\cdot\sqrt{y_2-y_3+a}=f_2(Y,U) \qquad (2.14)$$

$$\frac{dY_3}{dt}=k\cdot C_V(u_2)\cdot\sqrt{y_2-y_3+a}-k\cdot C_V(u_3)\cdot\sqrt{y_3-y_4+a}=f_3(Y,U) \qquad (2.15)$$

$$\frac{dY_4}{dt}=k\cdot C_V(u_3)\cdot\sqrt{y_3-y_4+a}-k\cdot C_V(u_4)\cdot\sqrt{y_4}=f_4(Y,U) \qquad (2.16)$$

Y and U are the vectors of pulp levels and, control actions; q is a measured disturbance of low frequency and; $\dot{Y} = F(Y, U)$ is the vector of derivatives. Then:

$$\dot{Y} = F(Y, U, Q) = [f1; f2; f3; f4] \qquad (2.17)$$

Linearizing around a symbolic operating point, $(Y_o, U_o) \Rightarrow$

$$\dot{Y} = F(Y, U, Q) \cong F(Y_o, U_o) + \frac{\partial F}{\partial Y}(Y_o, U_o)\cdot\Delta Y+\frac{\partial F}{\partial Y}(Y_o, U_o)\cdot\Delta U \qquad (2.18)$$

For pulp levels, the type of state space model being looked is the one expresses in equation 2.19, it can be noticed that A and B are the discretized version of Jacobian of F respect to Y and U, evaluated in the operating point (Y_o, U_o). Q_k is derived from the volumetric flow q and IWW. Further details are found in the process simulation chapter

$$y_{k+1} = Ay_k + Bu_k + Q_k \qquad (2.19)$$

Polat & Chandler (2000) collection zone recovery model: The general first order recovery equation is:

$$R(t)=R_{\infty}\cdot\left[\iint_0^{\infty}\left(1-e^{-kt}\right)\cdot F(k)\cdot E(t)\,dk\,dt\right] \qquad (2.20)$$

In which,

$R(t)$: Recovery at time t

R_{∞} : Maximum recovery (for $t = \infty$)

k : First order flotation rate constant, given in 1/s

$\left(1-e^{-kt}\right)$: Recovery of floatable mineral according to a first order process

$F(k)$: Kinetic distributions function for mineral species

$E(t)$: Residence time distributions function

E (t): for batch flotation tests, residence time is not distributed and then $E(t) = \delta(t)$, where $\delta(t)$ represents delta Dirac function. For continuous operations, equations (2.21) to (2.24) are correspondingly used for: a piston flow (2.21); a perfect mixer (2.22), a real mixer (2.23) and; a conventional mechanical cell according to Yianatos et al. (2007c).

$$E(t)=\delta\left(t-\theta\right) \qquad (2.21)$$

$$E(t)=\left({}^{1}/_{\tau}\right)\cdot e^{-t/\tau} \qquad (2.22)$$

$$E(t)=u(t-\theta)\cdot\frac{e^{-(t-\theta)/\tau}}{\tau} \qquad (2.23)$$

$$E(t)=\frac{e^{-t/\tau_G}-e^{-t)/\tau_P}}{\tau_G-\tau_P} \qquad (2.24)$$

Θ : Time delay

τ : mean residence time

τ_G : mean residence time of the big perfect mixer, $\tau_G > \tau_P$

τ_P : mean residence time of the small perfect mixer, $\tau_G > \tau_P$

F(k): Different simplifications are used for F(k). In this thesis, two kinetics distribution are used: a single, non-distributed rate constant for the whole ore sample as shown in equation (2.25) and; a rectangular distribution as shown in equation (2.26):

$$F(k)=\delta(k) \qquad (2.25)$$

$$F(k)=\begin{cases}1/k_m\,, & 0 \le k \le k_m \\ 0, & k > k_m,\ \ k < 0\end{cases} \qquad (2.26)$$

Resulting collection recoveries: As can be seen for above equations, several combinations of E (t) and F (k) are possible, but only some of them are herein used. For batch testing, (2.25) and (2.26) are used and the following recoveries are obtained, being (2.27) García-Zúñiga's (G-Z) (1935) equation and, (2.28) Klimplel's batch model (K)(1980):

$$R(t)= \left(1-e^{-kt}\right) \qquad (2.27)$$

$$R=R_\infty \left[1-\frac{1}{K_m \cdot t}\cdot\left(1-e^{-K_m \cdot t}\right)\right] \qquad (2.28)$$

For continuous operations, Garcia-Zúñiga kinetic distribution is used in conjunction with (2.24) and (2.25). Then, for a conventional cell:

$$R_{CONV}= R_\infty \int_{t=0}^{t=\infty}\left[\frac{e^{-t/\tau_G}-e^{-t/\tau_P}}{\tau_G-\tau_P}\right]\cdot\left[1-e^{-K_{gz}t}\right]dt \qquad (2.29)$$

Therefore, the continuous recovery for the collection zone is:

$$R_{CONV} = \frac{R_\infty}{\tau_G-\tau_P}\cdot\left(\tau_G-\tau_P-\tau_G\cdot e^{-t/\tau_G}+\tau_P\cdot e^{-t/\tau_P}\right) \qquad (2.30)$$

2.3. PROCESS CONTROL

Conceptual process control design includes the following definitions: optimization philosophy, control objectives, degree of centralization, control hierarchy, control structure, set-point policy and, control algorithms.

Optimization philosophy: The role of process control has to be considered as an integrated element of business planning in order to support feasibility and optimality of process operation (Goodwin et al., 2008). From a wider perspective, process control systems shall support asset management decision making through: dynamic optimization support systems, abnormal situation support systems and asset integrated information at central control room.

As stated by Edgar (2004), the control system formerly was a simple tool to achieve the predetermined goals of production, which had been set in the process design stage considering only the regulatory function of control systems. As such, associated measurements and controls are essential to manage and optimize. Furthermore, the ultimate aim of process control is to optimize the process performance and hence increase the economic efficiency (McKee, 1991).

Nowadays, business planning of process industries has become online and much less limited by the early decisions at the design stage. As such, new control systems have also inputs in terms of economic parameters and translate them into operational decisions. This has encouraged designers to consider the highest priority to process profitability and the roles of other control tasks are to realize the targeted economic objectives. Figure 2.8 shows the optimizing contextual scheme considered for a rougher flotation row within the concentration optimization context:

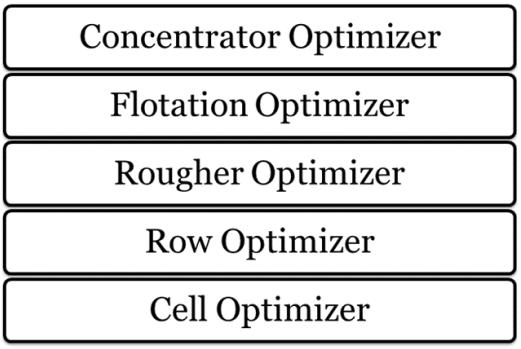

Figure 2.10: Optimization contextual scheme

Control Objectives (McKee, 1991): In any process control systems' design of, control objectives must be set as an essential prerequisite. Regarding flotation control system, he expresses that: "In the broadest sense, the objective of a flotation control system can usually be stated as optimizing the metallurgical performance". For him, the control objectives shall be: (i) to stabilize performance by minimizing the frequency and severity of erratic operation, (ii) to achieve nominated grade and/or recovery set points and, (iii) to maximize the economic performance. Then, the control objective should be to improve the metallurgical efficiency producing the best possible grade-recovery curve, and to stabilize the process at the concentrate grade which will produce the most economic return from the throughput (figure 2.11), despite disturbances in the circuit.

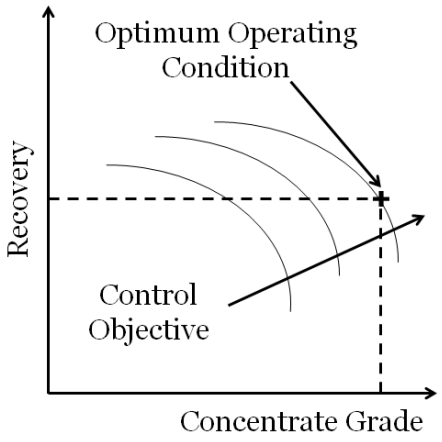

Figure 2.11: Flotation control objective, from Wills (2006)

Degree of centralization (Rawlings & Stewart, 2007): Level of independency of controls within a control structure, classified in: centralized control structures with a single objective function and a single model for decision-making; decentralized control structures in which the controllers are distributed and the interactions are ignored; communicated control structures in which each controller has his own objective function but employs an interaction model for communicating and; cooperative control structures that employ an objective function for the whole system, and the prediction of the last iteration of each controller is available to the others.

Control hierarchy: According to Downs and Skogestad (2011), industrial needs for simplicity discourage the application of highly complex control systems. The process control design problem needs to be resolved and decomposed into more manageable sub problems. Many authors suggested a hierarchical approach as a decomposition technique to reduce the flotation process problem complexities. A comprehensive review of hierarchical decompositions that are used for froth flotation process control design is done by Jovanović and Miljanović (2015). Qin and Badgwell (2003) state that the control hierarchy shall reflect the processing times related to decision making process for both people and controls. As Buckley (1964) recognizes, control structures has higher frequency control layers for stability and lower frequency control layers for quality control (specifications, recovery, grades). Furthermore, it is well-known that in multi-loop control systems, interactive loops with a significant difference in their time constants may demonstrate a decoupled performance, and can operate separately, (Ogunnaike and Ray, 1994).

Liu and MacGregor (2008) suggest a functional hierarchy, depending on the flotation control objectives as follows: (i) process stabilization by minimizing the frequency of variations and the intensity of disturbances, (ii) achieving nominal values of the concentrate grade and recovery. Then, regulatory layer(s) handle fast disturbances with a zero expected value in long-term and longstanding disturbances with significant economic effects are treated by the optimizing layers.

Control Structures (Skogestad, 2004): He develops an iterative top-down / bottom-up methodology for control structures' selection. The design approach in the top-down direction starts with meeting the operational objectives, optimizing the process variables for important disturbances and determining active constraints with emphasize on throughput/efficiency constraints. The bottom-up design starts with the most dynamic issues such as designing the control loops including instrumentation, basic controllers and valves and actuators supervisory control layer. The main elements of a control structure are manipulated variables (MVs) and controlled variables (CVs).

Manipulated Variables (Skogestad, 2004) are those degrees of freedom which are used for inserting the control action to the system. The desired properties of manipulated variables are to be consistent with each other, reliable, and able to affect controlled variables with reasonable dynamics. Two manipulated variables may be inconsistent when they cannot be adjusted simultaneously. Reliability is defined as the probability of failure to perform the desired action. Reliability of manipulated variables is important because it is not desirable to select a manipulated variable which is likely to fail. Also, the available degrees of freedom shall be sufficient to meet the controllability requirements. In addition, different operational modes may require different control structures.

Controlled variables (Qin and Badgwell, 2003): Selection of controlled variables is more complicated compared to manipulated variables. This is because controlled variables can be categorized based on two different tasks. Firstly, these variables are responsible for detection of disturbances and stabilizing processes within their feasible operational boundaries. Secondly, selection of controlled variables and their set points provide the opportunities to optimize profitability. The first category of controlled variables is selected for treatment of instability modes. The second category should be selected by technical and economic optimum criteria.

As both feasibility and optimality are related to process profitability, it can be said that controlled variables are those which set points are strongly related to process profitability.

Manipulated variables versus controlled variables (Froisy, 1994): to compare the quantity of manipulated and controlled variables provides insights about the control problem. At design stage, the manipulated variables often exceed the controlled variables and the control problem is intentionally over-determined. If this case remains in the operation phase, extra variables are available for economic optimization. However, the number of manipulated variables may decrease during operation because constraints activation, control valves saturation or control signals failures.

MPC-based control structures (Aske, 2009) are subject to dynamic changes in the dimension of the control problem during control execution. The reason is that the manipulated and controlled variables may disappear due to valve saturations, signal failures, or operator interventions in each control execution and return on the next one. These changes can make the control configuration under-determined and perfect control (maintaining controlled variables at their desired values) would be infeasible. However, it is still desirable to have the best possible control action. Unfortunately, these changes have a combinatorial nature and it is not possible to evaluate all of the alternative subspaces of a control problem at the design stage. Therefore, MPC systems have an online monitoring agent that is responsible for sub problem conditioning. The strategy is to meet the control objectives based on their priorities. In order to avoid saturation of manipulated variables in MPC-based systems, their nominal values are treated as additional controlled variables with lower priorities. In addition, when a manipulated variable disappears from the control structure (e.g. because the operator turns it into manual mode), it may be treated as a measured disturbance. Similarly, saturated valves are treated as one-directional manipulated variables. For instance, when a controlled variable is lost because of signal failure or delay in measurements, the practical approach is to use the predicted value for it. But, if the faulty situation persists for a too large number of execution steps, the contribution of the missing controlled variable will be omitted from the objective function.

Optimal selection of controlled variables (Skogestad, 2004): He states that the main purpose shall be to translate the economic objective into process control objectives. In other words, the main idea is to find a function of the process variables which, when held constant, leads automatically to the optimal adjustment of the manipulated variables, and with it, the optimal operating conditions. He shows that the costs associated with disturbances are not the same for two different controlled variables; the cost associated with maintaining one controlled variable at its set point could be significantly lower than to maintain other controller variable in its set point. This suggests that selection of controlled variables can be employed as a method for off-line optimization of process profitability.

Set point policy (Chachuat et al., 2009): When a control structure is selected for a process, the objectives for controlling that process such as stabilizing, safety concerns, environmental criteria, and profitability will be translated to maintaining a specific set of controlled variables at their set points. However, some of the targets of the above mentioned objectives may need to be updated time to time due to disturbances. The ability of the control structure to keep pace with these changes is crucial for feasibility and profitability of process operation. Two strategies are possible for ensuring process feasibility and profitability. They are: static set point policy - off-line optimization – and, dynamic set point policy - online optimization.

The motivation for the static set point policy is that, while the costs of development and maintenance of a model-based online optimizer are relatively high, selection of the controlled variables which guarantee a feasible and near optimal operation is by no means trivial. Static set point policy has a direct relation to the optimal selection of controlled variables. In this approach, online optimization of set points is substituted by maintaining optimal controlled variables constant. This is also consistent with the culture of industrial practitioners who would like to counteract the model mismatches and the effects of disturbances by feedback control.

Two approaches for dynamic set point policy may apply: model parameter adaptation, where on-line measurements are used to update the model and; model modifier adaptation where on-line measurements are used to update modifier terms in the objective function of the online optimizer.

Regarding feasibility and optimality criteria; the results of variability analysis have confirmed that feasibility is of a higher priority than optimality. The main challenge is to develop accurate and reliable models with a manageable degree of complexity and uncertainty. Online optimization using an inaccurate model may result in a sub-optimal or even infeasible operation.

Control algorithms currently in use in flotation plants: (i) conventional single-input single-output (SISO) proportional and integral (PI) algorithm, still the most used algorithm for basic SISO control loops; (ii) conventional multiple-input multiple output (MIMO), PI-based multi-loop controllers with additional non-integrated blocks for delays, non-linearity and constraint handling such as feedforward or smith predictor blocks; (iii) MPC family of control algorithms, as the "cutting edge" choice for multivariable control due to its embedded capacities to fully integrates: constraints handling, decoupling, delays, nonlinearities, disturbance rejection, dead time and lag management, among others; (iv) adaptive algorithms as the preferred choice for set point tracking and/or time variant systems and/or highly nonlinear loops and, (v) expert rule-based in conjunction with machine learning systems are the first choice for abnormal situation management and entire flotation plants optimization. In terms of control theory, while regulatory control schemes are related to fixed set points; profiling schemes are related to set point tracking.

Conventional SISO and MIMO algorithms are proved efficient in controlling flotation processes, because they have reliable operation and are understandable to plant people. However, conventional multi-loop controllers have a significant drawback leaving set points at constant values because disturbances and the changes in economic parameters can change the optimal set points and in extreme, require control structure reconfiguration, as worked by Downs and Skogestad (2011) together with economic losses due to constant-set point policy. Other drawbacks of multi-loop controllers are the required convoluted override logics for constraint handling, and interactions among control loops, (Stephanopoulos and Reklaitis, 2011).

2.4. MODEL PREDICTIVE CONTROL

Predictive control technique is very widely implemented within industry and hence it's both a standard topic in most controls curricula and a common practice for engineers in charge of advanced process control design and implementation. As such, main references for the synthesis done in this sub-chapter are books: Rossiter (2004), Camacho & Bordons (2004), Rawlings & Mayne (2015) and Bemporad et al. (2016).

According to Rossiter (2004), model predictive control describes an 'approach' to control design, not a specific algorithm. Therefore, a user would ideally interpret the approach to define an algorithm suitable for his needs. Rossiter adds that many effective control strategies have their origins in human behaviour. Moreover, humans are very good at control so a good start point for automation techniques. For example: proportional, integral and derivative (PID) controllers can be deconstructed as a simplification of a human technique for controlling simple systems. Similarly, the use of predictions of expected behaviour in determining a control strategy is intuitively obvious. It is clear that humans use anticipation, effectively prediction, in order to consider the impacts of different control strategies. They choose the strategy they expect to give the most desirable future outcome. Prediction underpins practical human control strategies and thus seems a logical concept to incorporate into automated strategies. The use of prediction seems logical, but many other advantages of predictive control can be listed, such as: (i) intuitive concept, easy to understand and implement for a variety of systems; (ii) systematic handling of constraints; (iii) handles MIMO systems and dead-time without any modification, (iv) feed forward to make good use of future target information is included implicitly and, (v) handles challenging dynamics.

Why popular in industry? A simple answer is that it has been proven to improve profits by giving superior control compared to conventional techniques. A typical argument is that, if one is confident that the variance of the output can be reduced, one can then safely operate closer to a constraint and therefore increase output quantity or quality. The ability to incorporate constraints explicitly enables 'optimum' constrained performance as opposed to the consequences of ad hoc fixes.

A more precise definition is that MPC is a particular branch of model-based design: a dynamical model of the open-loop process is explicitly used to construct an optimization problem aimed at achieving the prescribed system's performance under specified restrictions on input and output variables.

Similarly, Qin & Badgwell (2003) mention that MPC is a class of computer control algorithms that use an explicit process model to predict the future response of a plant. They add that at each control interval, the MPC algorithm optimize future plant behavior computing future manipulated variable adjustments. Then, the first input in the optimal sequence is sent to the plant, and the entire calculation is repeated at subsequent control intervals. According to Camacho & Bordons (2004), MPC is a closed-loop control where the current value of the manipulated variables is determined on line as the solution of an optimal control problem over a horizon of given length. Bemporad et al. (2016) explain MPC's structure using a figure similar to figure 2.10. He explains that as in every traditional closed-loop control problem, there is a process system to be controlled and a controller that manipulates the process input variables in order to obtain desired outputs of the plant.

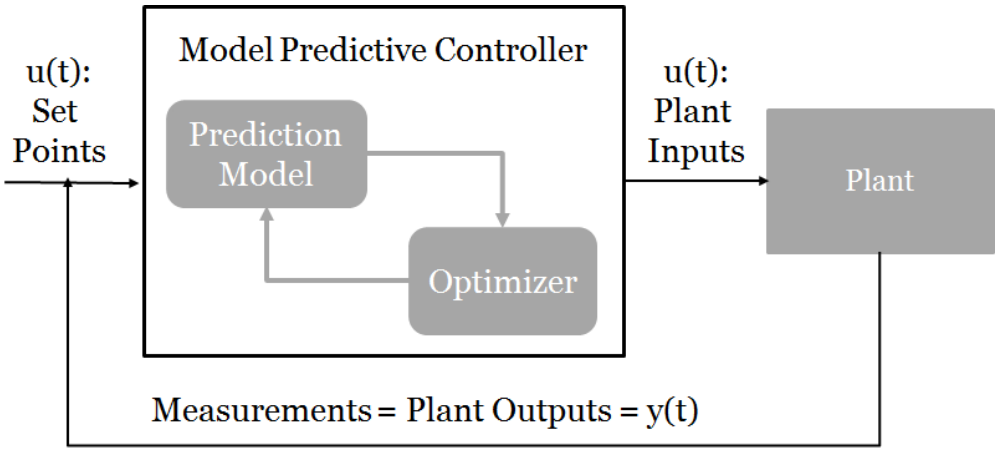

Figure 2.12: Basic MPC structure block diagram (from Bemporad et al., 2016)

The peculiarity of model predictive control approach is that it uses an explicit dynamical model of the process to predict its future evolution and choose the optimal control action. Then, the optimal control action is determined by a real time minimization of a cost function that considers both the error and the control effort. The canonical optimization problem is the minimization of the following cost function (Bemporad et al., 2016):

$$\min \sum_{k=0}^{N-1} \left\{ \left\| W^{y}(y_k - r(t)) \right\|^2 + \left\| W^{u}(u_k - u_{ref}(t)) \right\|^2 \right\} \qquad (2.31)$$

Subject to: $x_{k+1}=f(x_k, y_k, t)$; $y_k = g(x_k, u_k, t)$; constraints on u_k, y_k and; + $x_o = x_o(t)$

Where x_k , u_k and y_k are state, input and output vectors at sampling time k; r(t) and $x_0(t)$ are set point and receding initial state at time t; W^y and W^u are output and input weight matrices. As can be seen, the cost function to be minimized is a tradeoff between the tracking error (y_k-r(t)) and the actuation error (u_k-u_{ref}(t)). The tradeoff is expressed with weight matrices. One interesting feature of the canonical MPC formula is that constraints on u_k and y_k can be included in the minimization algorithm.

The optimization at time t is done over a period of N steps in the future and hence an N step optimal u_k sequence is obtained: $\{u_o, u_1 \ldots u_N\}$. But, only the first optimal move is applied, u_o and the rest of the sequence is thrown away. At time t+1, new measurements are obtained and the optimization is repeated under a shifted horizon between t+1 and t+N+1. As result, a new optimal u_{k+1} sequence are got: $\{u_1, u_2 \ldots u_{N+1}\}$ and so on…the controller keeps doing this repeated optimization at every single sampling step…that's because MPC is also called receding horizon control.

The main reason underlying this repeated optimization is that a feedback control law is needed. Therefore, in spite that open loop predictions are been used, the output shall always be a function of current states. A way to explain receding horizon feature is through an analogy with chess, where a chess player decide his next move based on a mental optimization with a sequence of inputs (his own moves) subject to a sequence of predicted outputs (his opponent's moves), but he usually repeat the optimization algorithm after his opponent move.

Among the advantages of the above approach, MPC is an extremely flexible control design approach. With almost the same formulation different type of processes can be addressed: (i) with wide number of input, output and state variables, (ii) either time variant or invariant systems and (iii) with substantial delays and disturbances.

Also, MPC has the ability to embed information about future if a disturbance and/or set point change is knowledge in advance. Then, available preview on future references and measured disturbances can be exploited and integrated.

The main components of a MPC-based control strategy are: modelling, prediction, receding horizon, performance index, degrees of freedom, constraint handling and multivariable approach.

While humans are very good at predicting outcomes, these predictions are based on a lot of experience which could be difficult to untangle and automate. In order to automate predictions, a model of system behaviour is required. However, what is not immediately obvious is defining or determining an appropriate prediction models.

As stated in sub-chapter 2.3 of this thesis, model should be as simple as possible, modular, incremental and fit for purpose. Additionally, it is mentioned that the most important purpose of the models implemented for process simulation is to represent fairly enough the relationships between the manipulated variables, controlled variables and measured variables. These features imply that a model for control purposes shall be dynamic, macroscopic, controllable and observable. A system is controllable if it has the ability to achieve stability of the outputs with the available manipulated variables. A system is observable if it has the ability to obtain the relevant output variables either directly or from measured variables. In the specific case of a model-based design of a model predictive control strategy, there are two types of models: models for process simulation and models for predictions. Prediction models almost always are built upon process simulation models and have the particular characteristics of being discrete, state space and linear. As prediction models summary, the simplest model that gives accurate enough predictions is usually the best. Accurate enough is ill-defined, but in practice predictions can often be 10% out in steady-state and still be highly effective as long as they also capture the key dynamic changes during transients. It is rarely beneficial to spend excessive effort improving accuracy as this is expensive, can give high order models but may have little impact on behaviour. Feedback will correct for small modelling errors as far as the model has the ability to give good long range prediction (Rossiter, 2004).

2.5. MPC STARTUP ALGORITHMS

Regarding the code implementation of the control simulation framework of this thesis; instead of using "out of the box" packaged coded MPC algorithms; they are developed "starting from scratch". In this sub-chapter, the basis of developed code is presented. Main references for the synthesis done in this sub-chapter are the following books: Rossiter (2004), Camacho & Bordons (2004) and Rawlings & Mayne (2015). In addition, Tao (2014) is used a specific reference for adaptive model predictive control.

As already stated, MPC has two main components, an embedded predictive model and an optimization algorithm given the cost function to optimize.

Regarding the predictive models, all of them are herein linear, state space and discrete. Linearity is always wished since it requires simple manipulation and algebra because superposition can be used. Then MPC deploys linear models whenever they are good enough and that's assumed to be the case of this work.

Discrete or continuous: all the predictive models are discrete. While processes operate in continuous time and indeed so do classical control laws such as PI, decision making tends to be more of a discrete process. Decision making requires processing time and thus cannot be instantaneous, especially where one is considering interacting inputs/outputs/constraints and performance. Also, common predictive control laws are implemented in discrete time as almost all commercial MPC applications.

State space models: in spite there are some variants, they are all very similar and at lastly, equivalents. In this thesis, the following formulation is used:

$$x_{k+1}=A\cdot x_k+B\cdot u_k \qquad (2.32)$$

$$y_{k+1}=C\cdot x_k+d_k \qquad (2.33)$$

Where x: states; u=inputs; y: outputs; d: disturbances.

State space predictions: discrete models are one step-ahead prediction models, that is, given data at sample k, data at sample 'k+1' is determined as can be seen in equation (2.35). Then, for data at example k+2 is given by:

$$x_{k+2}=A\cdot x_{k+1}+B\cdot u_{k+1} \qquad (2.34)$$

$$x_{k+2}=A\cdot(A\cdot x_k+B\cdot u_k)+B\cdot u_{k+1}=A^2\cdot x_k+A\cdot B\cdot u_k+B\cdot u_k \qquad (2.35)$$

$$x_{k+3}=A^3\cdot x_k+A^2B\cdot u_k+A\cdot B\cdot u_{k+1}+B\cdot u_k \qquad (2.36)$$

$$x_{k+4}=A^4\cdot x_k+A^3B\cdot u_k+A^2\cdot B\cdot u_{k+1}+A\cdot B\cdot u_{k+2}+A\cdot B\cdot u_{k+1}+B\cdot u_k \qquad (2.37)$$

Using the following nomenclature:

$$x_{\rightarrow k+1}=\begin{bmatrix} x_{k+1} \\ x_{k+2} \\ \dots \\ x_{k+n} \end{bmatrix} \qquad (2.38)$$

The pattern is trivial:

$$x_{\rightarrow k+1}=\begin{bmatrix} A \\ A^2 \\ \dots \\ A^n \end{bmatrix} x_k+\begin{bmatrix} B & 0 & 0 & 0 \\ AB & B & 0 & 0 \\ \dots & \dots & \dots & \dots \\ A^{n-1}B & A^{n-2}B & \dots & B \end{bmatrix} u_k \qquad (2.39)$$

Compacting:

$$x_{\rightarrow k+1}=P_x\cdot x_k+H_x\cdot u_k \qquad (2.40)$$

Similarly, assuming $d_{k+1} \cong d_k$ (fairly certain for the measured disturbances considered in this thesis):

$$y_{\rightarrow k+1}=\begin{bmatrix} CA \\ CA^2 \\ \dots \\ CA^n \end{bmatrix} x_k+\begin{bmatrix} CB & 0 & 0 & 0 \\ CAB & CB & 0 & 0 \\ \dots & \dots & \dots & \dots \\ CA^{n-1}B & CA^{n-2}B & \dots & CB \end{bmatrix} u_k+\begin{bmatrix} d_k \\ d_k \\ \dots \\ d_k \end{bmatrix} \qquad (2.41)$$

$$y_{\rightarrow k+1}=Px_k+H\cdot u_k+L_d \qquad (2.42)$$

The output prediction equations (one step ahead) must be the same as the current steady-state. As such, the aim is to estimate the expected steady-state values for the states and inputs to meet a given steady-state output and then; in effect, use deviation variables. Consistency can be ensured between predictions and the actual process if the estimated steady-state is simultaneously consistent with the process and model. A disturbance estimate is required to estimate the steady-state states and inputs for a given steady output. Typically, desired steady-state output can be selected as the target. The expected steady-state obeys the following:

$$y_{ss}=C\cdot x_{ss}+d;\ x_{ss}=A\cdot x_{ss}+B \qquad (2.43)$$

$$\begin{bmatrix} y_{ss}-d \\ 0 \end{bmatrix} = \begin{bmatrix} C & 0 \\ A-I & B \end{bmatrix} \cdot \begin{bmatrix} x_{ss} \\ u_{ss} \end{bmatrix} \qquad (2.44)$$

$$\begin{bmatrix} x_{ss} \\ u_{ss} \end{bmatrix} = \begin{bmatrix} C & 0 \\ A-I & B \end{bmatrix}^{-1} \begin{bmatrix} y_{ss}-d \\ 0 \end{bmatrix} \qquad (2.45)$$

Predict relative to the steady-state and deviation variables: a state space model is linear and thus superposition holds. Hence, defining the deviation variables as:

$$x_k=x_k-x_{ss};\ u_k=u_k-u_{ss};\ y_k=y_k-y_{ss}; \qquad (2.46)$$

$$y_k=C\cdot x_k;\ x_{k+1}=A\cdot x_k+B\cdot u_k \qquad (2.47)$$

Critically, the model in terms of the deviation variable no longer needs the disturbance term as this has been absorbed in the estimation of the correct steady-state.

As summary, in order to obtain unbiased predictions deviation variables are used. Then, the steps for developing the control simulation framework are:

(i) Estimate the steady-state values of disturbance/states/inputs to ensure consistency between the model and process.

(ii) Define the deviation variables.

(iii) Do predictions about the estimated steady-state using nominal process parameters.

Adaptive MPC (Tao, 2014): adaptive control systems are capable to ensure desired system asymptotic tracking performance and system stability under large parametric, structural and parametric disturbance uncertainties. Asymptotic tracking performance and stability are crucial for many tracking applications such as flotation profiling along the row. Adaptive MPC (AMPC) is capable to ensure them under large parametric, structural and parametric disturbance uncertainties. According to him, the most important principle of adaptive control is the certainty equivalence principle: for a plant with uncertain parameters, the adaptive estimated parameters are used in the feedback control design as if they were the true parameters. Two important technical foundations to implement the certainty equivalence principle are maximal plant uncertainty parametrization and stable controller parameter adaptation, making adaptive control a powerful and desirable methodology to deal with uncertainties. In figure 2.11, a schema of adaptive control is shown, where the control law and the online parameter estimator are the main components of an adaptive control strategy. The control law is MPC-based and the parameter estimator processes the data as it becomes available, unlike offline estimation where the data is processed after its gathering:

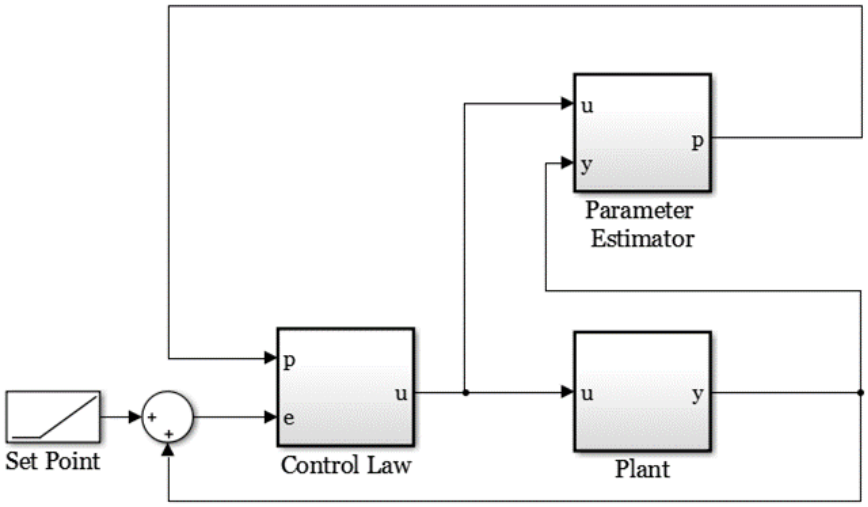

Figure 2.13: Adaptive Control Scheme, adapted from Tao (2014)

3. OBJECTIVES AND SCOPE

Objectives shall be functional to a work of thesis that seeks to displace knowledge's border. That border, together with the scope of the thesis, are known now, once the bibliographic review has been done.

3.1. OBJECTIVES

The main objective of this thesis is to understand, model and control the flotation process of a non-conventional flotation machine under different operating configurations and conditions.

As first particular objective, arises the characterization of pilot-scale non-conventional cells, studying phenomena such as the effect of wash water and feed composition. The second particular objective is to compare the performance of this equipment with that of conventional mechanical cells. The last particular objective of this thesis consists on implementing a hierarchical MPC advanced control strategy to support the solution to the challenges of flotation process control and optimization.

3.2. SCOPE

This thesis is focused on the characterization and controls of a row of rougher non-conventional mechanical cells. The test work is done with a relatively coarse grained porphyry copper ore (40-50 μm).

In order to achieve the objectives, a fit for purpose appropriate selection and comprehensive synthesis of existing first principle and/or semi-empiric models are done. Appropriate selection means that the models used should achieve the accuracy required by the application with minimal complexity.

Four successive experimental campaigns are considered in this thesis: industrial context, exploratory, variability and, continuous campaign. The main purpose of the experimental work is to implement, calibrate and simulate at pilot scale. Later on, the simulation framework is used to: (i) flotation machines technology selection and, (ii) MPC-based advanced control strategy.

4. FLOTATION MACHINES SELECTION

One of the specific applications of this thesis is flotation machines technology selection. In addition to the intrinsic value of the application itself, the experimental work herein done is also used afterwards for process simulation framework calibration and validation. Experiments are still indispensable for designing. They are not in competition with simulation methods; both approaches are ideal complements to each other. Experimental work is the main tool for the technology selection herein done.

Selection of a particular type of flotation machine is of great importance in designing a flotation plant and usually the subject of great debate (Araujo et al., 2005). According to them, the main criteria in assessing cell performance are: (i) metallurgical performance, i.e. product recovery and grade; (ii) capacity in tons treated per unit volume and; (iii) economics, e.g. initial costs, operating and maintenance costs.

Additionally, less tangible factors, such as the ease of operation and previous experience of personnel with the equipment, may contribute. Then, direct comparison of cells is by no means a simple matter. Even testing the same pulp in parallel streams, it's not trivial to ensure that a fair comparison is done.

Therefore, instead of a comparison criterion, the following selection criterion is herein considered as given: "The non-conventional flotation machine will be selected if its pilot prototype overcomes the metallurgical performance of a standard laboratory cell, under certain conditions".

The economics that supports the selection criterion are out of this thesis' scope. But, it's worth to emphasize that the technology selection herein done considers the specific characteristic of the feed mineral under consideration as well as specific previous definitions such as the circuit layout and assumptions regarding economics.

4.1. INDUSTRIAL CONTEXT

From an industrial perspective, this thesis is a reference for the integrated control and process design of a rougher collective flotation plant of project "N" in its feasibility study phase. Project "N" is a potential new 100 000 t/d concentrator, which flotation circuit is shown in figure 4.1, where [F], [C] and [T] are, correspondingly, the Cu contents in feed, concentrate and tailings. R, C1, C2, S are the corresponding metallurgical recoveries of rougher, first cleaner, second cleaner and scavenger stages.

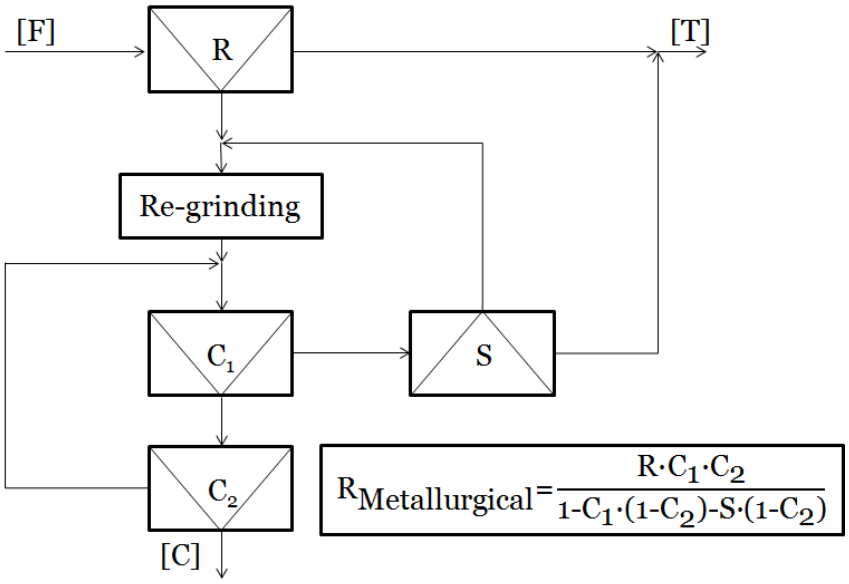

Figure 4.1: Collective flotation circuit

Geometallurgical background: the pre-feasibility work included the laboratory flotation tests of 200 samples from a 70x70 drill screen. With those samples, the main flotation geometallurgical units (FGU) were defined. Big trench samples are loaded in trucks from each one of main FGUs and considered as feed material for the experimental campaigns of this thesis. FGU's definitions, yearly distributions and, compositions are presented in next tables 4.1, 4.2, 4.3 and 4.4.

Table 4.1: Main FGUs and corresponding trench samples and trucks

Description	FGU	Trench	Trucks
Hypogene / Intrusive / All Alterations	NO IND	HYPF01	1, 2, 3, 5,
Hypogene / Wall Rock / Non-Potassic	IND NK	HYPF02	4, 6, 8
Hypogene / Wall Rock / Potassic	INDK	HYPF03	7, 9

Table 4.2: FGU's proportions according to mining plan

Year	No IND	IND NK	IND K
P1	12	87	1
P2	15	82	2
P3	22	69	9
P4	24	64	12
P5	48	36	17
P6	51	34	15
P7	7	81	12
P8	14	63	23
P9	24	48	28
P10	3	70	27
P11	8	66	27

Table 4.3: Main FGUs' mineralogical characteristics

Mineral Name	HYPF01	HYPF02	HYPF03
Cu Minerals	1.74	1.46	1.51
Pyrite	2.79	6.33	4.66
Quartz	42.81	32.68	28.94
Orthoclase	4.97	14.19	9.84
Muscovite/Sericite	28.91	32.81	32.75
Kaolinite	18.4	11.81	21.64
Others	0.38	0.72	0.66
Total	100	100	100

Table 4.4: Copper distribution in representative trench samples

	Specie	HYPF01	HYPF02	HYPF03
Sulphides	Cu_2S - $Cu_{1.2}S$	3.9	4.4	4.6
	$Cu_{1.2}S$ – CuS	2.5	4.2	2.8
	$CuFeS_2$	93.5	91.4	92.5
Oxides	Cu2Cl(OH)3	0.1	0.1	0.1
Total		100	100	100

Data from laboratory flotation tests was used as input for simulation considering: given flotation circuit, conventional technologies and, standard operating conditions. Then, a yearly-based mining plan was generated for the time period from year 1 to year 11. Figures 4.2 and 4.3 show the simulation results in terms of copper and molybdenum grades and recoveries:

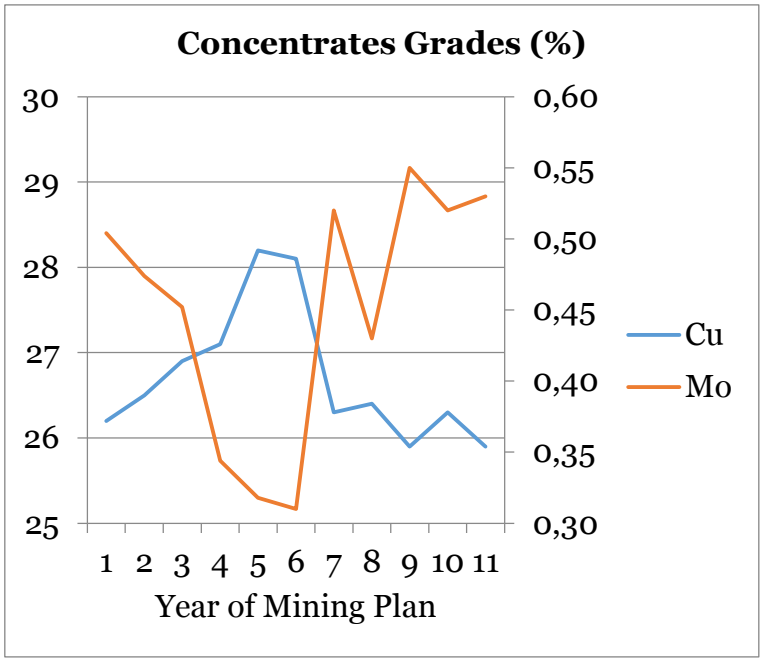

Figure 4.2: Simulated copper and molybdenum grades

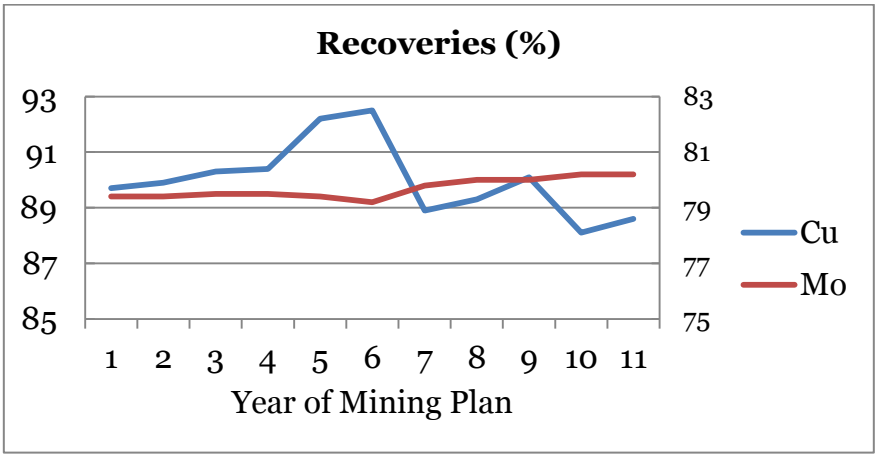

Figure 4.3: Simulated copper and molybdenum recoveries

Finally, project "N" went into feasibility phase and the thesis project "T" starts its experimental work. Project "T" is the "thesis project", a pilot plant consisting of four cells in series, called herein T_A regarding row "A".

4.2. FLOTATION MACHINES

From a conceptual point of view, a generic flotation machine can be observed as a sequence of two operations, 'reaction' and 'separation' (Yianatos, 2007a). As reaction and separation are different operations, it makes sense to physically separate them in order to optimize each one. The subjacent concept of operational units' separation has been applied across all the chemical industry. One emblematic example is the mixer-settler. In the context of this work, "reactor-separator" machine is defined as having two separated vessels for each one of the operations; "conventional" machine is a single vessel machine where both operations occur. A necessary condition for mineral separation in a flotation process is the existence of a froth zone with a distinctive pulp-froth interface. The critical boundary conditions for industrial flotation equipment in terms of bubble size and superficial gas rate, regarding the loss of the pulp–froth interface, froth stability and limiting carrying capacity has been reported by Yianatos and Henrıquez (2007b).

According to Gorain et al. (2000), mechanical cells are good mixers because the zone close to the impeller causes the needed turbulence for solids suspension, gas dispersion and, bubble-particle interaction for collection of minerals on the surface of the bubbles. On the other hand, with their lower turbulence, column machines are good displacement – separators. Gorain et al. (2000) also state that the conflicting functional requirements in different zones are a challenge in terms of cell design.

Regarding steady state metallurgical validation, the three compartment model reaches its maturity with Savassi's one (2005). Savassi's compartment model is one of the bases of the process simulation framework implemented herein. Nevertheless, it has to be mentioned that Savassi's model is a two compartment model regarding true flotation. The article titled "Modelling flotation with a flexible approach – integrating different models to the compartment model" (Alves dos Santos et al., 2014) is one of the bases for the methodology to integrate other models to the compartment model.

Savassi's model analysis: The flotation rate distribution in the collection zone is represented by the same rate constant distribution obtained from the batch test standardized as MFT (MinnovEX flotation test) from Savassi's work (2005). The test is designed to minimize the impact of the froth layer in lab results. Four concentrates are collected at specific times, with samples of the feed, tail, and combined concentrate being analyzed for size-by-size assays. The froth is removed at a speed of one crape every two seconds. Three parameters are used to characterize the cell performance: the effective collection volume V_c to represent the effective collection zone residence time, the entrainment factor ENT to describe the solid entrainment, and the froth recovery R_f to quantify the froth zone performance. According to Yianatos et al. (2010), the use of linear relationships and three empirical parameters constrain the model prediction for other conditions different than those observed during the model calibration.

An important Savassi's (2005) confirmed assumption is that true flotation and entrainment originate at different places: true flotation at the collection zone and entrainment at the quiescent one. Then, if technical optimization in the origin is wished, true flotation should be increased in the collection zone and entrainment should be decreased in the quiescent zone.

Reactor-separator (RS) machine is herein considered as a flotation machine which two main processes are physically separated in two vessels. The sketch of pilot RS machine used for experiments is shown in figure 4.4:

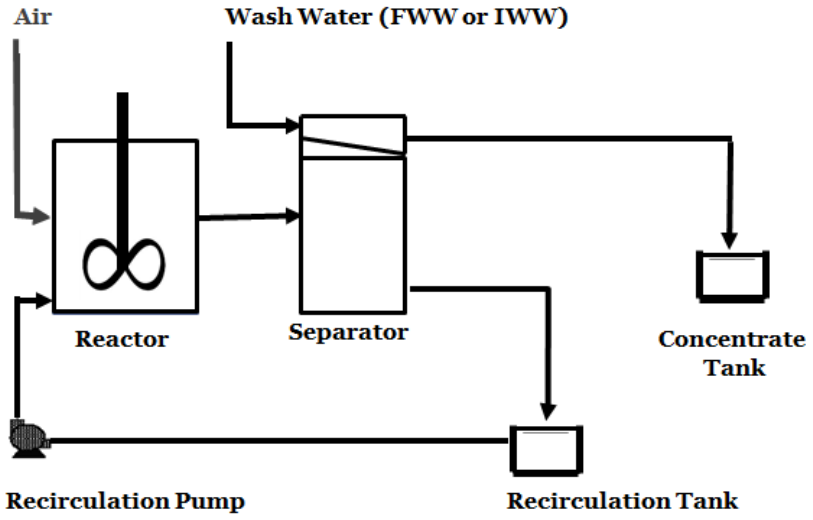

Figure 4.4: Reactor Separator (RS) Machine

The reactor unit (RU) includes a container, an impeller for breaking the air into fine bubbles and, means for introducing pulp and air; to produce an aqueous mixture containing gas bubbles carrying hydrophobic particles. The separator unit (SU) consists in a vessel and an adjustable ring sparser for introducing either froth wash water (FWW) or interface wash water (IWW), depending on the height of adjustment. The SU receives the bubble-particle aggregates from the reactor unit and permits the hydrophobic particle-carrying bubbles in the mixture to reach the surface. A concentrate fraction containing hydrophobic particles is discharged from the upper portion and a tailing fraction containing hydrophilic particles is discharged from the lower portion.

Reactor separator experimental setup: The single RS pilot setup provides the equipment for exploratory and variability phases. The RS rig operates at approximate 15 l/min of slurry feed. The tailings stream, after each pass through the RS, is collected and re-processed to emulate continuous multi-stage performance. The test work configuration, as illustrated in Figure 4.5, includes a complete RS unit as well as peripheral tanks, pumps, piping and instrumentation to provide an integrated rig for test work purposes.

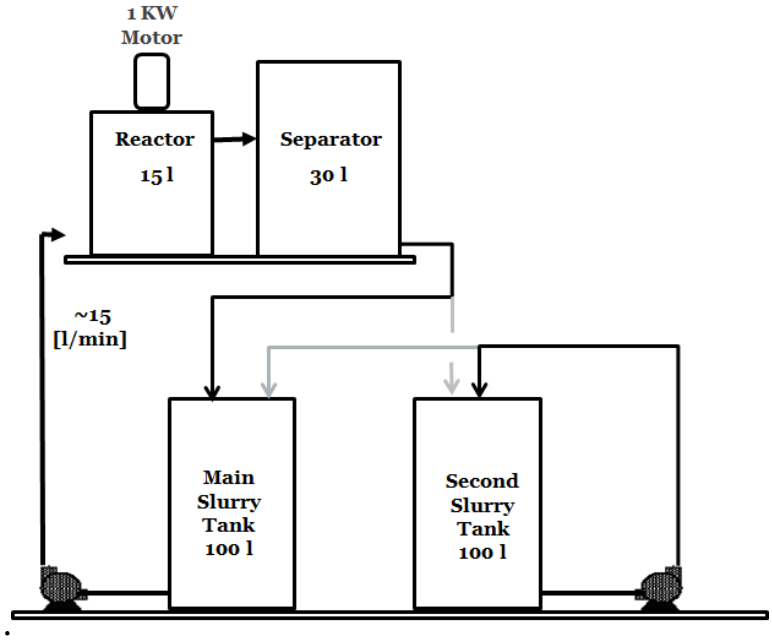

Figure 4.5: Mini-RS configuration schematic

4.3. EXPLORATORY ROUGHER CAMPAIGN

This experimental phase consists on both laboratory and pilot batch testing in parallel and its main purpose is to identify and define the variables that could already be frozen as design parameters and which have to remain as variables for the following phase. Other specific purpose is to select among FWW, IWW or not water at all. The rougher exploratory campaign covers 60 tests, shown in table 4.5:

Table 4.5: Summary of exploratory rougher tests

Test Number	Average Grade			Variable under exploration
	%Cu	%Mo	%Py	
01-20	0.55	0.039	3.7	Interface wash water (IWW)
21-30	0.59	0.040	4.5	Reagents Exploration
31-40	0.53	0.037	4.2	Froth wash water (FWW)
41-50	0.61	0.042	5.3	Slurry density
51-60	0.53	0.032	3.2	Reagents optimization

Experimental measurements: for each pilot run, the following information is generated and used for the grade/recovery calculations: (i) starting volume of feed slurry for each run, V_i [m^3]; (ii) feed's fractional solids content C_{PF} at the start of each test using a Marcy scale; (iii) feed assays, from a dedicated feed sample taken at the beginning of each test, (iv) concentrate and tails assays for each stage over the duration of the test and; (v) the mass of concentrate collected for each stage.

Calculation methods for data analysis: the main purpose of above information is to provide the grade and recovery over the whole test, and at any stage during the test. There are well-known relationships for the experimental measurements previously mentioned, based on mass or volumetric balances. Among them, the total starting volume corresponds to the addition of starting solids volume and starting liquid volume, thus obtaining:

$$V_i = \frac{H_{SF}}{W_{SF}} + \frac{(1\text{-}C_{PF})}{C_{PF}} \cdot \frac{H_{SF}}{W_{LF}} \qquad (4.1)$$

And, by definition:

$$H_{SF} = C_{PF} \cdot V_i \cdot W_{PF} \qquad (4.2)$$

Where:

H_{SF} : feed solids, in [kg].

C_{PF} : feed's fractional solids content.

W_{SF} : feed sample dry weight.

W_{PF} : feed sample wet weight.

W_{LF} : feed water weight (water density ~ 1000 [kg/m^3].

Therefore, feed solids H_{SF} [kg] is calculated from the measured volume of feed slurry at the start of each run; the measured feed fractional solids content (from feed sample wet and dry weights) and; assuming normal conditions for water density.

At steady state, solids shall be balanced:

$$H_{SF}=H_{SC}+H_{ST} \qquad (4.3)$$

As well as volumes shall be balanced at steady state:

$$\frac{H_{SF}}{\delta_{SF}}=\frac{H_{SC}}{\delta_{SC}}+\frac{H_{ST}}{\delta_{ST}} \qquad (4.4)$$

Concentrate solids over the duration of the run is calculated as follows:

$$H_{SC}=\sum_1^N H_{SC,i} \qquad (4.5)$$

Where:

$H_{SC,\,i}$: mass of concentrate solids at stage i, in [kg].

H_{SC} : concentrate solids collected over the duration of the run, in [kg].

N : number of concentrate samples within a run, twelve (12) in this case.

The Marcy value of C_{PF} is cross-checked against the wet/dry masses of RS feed sample and it is also back-calculated with the laboratory's sample dry mass and total volume. Then, for each stage, several cuts of the tails are taken over the duration of each stage, and submitted for solids contents and chemical analyses. The overall tails grade after 12 stages is as recorded from the chemical analysis of the tails sample. Afterwards, the weight distribution is calculated from the masses of concentrate collected at each one of the twelve stages of a run, $H_{SC,\,i}$. All the concentrate weights are summed, and each weight is divided by the total weight to give the fractional weight distribution per stage.

$$W_{C,i}=H_{SC.i}/H_{SC} \qquad (4.6)$$

The chemical assay of the feed sample taken at the beginning of each run is used as the feed grade of copper and molybdenum. The measured feed grade is compared with a back-calculated feed grade, just for data verification purposes. The back-calculated feed grade is calculated as follows:

$$L_{Cu,F,b} = (H_{SC} \cdot L_{Cu,C} + H_{ST} \cdot L_{Cu,T}) / H_{SF} \qquad (4.7)$$

Where:

$L_{Cu,F,b}$: back-calculated feed grade in %.

$L_{Cu,C}$: combined concentrate assay in %.

$L_{Cu,T}$: tails assay in %.

H_{SC} : concentrate solids collected over the duration of the run, in [kg].

H_{ST} : tails solids, in [kg].

H_{SF} : feed solids, in [kg].

Mineral Balance: For each test, the following elemental assays are reported per sample: Cu; Mo; S and Fe. In addition, CuS is reported per sample as an indication of the presence of oxide copper species and acid-soluble secondary copper species. Based on these assays, the following mineral species are accounted for: (i) copper sulphides: the simplifying assumption is that all copper reports as chalcopyrite ($CuFeS_2$) and calculated as (Cu ÷ 0.346); (ii) non-sulphide gangue (NSG) is calculated as all mass remaining after subtracting Cu, Mo, S and Fe. This is based on the assumption that all Cu, Mo, S and Fe are associated with sulphide species; (iii) Pyrite is accounted for as the remaining mass, after subtracting sulphide copper and NSG from total mass and; (iv) the following species (as defined above) are reported in all tables and figures: Cu, Mo, pyrite and NSG.

Non-conventional flotation machines with interface wash water (IWW): The potential advantage inherent in pulp washing of the high clay feed material is very important in rougher piloting. The results of four comparisons on the effect of IWW are shown in figures 4.6 & 4.7. Graphs of copper concentrate grade versus recovery are provided for Truck 6 (IND-NK), Truck 4 (IND-NK), Truck 1 (NO-IND) and Truck 1 (NO-IND) samples. As can be seen in figure 4.6, application of IWW is very beneficial for all comparisons, except the higher grade Truck 1. The application of IWW provided a higher concentrate grade, but also resulted in higher copper recovery. The increase in concentrate grade on the rougher is a direct result of increased gangue rejection. Figure 4.7 illustrates this, showing NSG recovery versus copper recovery for the four comparisons of Figure 4.6. The Truck 1 sample does not show a difference in performance with the addition of IWW. This suggests that some of the material could not benefit from wash water. However, it is clear that SE for any of the material with reasonably high clay levels will be enhanced through the application of IWW.

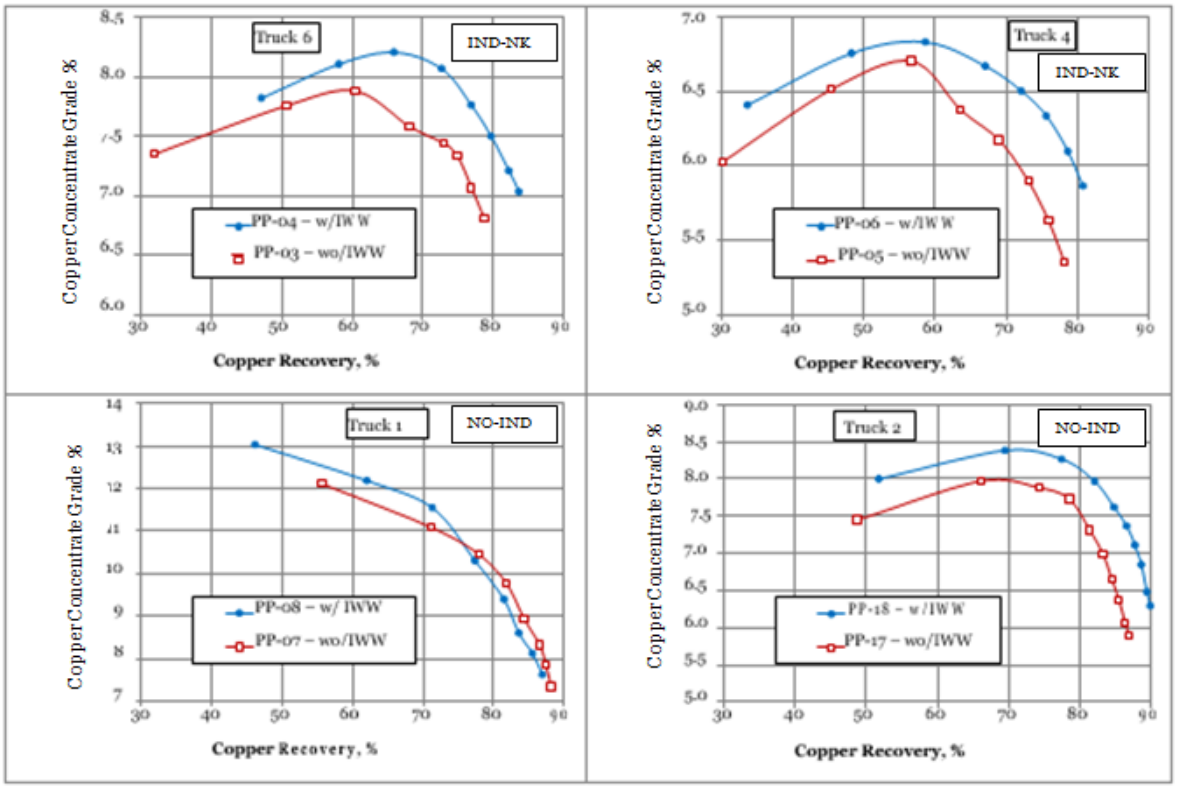

Figure 4.6: Copper grade versus recovery with and without IWW

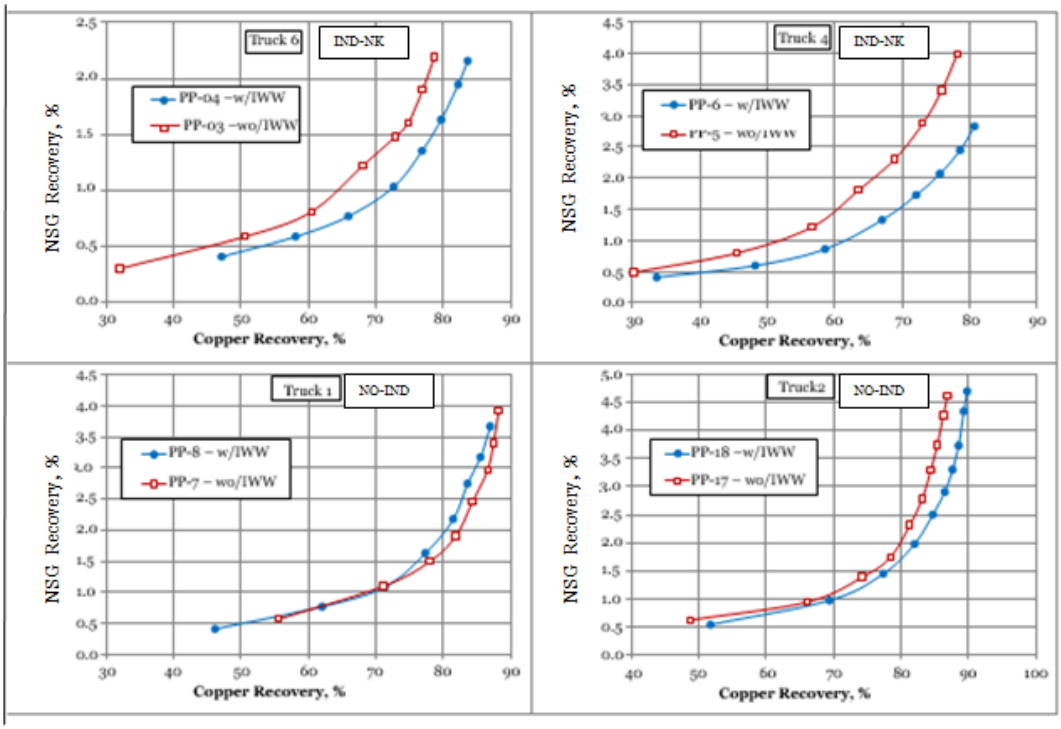

Figure 4.7: NSG versus copper recoveries with and without IWW

In next figure 4.8, RS froth at the first stage can be seen. In the left, before interface wash water addition; froth appears wet, slimy and dirty. In the right – after under-froth water addition; froth has rapidly become clean and heavily mineralized.

Figure 4.8: Effect of IWW - left with - right without

Non-conventional flotation machines with froth wash water (FWW): Adjusting the ring sparser over the froth, FWW is used with Truck 6 and Truck 4 samples. These samples are selected because they have an excellent performance with IWW. Nevertheless, the results do not show differences in metallurgical performances with the usage of FWW as can be seen in figure 4.9:

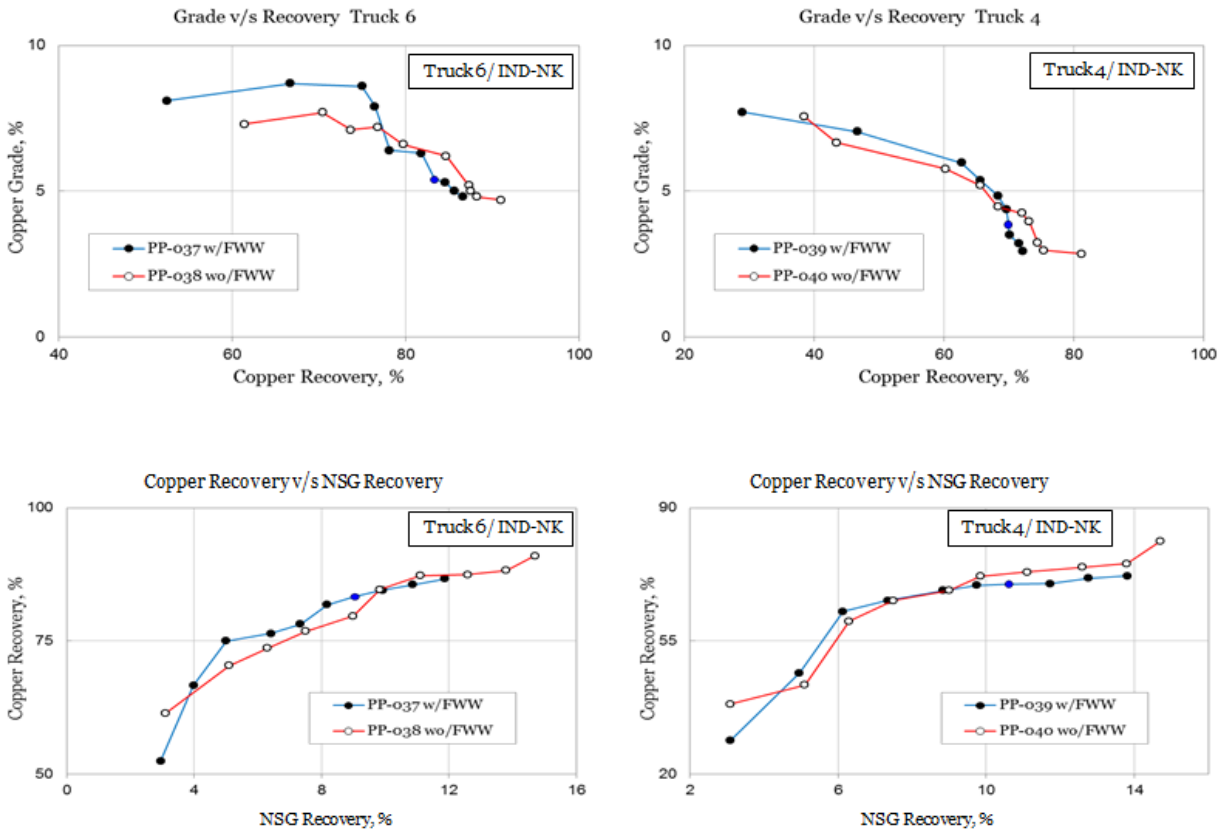

Figure 4.9: Effect of FWW for trucks 4 & 6 (FGU=IND-NK)

Slurry density: Truck 6 results at 26-27 % solids are shown in figure 4.10, together with three additional tests at 31-34 % solids. Concentrate grade is significantly reduced at higher slurry density, even when IWW is applied. For the Truck 6 material, feed density needs to be maintained below 30 % solids.

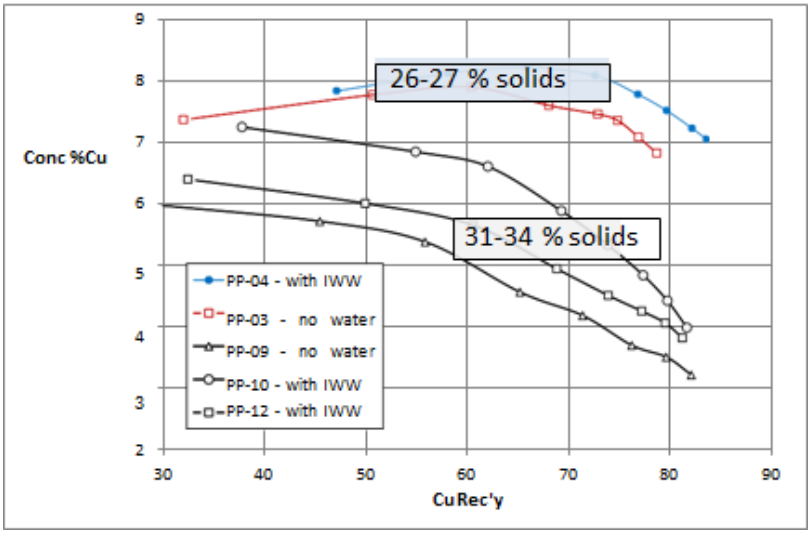

Figure 4.10: Impact of slurry density on copper grade versus recovery for Truck 6

4.4. ROUGHER VARIABILITY CAMPAIGN

This phase of work includes 100 pilot runs for the hypogene ores (tests 6-PP-401 to 500). Materials consisted on 100 variability ore samples, classified into three different categories: No IND, IND NK and, IND-K. The tests are summarized in Table 4.6.

Table 4.6: Summary of variability campaign ore types

Geologic Group	Ore Type	# of Tests
HYPOGENE	No IND	43
	IND NK	33
	IND K	24

The primary objective of this phase is to obtain a significant quantity of metallurgical data, including RS machine performance on drill core samples; that represents the hypogene resource, to be applied toward the geometallurgical mine plan. In parallel with each pilot run, each variability sample is subject to partial extraction analysis, full ICP analysis, sample characterization test work, QEMScan mineralogy and a standard Denver bench float test (Denver Seca). As per standard operating protocol, a Denver float test is performed on the RS feed pulp (Denver Pulp).

Samples and initial characterization for variability test work: Prior to the running of each test in the pilot plant, assay and mineralogical data are given. Having this information prior to each test is vital to help the team to better read and understand the flotation performance of each variability sample, and guide for the test operation accordingly. These responses included adjustments to mass pull, and in few cases, adjustments to reagent addition. A summary for variability phase test work is shown in Table 4.7. To gain a clear understanding of the ore body numerous tests are completed including flotation performance, hardness, density and mineralogy.

Table 4.7: Testing done on variability campaign

Category	Test	Total
RS and Denver	RS Pilot Test	100
	Pulp Denver Laboratory Test	100
	Pulp Denver Laboratory Test with NaHS	8
	Dry Denver Laboratory Test	100
Standard Flotation	MFT	96
	Chemical Assays	96
	PMA at P80 150 um	96
	Parameter Extraction	96
Chemical Assays	Partial Extraction	100
	ICP	100
Hardness	SPI	81
	Modified BWI	81
	Standard BWI	17
	Abrasion Test	53
Mineralogy	QEMScan	100
	NIR	100
	XRD	75
	XRD Clay Speciation	25
	CEC	25
Density	Density	100

Procedures and Observations: Each variability sample is delivered as two grounds and slurred feed charges; each charge of 20.6 kg ground solids as slurry in two buckets, together with two additional buckets containing process water. The solids plus the combined water in the four buckets add up to the required solids content for each charge.

The same fixed mass of lime is added to the feed before grinding. Grinding takes place in a 10kg rod mill. A grind-time is established for each of the variability samples, to achieve the grind target P80 of 150 μm, based on milling kinetics. The water comes from a desalination plant, including interface wash water (IWW) and water added to the laboratory flotation tests over the duration of the tests. In addition, IWW is prepared to a pH of 10, so as to not cause any significant deviation in the slurry pH over the duration of a run. Likewise, the water added in lab float tests is also adjusted to pH 10.

Although the pyrite content of all variability samples varies heavily, there is no protocol to adjust the collector additions into the grinding mill, according to the pyrite content. Each one of the four buckets per run (two buckets of slurry and two buckets of water) are weighted before the start of each run, to confirm the feed pulp density. The actual feed solids content; known at the start of the test by knowing the masses of water and solids added; and also cross-checked and confirmed through the wet and dry mass of the feed sub-sample; are the numbers that are reported in this document. All solids contents arise from wet and dry masses of the samples. Because of the importance of consistent wet and dry masses for all samples, the tare weights on the sample buckets are checked and confirmed regularly over the course of this program.

The slurry pH is checked at the start of each test, and adjusted to a standard pH 10 for all tests. In the case of the samples where the 'as-received' pH is above 10.25, a small amount of H_2SO_4 is used to bring the pH back to the standard pH of 10. Five hypogene samples are received with a pH above 10 and three of those are above pH 10.25. In all cases, an initial addition of 25 g/t of frother is added to the pulp prior to extracting the 2L sample for the Denver lab flotation test; the 2L sample for the feed size distribution analysis; and the RS feed sub-sample. For all the pilot runs and their corresponding Denver tests, the frother used is 70:30=X-133: Pine Oil.

Analysis: The RS machine performance after 7 stages is compared with Denver Pulp results after 20 minutes. Figure 4.11 presents the complete body of data (100 tests – 5 culled results = 95 valid test results), as Cu recovery in the RS after 7 stages versus Cu recovery in the Denver Pulp test after 20 minutes.

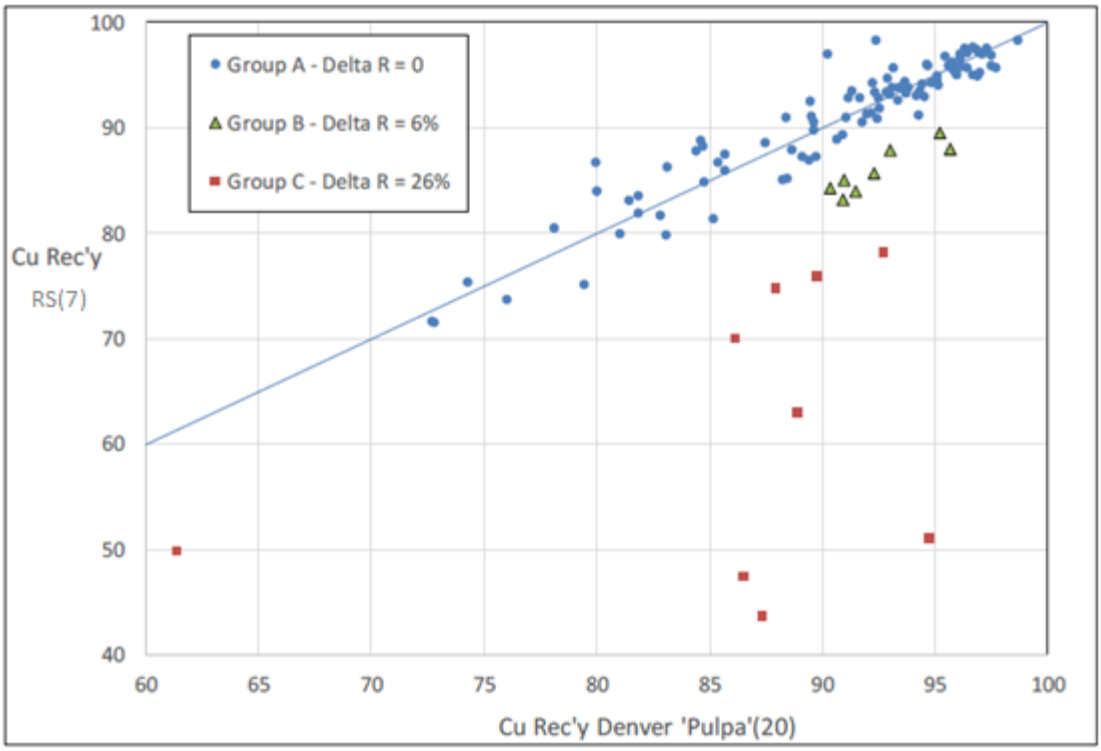

Figure 4.11: Copper Recovery – Denver versus RS

These data clearly fall into three groups: Group A in blue (98 samples) – Delta Recovery average = 0. Group B in green (8 samples) – Delta Recovery average = 6%. Group C in red (9 samples) – Delta Recovery average = 26%. Delta Recovery is (Cu Recovery Pulp, %) – (Cu Recovery RS, %). The blue unity line clearly indicates that for Group A samples, there is a simple 1-to-1 direct comparison between copper recovery in the RS (7 stages) and Denver recovery at 20 minutes. Figure 4.12 presents the same data; this time, plotting mass recovery from the Denver bench test versus feed percent sulfides (pyrite + copper sulfide).

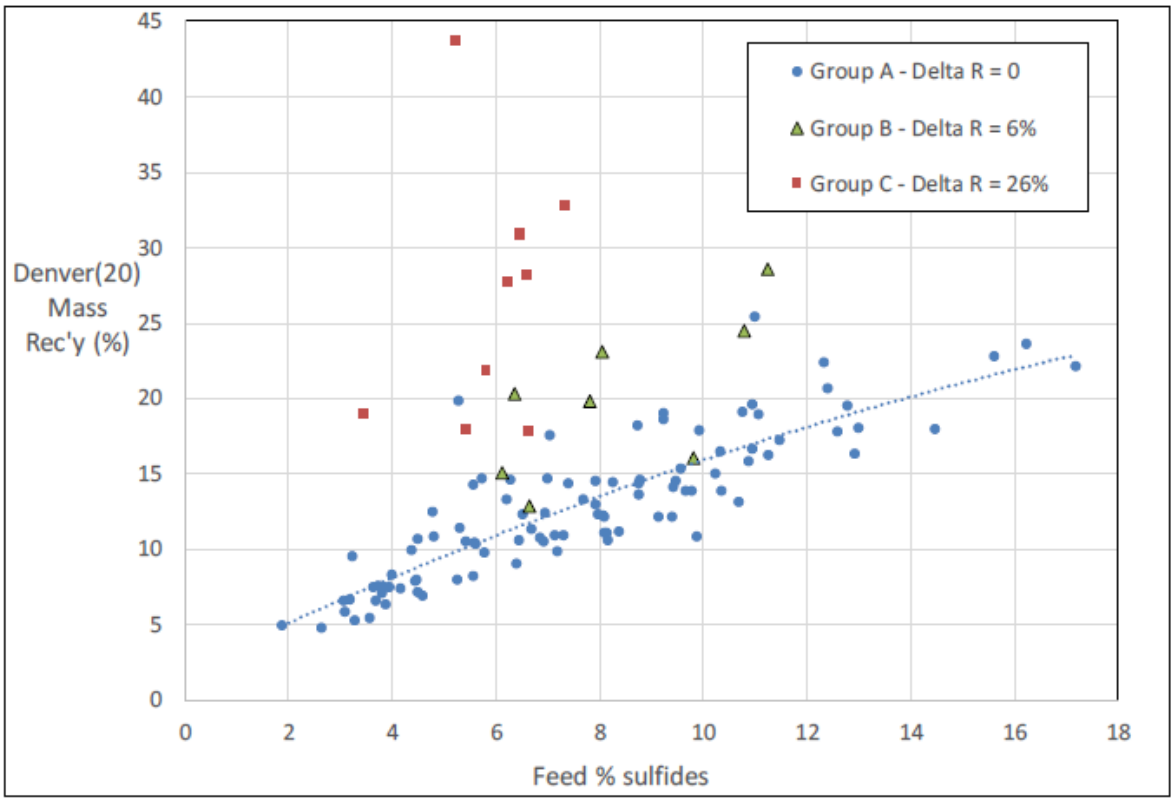

Figure 4.12: Denver Cu Recovery as a function of feed % Sulphides

Group A follows the expected trend, with a slope of about 1.6. Group B shows mass recovery that is, in general, significantly above the relationship set by the Group A tests, and the Group C mass recovery is dramatically higher.

The average Denver concentrate grade (for the hypogene samples) for Group A is 3.8 %Cu, versus only 2.1 %Cu for Groups B and 1.8 %Cu for Group C. In other words, for most of the Group B and C samples, the lab tests were pulled much harder than will occur in the plant, resulting in very high entrainment levels (average mass recovery for Group C is 26.6% versus 20.0 for Group B and 12.8% for Group A).

Presenting the data set as Delta copper recovery (Denver - RS) against Delta mass recovery (Denver - RS), Figure 4.14 confirms that the difference in performance between the RS and Denver test in Groups B and C can be wholly attributed to the difference in mass recovery between the two systems.

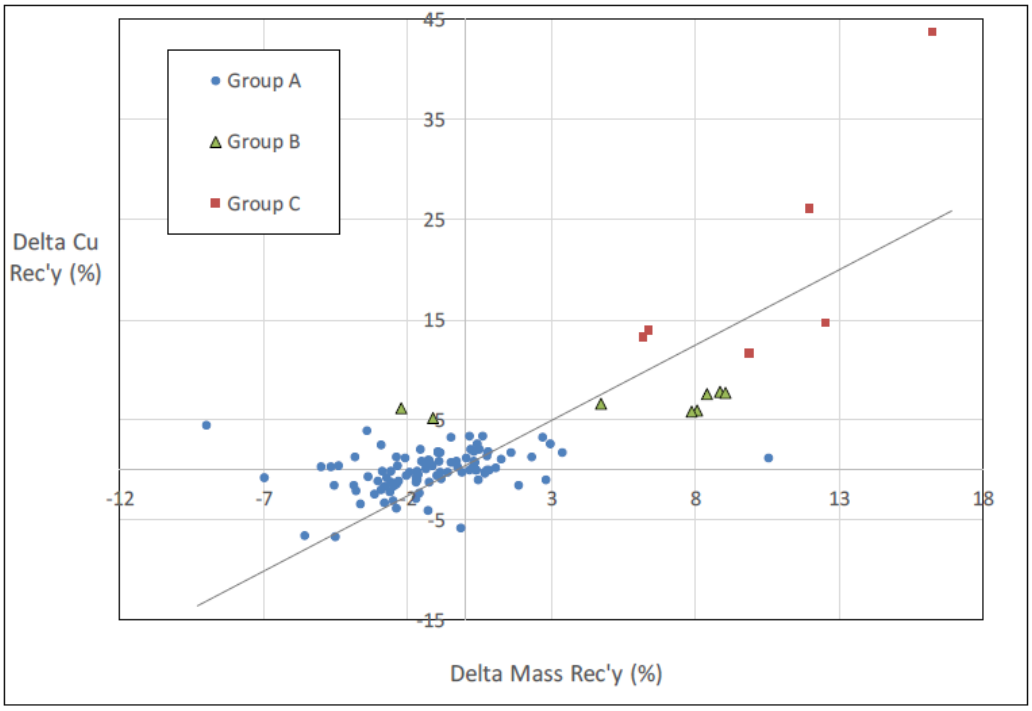

Figure 4.13: Delta Mass Recovery versus Delta Cu Recovery

Should be a key driver towards explaining these divergences in metallurgical performance (B and C) from the typical performance (A), Table 4-1 considers the Group C sample characteristics.

Table 4.8: Group C Sample Characteristics

Sample	% from QEMScan				% -400 #	Comments
	Kaolinite	Muscovite	Biotite	Chlorite		
PP-101	19	34	0	0	46	High Muscovite & Kaolinite
PP-102	20	32	0	0	55	High Muscovite & Kaolinite
PP-103	12	29	8	2	52	High Biotite & Chlorite
PP-104	33	20	0	0	50	High Kaolinite
PP-105	17	37	0	0	54	High Muscovite & Kaolinite
PP-106	21	13	5	0	51	High Biotite & Kaolinite
PP-107	16	35	0	0	49	High Muscovite & Kaolinite
PP-108	11	18	9	2	53	High Biotite & Chlorite
PP-109	10	16	4	1	51	High Biotite & Chlorite
Average	10	26	2	0	44	100 Samples

As draft analysis, it can be seen that for Group C, the combination of mineralogical characteristics results in a higher fines proportion in the feed ore, as quantified by the percent -400mesh fraction, and is shown in Figure 4.15.

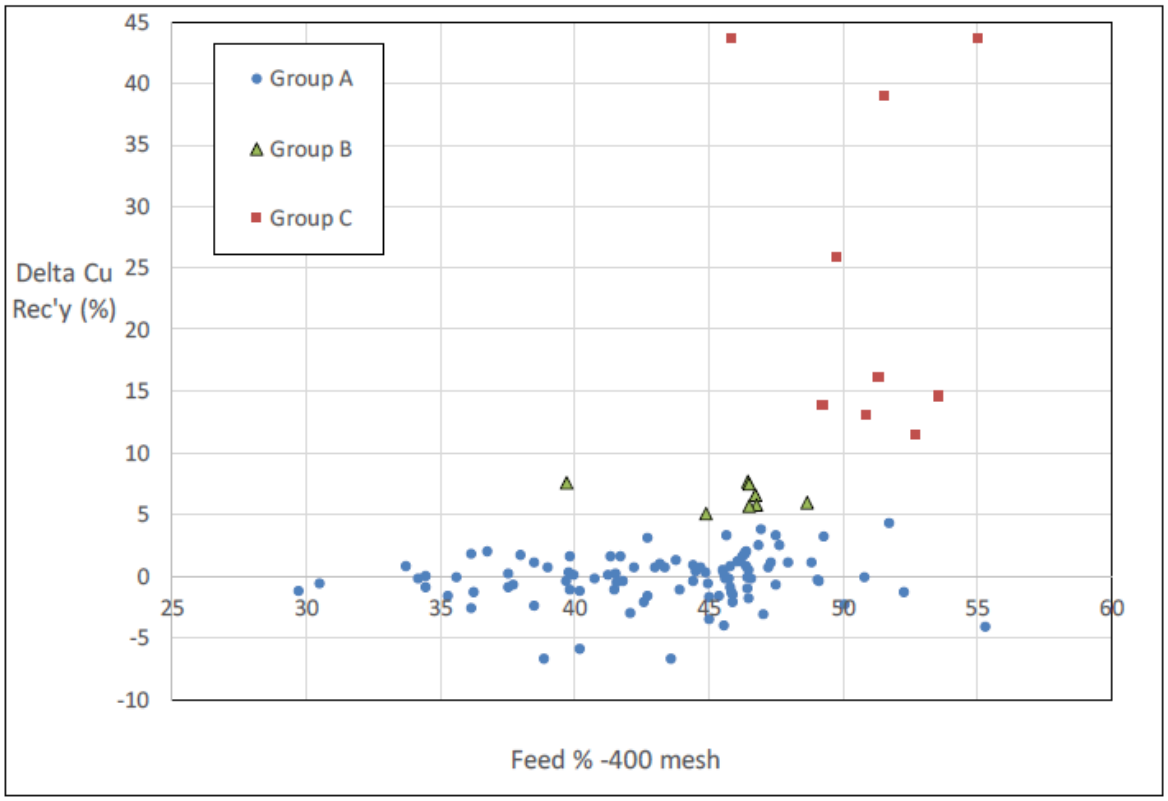

Figure 4.14: Delta Recovery versus feed -400 mesh fraction

The specific conclusions from this phase can be summarized as follows: (i) further analysis of gangue with a potential clustering of clays in families could be very important; (ii) the results' analysis focuses on the performance of three groups of samples, denoted Group A, Group B and Group C; (iii) Group A represents typical performance of RS accompanying Denver Pulp test. Groups B and C represent divergent performance, as a result of feed sample mineralogical characteristics.

Regarding the specific application of this chapter, the final conclusion is: **"The non-conventional flotation machine technology is selected together with interface wash water"**.

5. PROCESS SIMULATION FRAMEWORK

According to integrated process and control design (IPCD) approach, the process simulation framework is built upon modelling, simulation and experiments. The unifying methodology is based on systems identification theory. In this chapter the first focus is on steady state modelling followed by instrumental setup and ending with dynamic modelling and implementation.

5.1. SYSTEMS IDENTIFICATION STRATEGY

System identification is a methodology to build dynamic models that has been mostly applied for data driven box models but it´s now also referred for grey box models. The aim of system identification is to model systems dynamics that can't be easily described using first principles. In next figure 5.1., Ljung's system identification iterative work scheme is shown. Formerly used mainly for black box models; nowadays is utilized also for grey box) models.

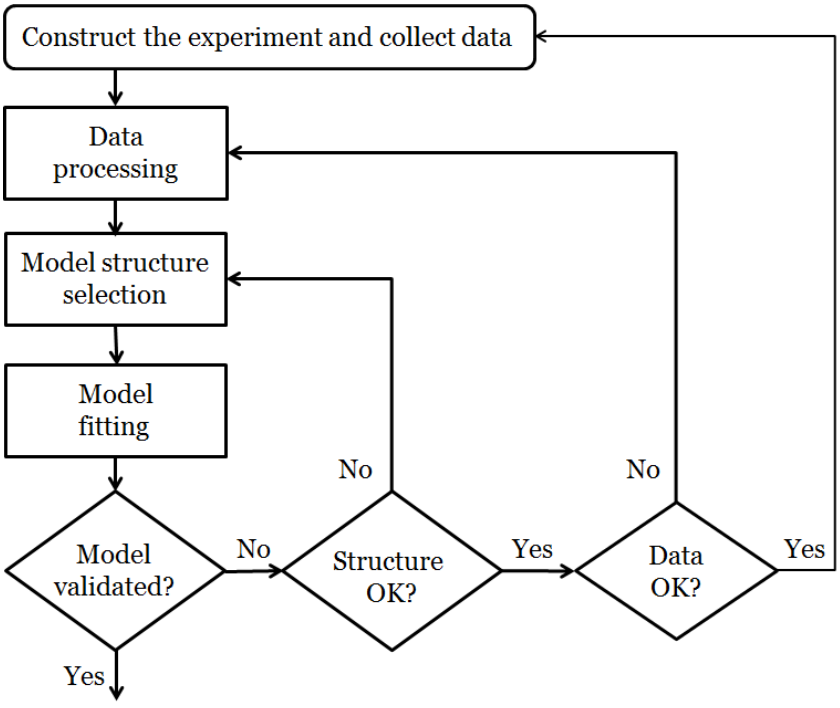

Figure 5.1.: System identification iterative work, from Ljung, 1990

Construct the experiment and collect the data: the experimental work of this phase consists mainly on continuous pilot testing. Even though, both laboratory and pilot continuous testing are run in parallel. Extensive and intensive usages of both off-line and on-line measurements are executed. By the exception of third party packaged expert system, all the instruments are tested in this phase. In terms of process control, the first layer of the control structure is presented in this sub-chapter: instrumentation and controls. The upper layers of the control structure are presented in chapter 6.

Continuous experimental phase: the main purpose of this campaign is to identify and implement the process simulation framework and the MPC predictive models for the control simulation framework. Other specific purposes are: instrumentation startup and testing and; proportional and integrative (PI) controllers' tuning. The continuous campaign covers 122 tests divided in three sub phases as shown in tables 5.1, 5.2 and 5.3:

Table 5.1: Experimental sub phase I: Instrumentation and Control

Test Number	Tuned loops and/or instruments
1-8	Cell single loops: level, air flow, wash water flow
9-10	Concentrate area-velocity volumetric flowmeter
11	Volumetric flow meters for feed and tailings
12-15	Feed densitometer
16	Reagents mass flowmeters
17-20	Metallurgical analysers
21-24	Conductivity meters

Table 5.2: Experimental sub phase II: Single RS Cell Characterization

Test Number	Name of calibrated and validated model
25-35	Mass and volumetric balance
36-45	Three compartments
46-55	Polat and Chandler – RTD

Table 5.3: Experimental sub phase III: Row Characterization

Test number	Description
56-62	Mass and volumetric balance - two (2) cells
63-65	Mass and volumetric balance - three (3) cells
66-70	Mass and volumetric balance - four (4) cells
71-84	RS versus SALA pilot plant (SPP)
85-97	RS versus conventional mini pilot plant (CMPP)
98-122	Variability Testing with three (3) main FGU's

Data processing: both data reconciliation and data filtering are considered within data processing. While both exploratory and variability campaigns are subject to partial data reconciliation; from here till the end of this thesis, full data reconciliation is done; either offline and/or online. Matlab routines for offline and online data reconciliation and parameter estimation are implemented for the purposes of this thesis.

Process model structure selection: the base models, to be adapted and/or modified and; synthetized in this chapter are: Savassi's compartmental model; Jämsä-Jounela dynamic model for pulp levels; Polat & Chandler for collection zone characterization and; Gorain et al. (2000) and, Bergh & Yianatos (2009) for both hydrodynamic and kinetic models. In addition to mentioned models, well known mass balance relationships among control variables are used together for simulation framework build-up.

Predictive model structure selection: all the predictive models considered in this thesis, are linear, state space and discrete. When the MPC's are in profiling mode, they mutate to adaptive MPC in which case, the models are time variant. In all the other cases, the models are time invariant. As it is already mentioned in sub chapter 2.5, a traditional discrete space model representation is used in this thesis, given by equations (2.35) and (2.36). In the case of adaptive model predictive control, matrices A and B are time dependant. Regarding the application, three types of MPC's are developed in this thesis: (i) row optimizer MPC, MPC_R; (2) individual cells MPC's, MPC_n (where n is the cell number) and; row levels MPC, MPC_L. While in case of MPC_L the matrices A (t) and B (t) are symbolic; for MPC_R and MPC_n, A (t) and B (t) are numerical.

Model fitting strategy: From a high level point of view, it can be hereupon observed that the cells are over-characterized with the instrumentation available at continuous experimental phase. The available degrees of freedom are used for parameters' estimation and data reconciliation. According to the specific experiments and models under resolution; different parameters are calibrated and validated. As such, the proportion between degrees of freedom used for parameters' estimation and those used for data reconciliation varies. The following model fitting stages are successively considered: (i) individual cell overall masses and volumes steady state parameters; (ii) individual zones steady state recoveries; (iii) collection and froth zones models' parameters; (iv) two, three and four cells rows' parameters and; (v) "enhanced" Jämsä-Jounela dynamic model parameters estimations.

Model fitting implementation: multiple data sources; including previous experimental phases such as variability tests and; the continuous experimental phases described in this chapter; are successfully integrated to maximise both the steady state and dynamic characterization of the machine-mineral system. Such characterization details are further explained later on in this chapter, but a brief follows.

Single cell model fitting: the proposed three compartment model has three main parameters, the corresponding zones recoveries R_C, R_F and R_Q; well determined, reconciled and validated by the experimental data as well as the total recoveries R_{RS} or R_{CONV}. While collection zone recoveries obtained from three compartmental model fitting, are tested and compared against Polat & Chandler model fitting; both froth and quiescent recoveries are kept as obtained from three compartmental fitting.

Collection zone model fitting: the assumption that the collection sub-process happens only within the reactor unit is used and tested. While kinetic characterization is done using parallel batch tests, residence time distribution parameters are experimentally determined for both the reactor unit and the whole RS machine, through conductivity testing in both RS's compartments. For RS machines as well as for conventional ones, comparisons are done between results from Polat & Chandler parameters' fitting and three compartmental R_C fitting.

Row model fitting is related to grades and recoveries obtained from both cell-based and row-based manipulated variables. Regarding row-based controlled variables (reagents), model fitting is based on data driven models. Also, as the startup dynamic model (Jämsä-Jounela) is row based, the dynamic model structure and fitting is described within the row characterization sub-chapter.

Dynamic model fitting: Experimental input signals need to be designed with few basic properties, to extract informative dynamical response from the process. The main idea for performing dynamic model fitting tests is to design input signals which: are rich enough to reveal the system dynamics; let the system perform around nominal operating points and; are chosen according to the bandwidth of expected dynamics.

Models' validation: All the estimated models are validated with independent data sets. The validation data set is pre-processed in the same way as the estimated data set.

5.2. INSTRUMENTATION AND CONTROL

Single cell measurements and basic controls: each cell "n" has the following basic control loops: pulp level control loop (LIC-n1); air control loop (FIC-n1) and; interface wash water control loop (FIC-n2). Next figure 5.2 shows the basic instrumentation and controls of each cell using ISA 95 standard. FT-03 is a concentrate volumetric flow transmitter.

Set points (SP) could be either managed independently by the operator or could be manage by the levels' MPC in case of level control loops or; "Cell n" MPC_n in case of both wash water and air flows. MPC's are described in chapter 6, as well as all the other components of the control structure.

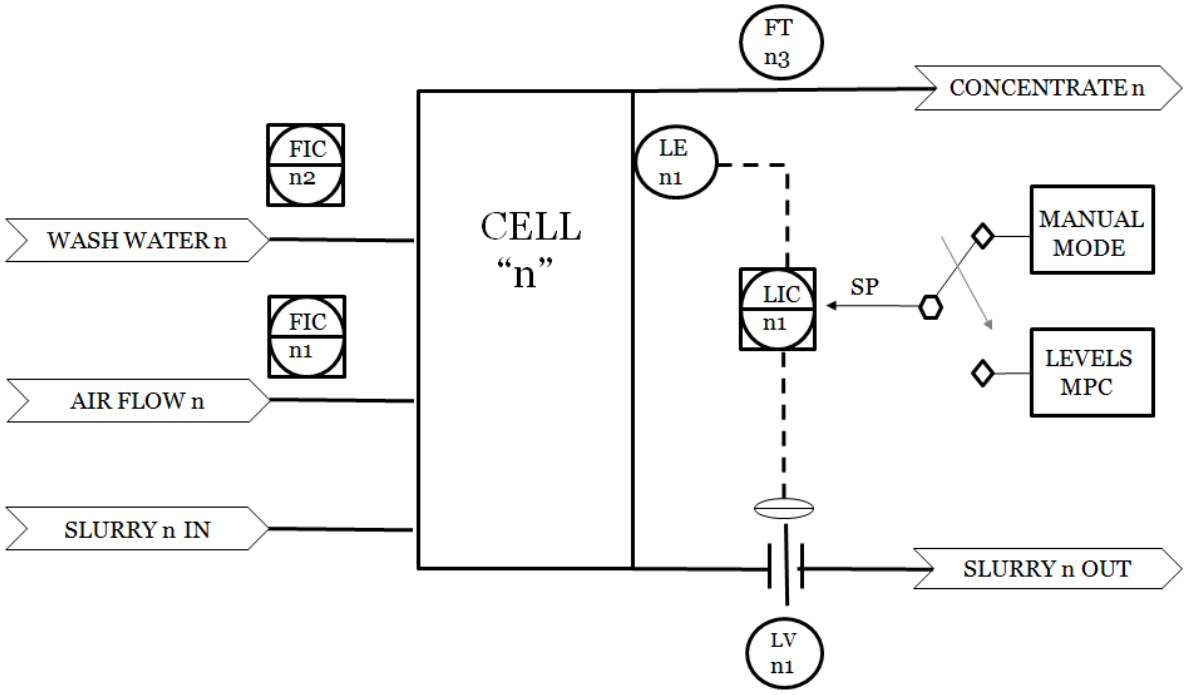

Figure 5.2: Cell n instrumentation and basic control scheme

Pulp level control loop - LIC-n1 - contains a modulating knife gate valve and a magnetostrictive double float / double level measuring unit. The first float sits at the froth/slurry interface – "LE-n1" - and the second float sits on top of froth – "LE-n2".-. This loop is managed by a PI controller, but its set point is stablished either by the operator or by the MPC that controls all the levels along the row (MPC_L). LE-n1 represents the pulp level and LE-n2 represents froth height over the lip and is afterwards used for the supervisory purposes described in chapter 6.

The air control loop (FIC-n1) manages the airflow. It contains a pneumatic globe air control valve and; a vortex flowmeter, located upstream of the control valve. This loop is managed by a PI controller, but its set point is stablished either by the operator or by the MPC that controls all the levels along the row (MPC_n). In next figure 5.3, the air control loop is shown:

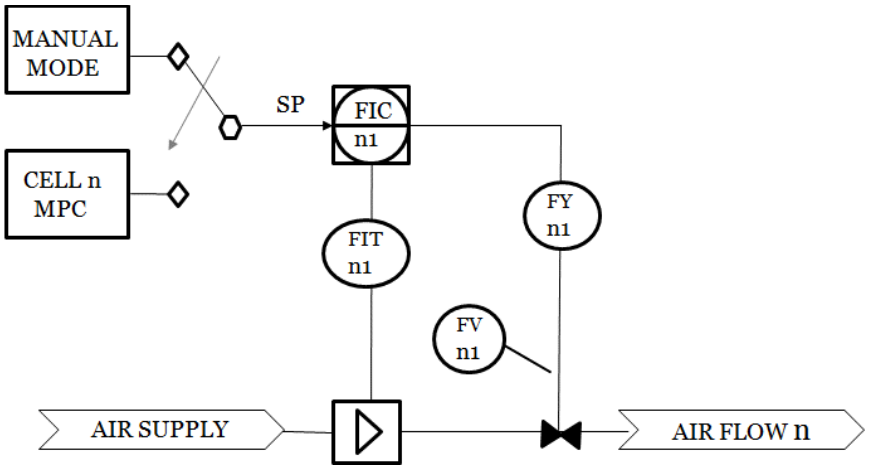

Figure 5.3: Cell n, air flow control loop

The wash water loop (FIC-n2) is used to control and change the interface wash water flow (IWW) and shown in figure 5.4. It contains a globe pneumatic water control valve and a magnetic flow meter. The magnetic flow meter is located upstream of the control valve. This loop is managed by a PI controller, but its set point is stablished either by the operator or by the MPC that controls all the levels along the row (MPC_n).

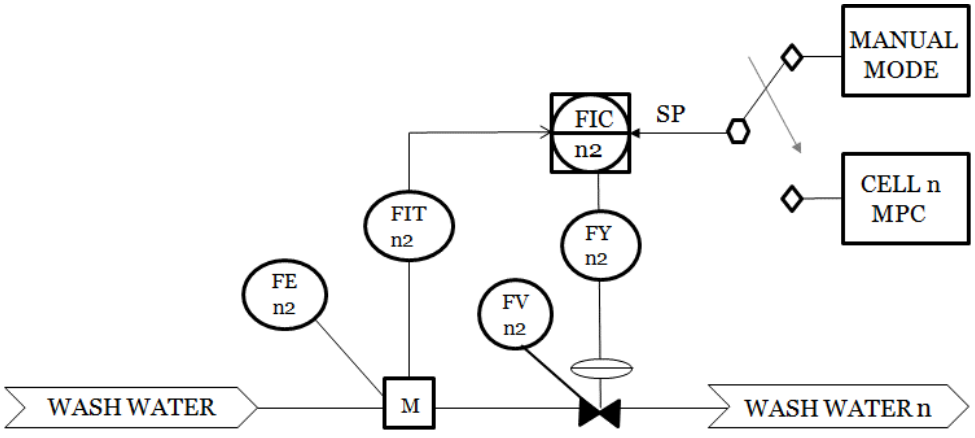

Figure 5.4: Cell n, wash water flow control loop

Row instrumentation - direct measurements: For each stream (F: feed, C: concentrate, T: tailings), there is an on-line XRF metallurgical analyzer that delivers copper, molybdenum, iron and arsenical grades, together with solids percentage C_P. Copper and molybdenum grades ($L_{Cu,F}$, $L_{Mo,F}$, $L_{Cu,C}$, $L_{Mo,C}$, $L_{Cu,T}$, $L_{Mo,T}$) are used by the optimization layer after being subject to on-line data reconciliation using iron and arsenical grades ($L_{Fe,F}$, $L_{As,F}$, $L_{Fe,C}$, $L_{As,C}$, $L_{Fe,T}$, $L_{As,T}$). In addition, on-line volumetric flowmeters deliver the corresponding measurements Q_F, Q_C and Q_T. While the volumetric flowmeter for feed is magnetic, the other two ones are area-velocity ones. Additionally, the feed pulp density (δ_{PF}) is measured by means of an electro-tomography instrument (non-radioactive). Finally, mass flowmeters (G_i) are available for the following reagents: lime, primary and secondary collector and, frother blend. In next figure 5.5, row measurements are shown, where X represents Cu, Mo, Fe and Arsenic; and i represents lime, primary collector, secondary collector and frother blend.

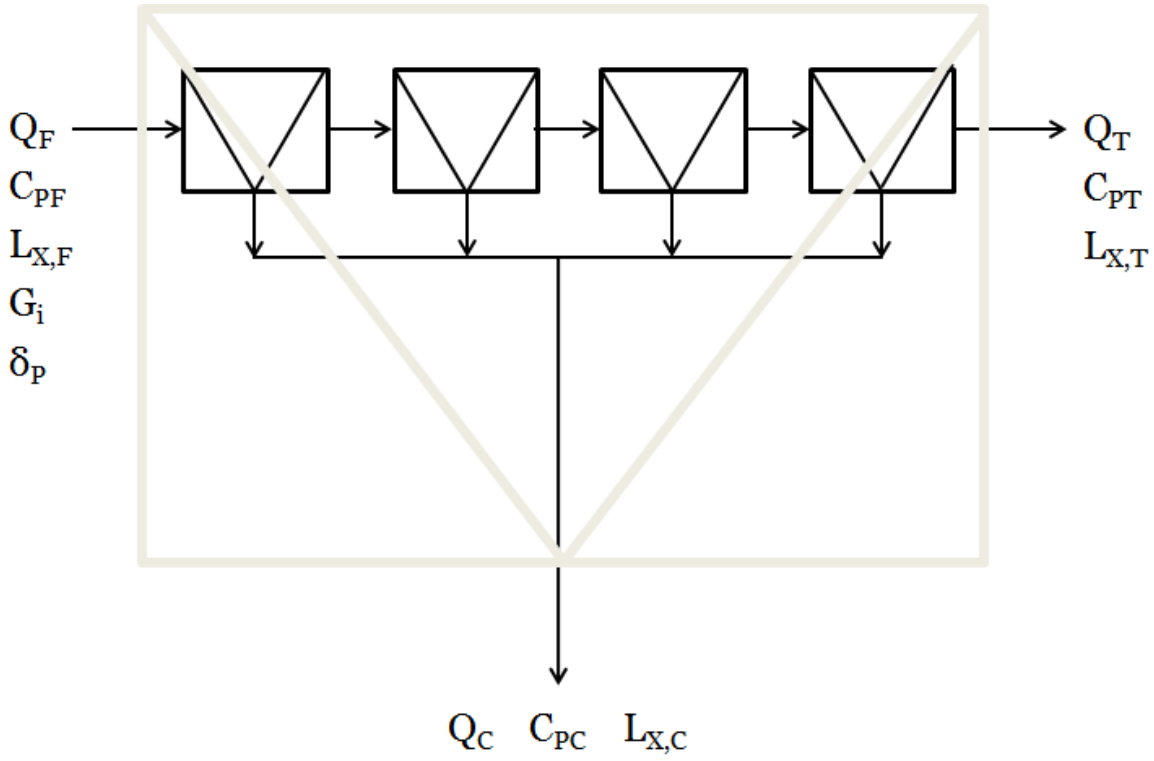

Figure 5.5: Row instrumentation

5.3. SINGLE CELL CHARACTERIZATION

Compartmental model synthesis: as mentioned in sub chapter 2.3, Savassi's compartmental model has two compartments regarding "true flotation": collection zone and froth zone and, can be represented by figure 5.6 and equation 5.1:

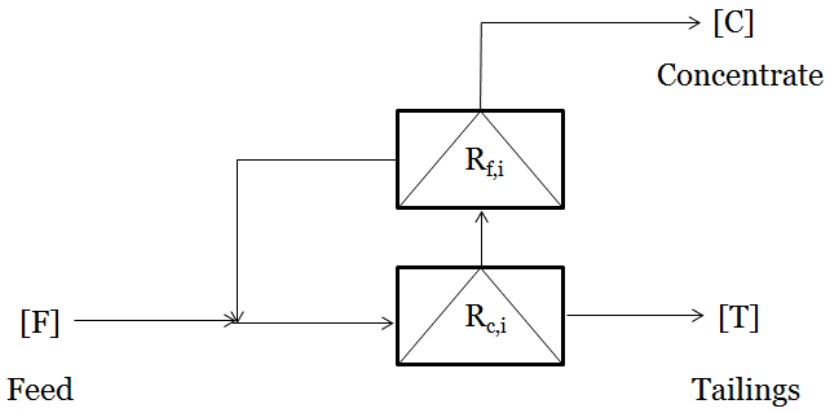

Figure 5.6: Two compartment model (adapted from Savassi, 2005)

$$R_{tot} = \frac{R_{c,i} \cdot R_{f,i}}{1 - R_{c,i} \cdot (1 - R_{f,i})} \qquad (5.1)$$

Where,

R_{tot} : Total cell recovery due to true flotation

$R_{c,i}$: Collection recovery of specie i

$R_{f,i}$: Froth recovery of specie i

$[F_i]$: Feed solids flow

$[C_i]$: Concentrate solids flow

$[T_i]$: Tailings solids flow

Specie i could be water, gangue particle, valuable particle or mixed particle. Additionally, either dynamic or steady state analysis can be done if dynamic mass accumulation is considered for each compartment.

A full three compartmental approach is proposed in this thesis. With $R_{q,i}$ representing quiescent zone recovery of specie i; the models of both conventional RS cells; are correspondingly shown in figures 5.7 and 5.8:

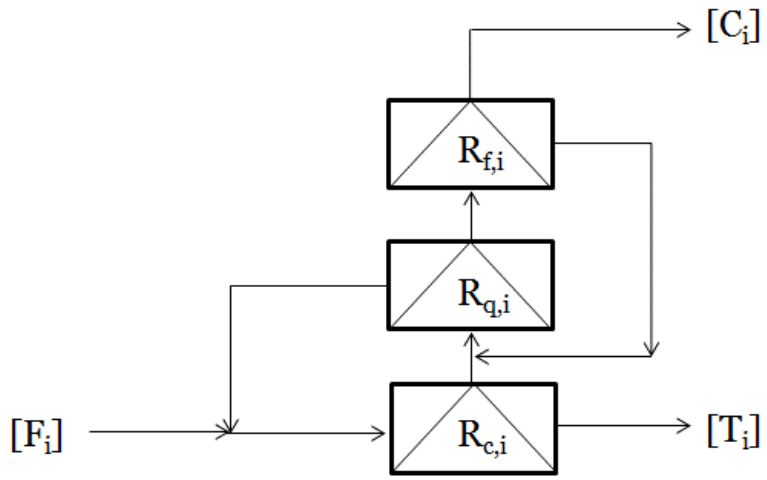

Figure 5.7: Full three compartmental model of conventional mechanical cell

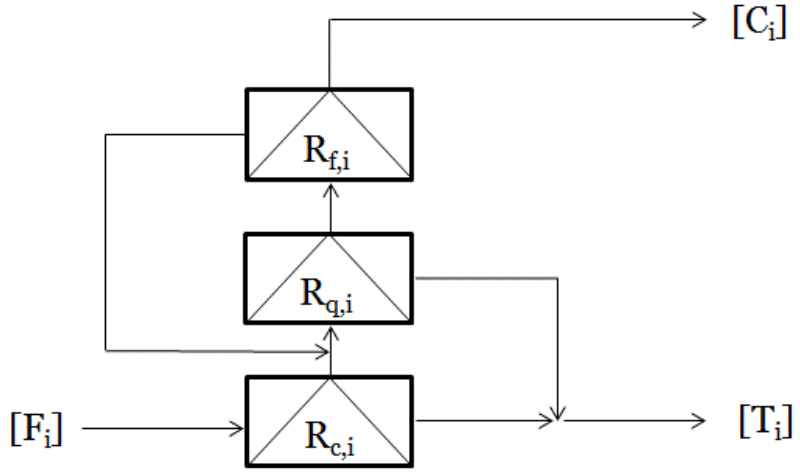

Figure 5.8: Full three compartmental model of a RS flotation machine

Then, the total recoveries for specie "i" in a conventional cell ($R_{conventional}$) and in a RS machine (R_{RS}); can be expressed by:

$$R_{conventional} = \frac{R_{c,i} \cdot R_{q,i} \cdot R_{f,i}}{1 - R_{c,i} \cdot (1 - R_{q,i}) - R_{q,i} \cdot (1 - R_{f,i})} \qquad (5.2)$$

$$R_{RS,i} = \frac{R_{c,i} \cdot R_{q,i} \cdot R_{f,i}}{1 - R_{q,i} \cdot (1 - R_{f,i})} \qquad (5.3)$$

It can be noticed that; if the zone recoveries were the same, the recovery of the conventional machine would be bigger. This structural difference is due to the fact that in case of RS flotation machine, particles detached in the separator tank report to the tailings because they do not have the probability return to the RU to be collected again.

Mass balance experimental synthesis: As part of the integrated process and control design (IPCD) approach, both cell layer and row layer instrumentation are available for pilot cell characterization. All of them are herein successively used for one cell, two cells and the entire row of four cells. Next figure 5.9, shows row layer's instrumentation applied to one cell characterization. It represents a model by itself, herein called "single cell – row model" (SCRM). While SCRM is presented here, "double cell – row model" (DCRM) and "multiple cell – row model" (MCRM) are presented in next sub-chapter.

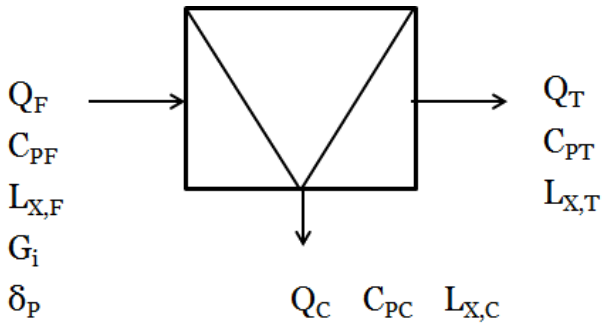

Figure 5.9: Single cell row direct measurements applied to one cell

Correspondingly, synthetizing the SCRM with the proposed three compartment model, the following figures 5.10 and 5.11 arise for conventional and RS cells:

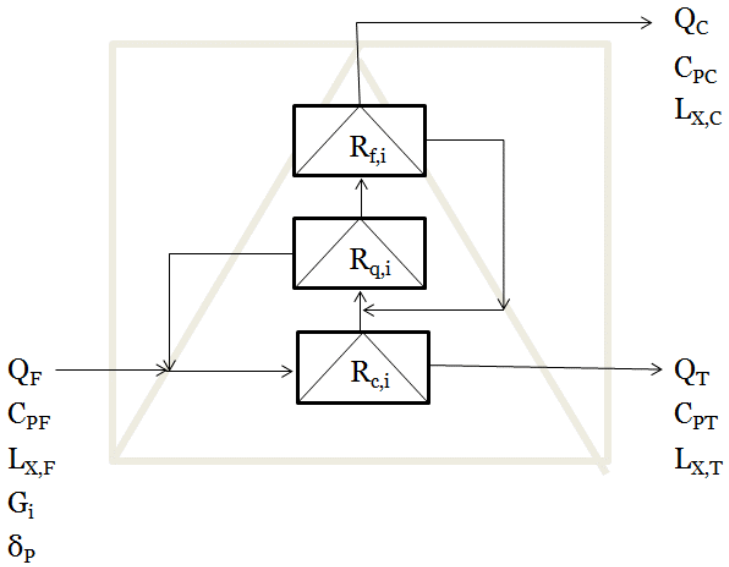

Figure 5.10: SCRM + conventional cell three compartment model

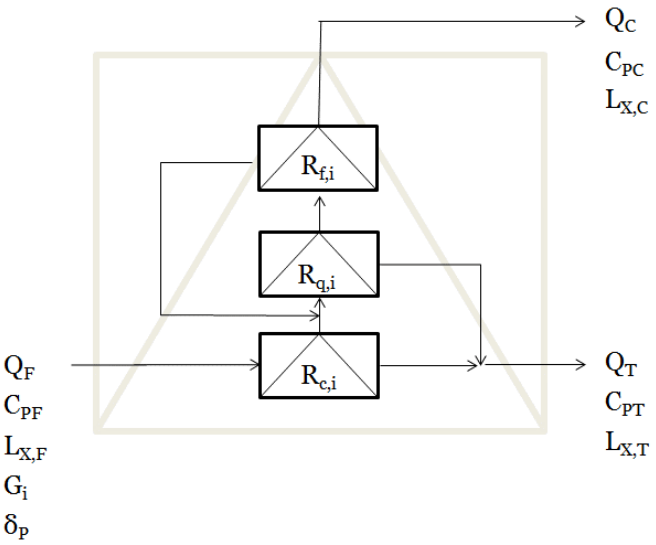

Figure 5.11: Single cell row model + RS three compartment model

At steady state, the following equations are used for resolving parameters R_q , R_f and R_c for each one of both types of cells: one (1) recovery equation (5.4 or 5.5); four (4) mass pulls obtained from (5.15); one (1) recovery (Cu) from (5.14) and; the mentioned 4x4 system given by equations (5.4), (5.5), (5.11) and (5.12). As can be observed, three degrees of freedom are needed from six available. Then, three degrees of freedom are available for: data reconciliation and; instruments' validation. While cells' parameters from vendors are shown in table 5.4; three compartmental models fitting results are presented in tables 5.5 and 5.6. Number of cells and row residence times are shown only for context and for reference afterwards in this thesis.

Table 5.4: Cells' operational parameters

Cell type	Cells #	Cell Volume	Pulp flow	τ_{ROW} min	τ_{CELL} min
RS (*)	4	15/45 l	≈15 l/h	≈4/12	≈1/3
ERIEZ	3	1.7 l	16.2 l/h	15.5 – 17.0	5.2 - 5.7
SALA	8	80 l	0.86 m3/h	37.4 - 38.1	4.7 - 4.8

(*) In the case of RS machines, there are two values for volume, flow and residence times: reactor unit parameters and, entire RS machine ones.

Table 5.5: RS three compartmental model fitting

				R_{RS}		
	R_C	R_F	R_Q	Experimental	R^2	Theory
HYPF-01	0.807	0.577	0.732	0.503	0.922	0.494
HYPF-02	0.806	0.553	0.701	0.472	0.934	0.455
HYPF-03	0.794	0.557	0.698	0.463	0.907	0.447
Average	0.804	0.564	0.717	0.485	-	0.464

Table 5.6: RS versus conventional three compartmental model fitting

				R_{TOTAL}		
	R_C	R_F	R_Q	Experimental	R^2	Theory
SALA	0.709	0.450	0.513	0.444	0.831	0.439
ERIEZ	0.759	0.406	0.601	0.558	0.844	0.544
RS	0.804	0.564	0.717	0.485	>0.907	0.464

As first insight, it can be observed that: (i) the RS model fitting shows better fittings (R^2) than conventional cells; (ii) even though, RS residence times are considerable smaller, total recoveries are not so different; (iii) RS zone recoveries are bigger than conventional cells' zone recoveries but, as an structural effect of direct reporting to tailings (figures 5.7 & 5.8, equations 5.2 & 5.3), RS total recoveries are smaller; (iv) almost always, experimental total recoveries are greater than theory and; (v) among zone recoveries, the collection zone shows better adjustment.

Continuous operation – collection zone recovery model: for conventional cells there is a synthesis done in the literature as mentioned in sub chapter 2.4. That's not the case for RS machines as far as they are "non-conventional". Therefore, a synthesis of Polat & Chandler (2000) model (2.20) is needed. For a RS machine; (5.4) is herein proposed as residence time distribution and both García-Zúñiga (G-Z) (1935, figure 2.25) and, Klimpel (K) (1980, figure 2.26), are here used as kinetic batch models.

$$E(t)= \; u(t-\theta)\cdot\frac{e^{-(t-\theta)/\tau_G}-e^{-(t-\theta)/\tau_P}}{\tau_G-\tau_P} \qquad (5.4)$$

Θ : Time delay

τ : mean residence time

τ_G : mean residence time of the big perfect mixer, $\tau_G > \tau_P$

τ_P : mean residence time of the small perfect mixer, $\tau_G > \tau_P$

Then, the following expressions (5.5) and (5.6) are considered to be further developed; being (5.5) from GZ batch kinetic distribution and; (5.6) from K one:

$$R_{RS,GZ}= R_\infty \int_{t=0}^{t=\infty} u(t-\theta)\cdot\left[\frac{e^{-(t-\theta)/\tau_G}-e^{-(t-\theta)/\tau_P}}{\tau_G-\tau_P}\right]\cdot\left[1-e^{-k_{gz}t}\right]dt \qquad (5.5)$$

$$R_{RS,K}= R_\infty \int_{t=0}^{t=\infty} u(t-\theta)\cdot\left[\frac{e^{-(t-\theta)/\tau_G}-e^{-(t-\theta)/\tau_P}}{\tau_G-\tau_P}\right]\cdot\left[1-\frac{1}{k_m t}\cdot(1-e^{-k_K t})\right]\left[1-e^{-k_m t}\right]dt \qquad (5.6)$$

Integrating, the continuous recovery for the collection zone is:

$$R= \frac{R_\infty}{\tau_G-\tau_P}\cdot\left[\alpha(t)-\beta(t)+\gamma(t)\right] \qquad (5.7)$$

Where for García-Zúñiga, $\beta=\gamma=0$, and for García-Zúñiga and Klimpel:

$$\alpha(t)=u(t-\theta)\cdot\left(\tau_G-\tau_P-\tau_G\cdot e^{-(t-\theta)/\tau_G}+\tau_P\cdot e^{-(t-\theta)/\tau_P}\right) \qquad (5.8)$$

For Klimpel:

$$\beta(t)=\beta_1(t)-\beta_2(t)-\beta_3(t);\ \gamma(t)=\gamma_1(t)-\gamma_2(t) \qquad (5.9)$$

$$\beta_1(t)=u(t-\theta)\cdot e^{\theta/\tau_G}\cdot Ei\left(\theta/\tau_G\right) \qquad (5.10)$$

$$\beta_2(t)=u(t-\theta)\cdot\left(e^{\theta/\tau_G}\cdot Ei(t/\tau_G)-e^{\theta/\tau_P}\cdot Ei(t/\tau_P)\right) \qquad (5.11)$$

$$\beta_3(t)=u(t-\theta)\cdot e^{\theta/\tau_P}\cdot Ei\left(\theta/\tau_P\right) \qquad (5.12)$$

$$\gamma_1(t)=u(t-\theta)\cdot\left[e^{\theta/\tau_G}\cdot\left(Ei\left(\theta\cdot(K_m\cdot\tau_G+1)/\tau_G\right)-Ei\left(t\cdot(K_m\cdot\tau_G+1)/\tau_G\right)\right)\right]/K_m \qquad (5.13)$$

$$\gamma_2(t)=u(t-\theta)\cdot\left[e^{\theta/\tau_P}\cdot\left(Ei\left(\theta\cdot(K_m\cdot\tau_P+1)/\tau_P\right)-Ei\left(t\cdot(K_m\cdot\tau_P+1)/\tau_P\right)\right)\right]/K_m \qquad (5.14)$$

It can be commented that even though above symbolic expressions are manageable for a single cell, that's no appear to be true for a row of RS machines. In this thesis, these formulas are not used for a row; but it's worth the effort to herein suggest the usage of numerical methods for that case.

Collection zone experimental work: while kinetic constants are obtained from variability campaign, residence time distributions (RTD) shall be experimentally obtained. In following figures 5.12 and 5.13, the experimental schemes are presented:

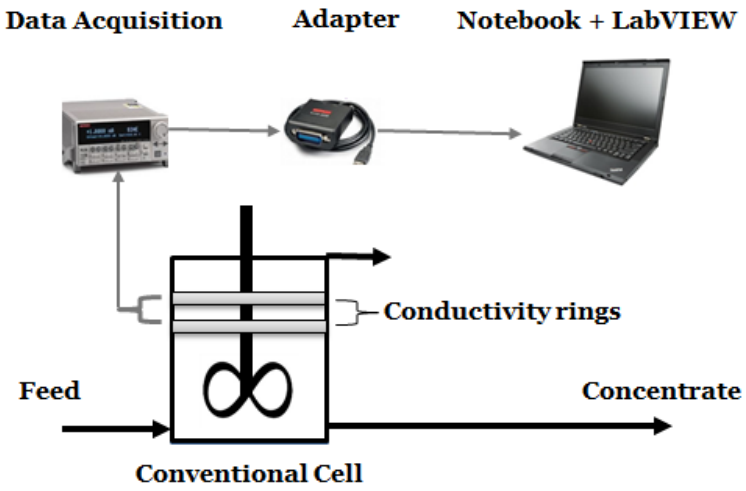

Figure 5.12: Experimental setup for conventional machine RTD

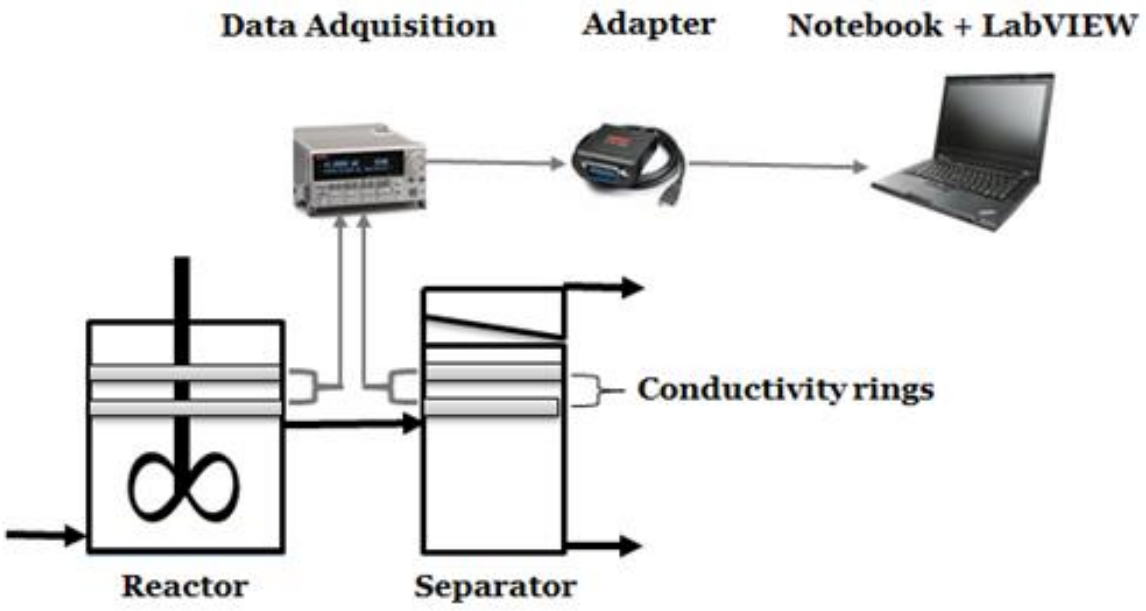

Figure 5.13: Experimental setup for RS machine RTD parameter fitting

Collection zone residence time experimental procedure: RTD tests are performed for RS machines. A brief description of the test follows:

(i) Installation of conductivity electrodes in the column and subsequent connection of to a signal adapter system. Then, the signal adapter system to a data acquisition card embedded in a notebook that has data acquisition software.

(ii) Conditioning of 72 liters of pulp, 2 kg of fine salt and 500 cm3 of 0.2 M hydrochloric acid into the "Conductive Pond".

(iii) Starting the pumping together with data acquisition → export of data generated by to Excel → import of data from Excel to MATLAB → reconciliation of experimental data → model fitting through script routines.

Collection zone residence time results are shown in following tables 5.7 and 5.8. All the tests are performed with the same material (truck 4) for the same FGU. In table 5.7, the LTST (large tank – small tank) model (Yianatos et al., 2007c) is used for conventional SALA cells. Then, in table 5.8, the real mixer model is used for fitting the residence time distribution of the reactor unit and; the herein proposed model (5.4) is used for fitting the residence time distribution of the entire RS machine. The estimator R^2 is shown as adjustment quality index.

Table 5.7: Conventional SALA cells' RTD model fitting (time in seconds)

	Test 48	Test 49	Test 55	τ_{theory}
	HYPF1	HYPF1	HYPF1	V_T/Q
τ_G [s]	203.44	209.82	205.32	-
τ_P [s]	37.65	43.16	46.55	-
τ [s]	241.09	252.98	251.87	284.47
R^2	0.90	0.89	0.88	-

From table 5.7, it can be noticed that the total fitted time residence is less than the "actual" residence time, calculated by the ratio between total volume and flow. That result is logical and it's commonly related to 2 problems: short circuits and/or material that remains a lot of time in the reactor occupying the place of fresh feed. Regarding the quality of the adjustment, R^2 is good enough.

Table 5.8: RS-RTD model fitting

	Test 47		Test 50		Test 53		τ_{theory}	
	T_47a	T_47b	T_50a	T_50b	T_53a	T_53b	V_{RU}/Q	V_T/Q
τ [s]	57.89	162.22	57.27	158.70	57.55	160.70	61.20	183.60
τ_G [s]	-	118.73	-	116.10	-	117.20	-	-
τ_P [s]	-	58.37	-	55.90	-	56.30	-	-
Θ [s]	2.92	5.21	3.08	6.30	3.17	7.40	-	-
R^2	0.93	0.91	0.94	0.92	0.93	0.92	-	-

From table 5.8, it can be observed that the reactor unit adjustments give smaller, but very similar times than the ratio between the reactor unit volume and the flow. Also, all the adjustments have good quality indices.

Table 5.9: Polat & Chandler (R_{cp}) and compartmental recoveries

	P&C	Compartmental recoveries		
	Rcp	Rcc	Rf	Rq
T_47a	0.798	0.793	0.571	0.724
T_47b	0.851	0.812	0.565	0.711
T_48	0.724	0.690	0.569	0.531
T_49	0.667	0.638	0.559	0.516
T_50a	0.805	0.813	0.566	0.715
T_50b	0.844	0.806	0.561	0.729
T_53a	0.822	0.791	0.561	0.705
T_53b	0.855	0.799	0.556	0.723
T_55	0.654	0.595	0.558	0.533

In table 5.9, zone recoveries are presented. For the collection zone there are two models: Polat & Chandler collection recovery (R_{cp}) and, three compartment's collection recovery (R_{cc}). It can be observed that $R_{cp} > R_{cc}$ in all the cases and, more than 5% bigger, in average. As for RS cells the residence times are very similar to the "real" residence times, it could be conjectured that the reason is not related to deficiencies as short-circuits.

In next table 5.10, total recoveries are presented. For conventional tests (T_48, T_49 and, T_55), equation (5.2) is used; while for RS tests (T_47, T_50 and, T_53), equation (5.3) applies. While in the first results' column, the Polat & Chandler collection recoveries are applied correspondingly to formulas (5.2) and (5.3); three compartmental model's collection recoveries are applied in second results' column.

Table 5.10: Total recoveries and errors related to experimental results

	Total recoveries			Recoveries' errors %	
	w/Rcp	w/Rcc	Experimental	w/Rcp	w/Rcc
T_47a	0.479	0.476	0.455	5.32	4.66
T_47b	0.494	0.472	0.445	10.98	5.90
T_48	0.507	0.483	0.460	10.17	4.94
T_49	0.428	0.410	0.404	6.12	1.48
T_50a	0.472	0.477	0.465	1.44	2.45
T_50b	0.508	0.485	0.485	4.76	0.05
T_53a	0.470	0.453	0.451	4.24	0.32
T_53b	0.506	0.473	0.449	12.66	5.29
T_55	0.424	0.386	0.380	11.48	1.40

Regarding RS tests, it can be noticed that the collection recoveries obtained from the three compartmental models, have considerable smaller errors than the recoveries calculated using P&C. Nevertheless, it's worth to mention that the P&C collection recoveries used are the ones from the proposed model, not using the simpler "real mixer" model for reactor unit. In that case, the error is smaller and that can be seen observing that the residence times of the reactor unit obtained by DTR's are very similar to the "real" ones. In practical terms, conductivity measurements are recommended herein in the reactor unit compartment.

For conventional tests (T_48, T_49 and, T_55), it can also be observed that the collection recoveries obtained from the three compartmental models, have considerable smaller errors than the recoveries calculated using P&C. But, from table 5.8 it can be noticed that the fitted residence times are around ten percent smaller than the "real" residence times calculated by means of the ratio between volume and flow.

5.4. ROW CHARACTERIZATION

Next figures 5.13, 5.14 and 5.15 show row layer's instrumentation applied successively to two, three and four cells row characterization. They represent models by themselves, related mainly to masses and volumes balances.

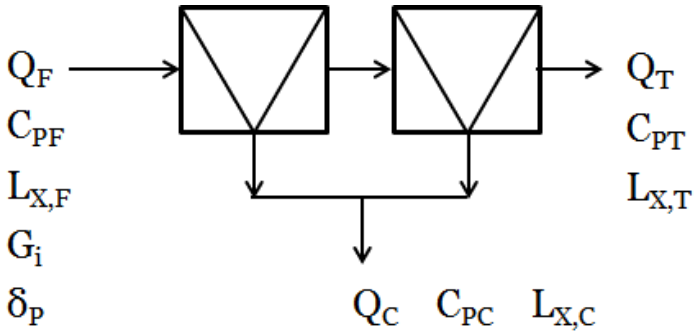

Figure 5.13: Double cell row model

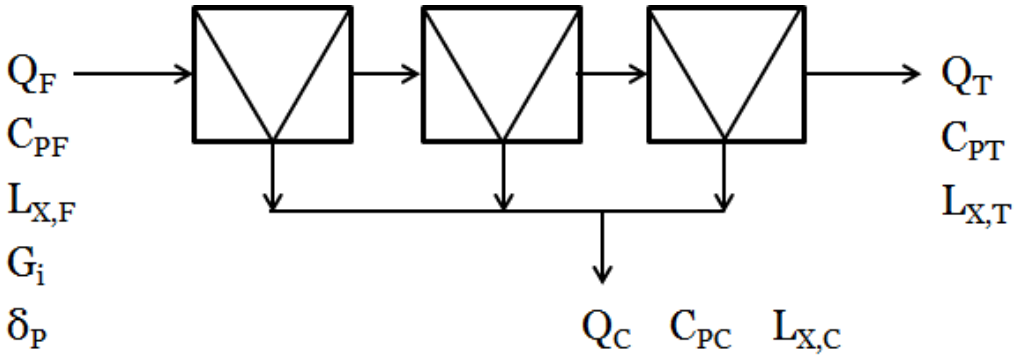

Figure 5.14: Triple cell row model

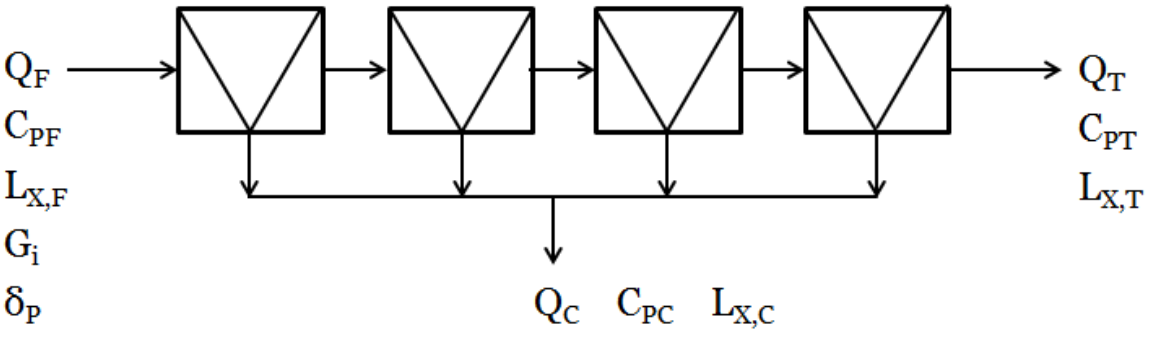

Figure 5.15: Four cell row model

Row balance models: there are well-known relationships for volumetric flows, fractional solids contents, solids flows and densities. Among them, the total volumetric flow of each stream corresponds to the addition of solids volumetric flow and liquid volumetric flow, obtaining:

$$Q_F = \frac{G_{SF}}{\delta_{SF}} + \frac{(1-C_{PF})}{C_{PF}} \cdot \frac{G_{SF}}{\delta_{LF}} \qquad (5.15)$$

$$Q_C = \frac{G_{SC}}{\delta_{SC}} + \frac{(1-C_{PC})}{C_{PC}} \cdot \frac{G_{SC}}{\delta_{LC}} \qquad (5.16)$$

$$Q_T = \frac{G_{ST}}{\delta_{ST}} + \frac{(1-C_{PT})}{C_{PT}} \cdot \frac{G_{ST}}{\delta_{LT}} \qquad (5.17)$$

As feed pulp density is known, solids feed density (δ_{SF}) can be obtained from:

$$C_{PF} = \frac{\delta_{SF} \cdot (\delta_{PF} - \delta_{LF})}{\delta_{PF} \cdot (\delta_{SF} - \delta_{LF})} \qquad (5.18)$$

From equation (5.15) and assuming $\delta_{LF} = \delta_{LC} = \delta_{LT} = 1[g/cm3] = 1000[kg/m3]$,

$$\delta_{SF} = (\delta_{PF} \cdot C_{PF}) / [1 - \delta_{PF} \cdot (1 - C_{PF})] \qquad (5.19)$$

In addition, G_{SF} is given by:

$$G_{SF} = C_{PF} \cdot Q_F \cdot \delta_{PF} \qquad (5.20)$$

A mass balance for solids flows:

$$\frac{dG}{dt} = G_{SF} - G_{SC} - G_{ST} \qquad (5.21)$$

The corresponding volumetric balance:

$$\frac{dV}{dt} = Q_{SF} - Q_{SC} - Q_{ST} \qquad (5.22)$$

Equations (5.21) and (5.22) are used for dynamic systems identification. At steady state, both solids mass flows and volumetric flows shall be balanced:

$$G_{SF} = G_{SC} + G_{ST} \qquad (5.23)$$

As well as solids volumetric flows shall be balanced at steady state:

$$\frac{G_{SF}}{\delta_{SF}} = \frac{G_{SC}}{\delta_{SC}} + \frac{G_{ST}}{\delta_{ST}} \qquad (5.24)$$

Equations (5.4), (5.5), (5.11) and (5.12); conform a 4x4 system regarding to G_{SC}, G_{ST}, δ_{SC} and, δ_{ST}. Then, for all streams (feed, concentrate and tailings), solids flows and solids densities are well defined at steady state. In addition, the row mass pull can be obtained in terms of solids mass flows:

$$Y = \frac{G_{SC}}{G_{SF}} \qquad (5.25)$$

From grades measurements, the following information is obtained: row metallurgical recoveries and row mass pulls:

$$R_X = \frac{L_{X,C}\cdot(L_{X,F}-L_{X,T})}{L_{X,F}\cdot(L_{X,C}-L_{X,T})} = \frac{L_{X,C}\cdot G_{SC}}{L_{X,F}\cdot G_{SF}} \qquad (5.26)$$

$$Y_X = \frac{(L_{X,F}-L_{X,T})}{(L_{X,C}-L_{X,T})} = \frac{G_{SC}}{G_{SF}} \qquad (5.27)$$

Where sub index "X" can represent Mo, Cu, Fe or As.

Then, five mass pulls are available, four from equation (5.26) and one from equation (5.25). As mass pulls shall be equal, four mass pulls are available for additional variables resolution and/or data reconciliation, as it is further explained wherever applies. Now, it can be said that degrees of freedom are used in the following section for dynamics' estimation.

Dynamic models synthesis: as mentioned in sub chapter 2.3, Kämpjärvi & Jämsä-Jounela dynamic model is selected as "startup model". In this sub chapter, some simplifications of the mentioned model are taken out. Here, there is interface wash water (IWW) flow and a concentrate flow. Additionally, pulp densities do vary along the row. Also, there is a volumetric air holdup (E_g). Therefore, instead of equation (2.4), the following equation (5.28) applies for each cell along the row; considering that: $Q_{W,i}$ and $E_{g,i}$ are correspondingly, the interface wash water and the volumetric gas holdup of cell i:

$$\frac{dV_i}{dt} = Q_{Fi} - Q_{Ci} - Q_{Ti} + Q_{Wi} + E_{g,i} \qquad (5.28)$$

It's important to mention that herein the air holdup is not in percentage, but it is considered as volumetric gas holdup.

From (5.21) & (5.22) & (5.23), for cell i:

$$\frac{dG_i}{dt} = G_{SFi} - G_{SCi} - G_{STi} \qquad (5.29)$$

For dynamic balances of valuable solids contents:

$$\frac{dG_{X,i}}{dt} = G_{SF,X,i} - G_{SC,X,i} - G_{ST,X,i} \qquad (5.30)$$

Then, considering that Q_{in} is feed flow; S is the area; c is the physical difference in height between the cells; K is a constant coefficient; C_v is the valve coefficient, given by valves' vendor and; y_i, u_i are respectively, the pulp level and control signal of cell i:

$$\frac{dy_1}{dt} = \frac{Q_{F1}}{S} - \frac{Q_{C1}}{S} - \frac{K}{S} C_v(u_1)\sqrt{\delta_1 y_1 - \delta_2 \cdot (y_2 - c)} + \frac{Q_{W1}}{S} + \frac{E_{g1}}{S} \qquad (5.31)$$

$$\frac{dy_2}{dt} = \frac{K}{S} C_v(u_1)\sqrt{\delta_1 y_1 - \delta_2 \cdot (y_2 - c)} - \frac{K}{S} C_v(u_2)\sqrt{\delta_2 y_2 - \delta_3 \cdot (y_3 - c)} - \frac{Q_{C2}}{S} + \frac{Q_{W2}}{S} + \frac{E_{g2}}{S} \quad (5.32)$$

$$\frac{dy_3}{dt} = \frac{K}{S} C_v(u_2)\sqrt{\delta_2 y_2 - \delta_3 \cdot (y_3 - c)} - \frac{K}{S} C_v(u_3)\sqrt{\delta_3 y_3 - \delta_4 \cdot (y_4 - c)} - \frac{Q_{C3}}{S} + \frac{Q_{W3}}{S} + \frac{E_{g3}}{S} \quad (5.33)$$

$$\frac{dy_4}{dt} = \frac{K}{S} C_v(u_3)\sqrt{\delta_3 y_3 - \delta_4 \cdot (y_4 - c)} - \frac{K}{S} C_v(u_4)\sqrt{\delta_4 y_4} - \frac{Q_{C4}}{S} + \frac{Q_{W4}}{S} + \frac{E_{g4}}{S} \qquad (5.34)$$

A symbolic process simulator is implemented. It's based on a library of configurable functions with symbolic parameters linearized around symbolic operating points. The linearization is the traditional. If state space derivative vector is defined as:

$$\dot{X} = G(X, U) \quad (5.35)$$

If $\hat{Y}$ and $\hat{W}$, are the operating points column vectors inputs and outputs:

$$\dot{X} = F(Y, W) - F(\hat{Y}, \hat{W}) \qquad (5.36)$$

Applying Taylor's first order approximation:

$$\dot{X} = \nabla F\left(Y; (\hat{Y}, \hat{W})\right) \cdot (Y - \hat{Y}) + \nabla F\left(W; (\hat{Y}, \hat{W})\right) \cdot (W - \hat{W}) \qquad (5.37)$$

Where, Y is the column vector of pulp levels; W is the column vector of control signals; F is the column vector of pulp level derivatives, X=Y- $\hat{Y}$, U=W-$\hat{W}$, and ∇F(Y ;($\hat{Y}$, $\hat{W}$)) and ∇ F (W ;($\hat{Y}$, $\hat{W}$)) are the correspondingly Jacobeans evaluated in the operating point. The objective is to obtain state space matrices A, B, C, D and E; for both process simulation and for predictive model building. Regarding predictive models, one set of state space matrices are needed for each one of the MPC's. For pulp levels MPC, MPCL and, for individual cell MPC, MPCn; matrices A and B are symbolic. Matrices C and D are data driven for all the MPC's.

Regarding pulp levels process simulation blocks, pulp level control valves used for this work are a special type of knife gate valves for control applications with special seat plates. The inherent characteristic is a compromise between equal percentage & linear flow characteristics. From the vendor technical specifications, C_v (w) relation is obtained where C_v is the valve coefficient and w the control signal, both normalized from 0 to 1.

Non-zero elements of A, B are shown in equations (5.38) to (5.47). For first row:

$$A(1,1) = \frac{-KC_v(w_1)}{2S\sqrt{c+y_1-y_2}}, A(1,2) = \frac{KC_v(w_1)}{2S\sqrt{c+y_1-y_2}} \qquad (5.38)$$

For intermediate A components, 1 < i < n and, then:

$$A(i, i-1) = \frac{KC_v(w_{i-1})}{2S\sqrt{c+y_{i-1}-y_i}} \qquad (5.39)$$

$$A(i, i) = -\frac{KC_v(w_{i-1})}{2S\sqrt{c+y_{i-1}-y_i}} - \frac{KC_v(w_i)}{2S\sqrt{c+y_i-y_{i+1}}} \qquad (5.40)$$

$$A(i, i+1) = \frac{KC_v(w_i)}{2S\sqrt{c+y_i-y_{i+1}}} \qquad (5.41)$$

For i=n:

$$A(n, n-1) = \frac{KC_v(w_{n-1})}{2S\sqrt{c+y_{n-1}-y_n}} \qquad (5.42)$$

$$A(n, n) = -\frac{KC_v(w_n)}{2S\sqrt{y_n}} - \frac{KC_v(w_{n-1})}{2S\sqrt{c+y_{n-1}-y_n}} \qquad (5.43)$$

The first row of B matrix is given by:

$$B(1,1) = \frac{-K\frac{dC_v}{dw}(w_1)\sqrt{c+y_1-y_2}}{S} \qquad (5.44)$$

While for 1<i <n, then:

$$B(i, i-1) = \frac{K\cdot\frac{dC_v}{dw}(w_{i-1})\sqrt{c+y_{i-1}-y_i}}{S} \qquad (5.45)$$

For i=n:

$$B(n, n-1) = \frac{K\frac{dC_v}{dw}(w_{n-1})\sqrt{c+y_{n-1}-y_n}}{S} \qquad (5.46)$$

$$B(n, n) = \frac{-K\frac{dC_v}{dw}(w_n)\sqrt{y_n}}{S} \qquad (5.47)$$

Other predictive models' descriptions are done in next chapter.

6. ADVANCED CONTROL AND OPTIMIZATION

6.1. ADVANCED CONTROL PERSPECTIVE

The problem addressed in this chapter is the need of further approaches that can provide both powerful and integrated solutions for advanced process control and optimization of flotation plants. The solution proposed in this study is a hierarchical and dynamic approach that takes advantage of available powerful techniques in the family of model predictive control algorithms together with cutting edge or novel instrumentation systems.

Until nowadays, the attitude at flotation plants has commonly been in the comfort zone due to former wealthy period. That unambiguously determines the need for more productivity and efficiency in the use of available resources.

Traditionally, process design and control design are strictly sequential tasks. The process is designed first to achieve the design objectives, and then, the operability and controllability aspects are considered through control design. This sequential approach is often inadequate since many process control challenges arise because of poor design of the process and may lead to overdesign of the process, dynamic constraint violations, and may not guarantee the required performance (Malcom et al., 2007).

As discussed by Edgar (2004), the priorities of the objectives have been reversed. In the early approaches, the control system was simply a tool to achieve the predetermined goals of production, which had been set in the process design stage. The operation personnel did not think of the control system as an optimization tool to improve profitability of the process. Therefore, economic optimization had the lowest priority. However nowadays, business planning of process industries has become online and much less limited by the early decisions at the design stage. Consequently, the new control systems have also inputs in terms of economic parameters and translate them into operational decisions. This has encouraged designers to consider the highest priority to process profitability and the roles of other control tasks are to realize the targeted economic objectives. In spite of the fact that economics are not under the scope of this work, the hierarchical approach based in temporal decomposition, give the needed and enough time for management decision making integrating both technical and commercial aspects.

6.2. ADVANCED CONTROL METHODOLOGY

Model-base design is the systematic and methodological approach for the whole work presented in this chapter. As such, the methodology framework includes specific model-base methods for: (i) process control design, (ii) control simulation framework implementation (ii) process modelling and,. Process models are the base for both the simulation of the process and, the controllers' implementation. Also, the main objective of this chapter is froth flotation control. Then, the model framework shall emulate the froth flotation process with needed and enough precision for process control purposes

In terms of process control, the model framework shall represent the relationship between the measured, controlled and manipulated variables in order to achieve the control objectives in spite of measured or unmeasured disturbance variables. This article is entirely model-based, including the control strategies. As such, both process simulator sub system and controller simulator sub-system are built upon an appropriate and comprehensive selection and synthesis of existing first principle models (white box), data driven models (black box) and/or a combination of both (grey box). It's important to state that both process and prediction models for control implementation, are calibrated and validated using pilot and/or industrial data. From a process control perspective, while process simulation framework is open loop, control simulation framework is closed loop. Then, the process simulator is used for both process simulation and controller implementation and; the control simulator is used to test control strategies by simulation without full closed loop experimental calibration or validation. That´s in the essence of model and simulation based methodologies: there could be a simulation framework without full experimental background, as long as the thoroughness and rigor, for the moment to arrive at the conclusions, is preserved.

Regarding simulation framework implementation, the methodology used to incrementally and systematically merge and combine first-principle models and empirical models in a comprehensive simulation framework is mainly based on Ljung's systems identification book (1990).

6.3. CONTROL DESIGN

Conceptual control design includes the following definitions: degree of centralization; control hierarchy; control structure and; set point policy.

Degree of centralization: An approach between pure decentralized and full centralized is used herein. Specifically, a cooperative control structure is selected for this thesis because while neither a pure decentralized control structure nor a communicated one ensures an optimal operation, there are many concerns reliability and maintainability of a large-scale centralized control structure. A cooperative control structure employs an objective function for the whole system, and the prediction of the last iteration of each controller is available to the others.

Control Hierarchy: A fit for purpose three layered hierarchy is used in this work. Also, the control structure is decentralized vertically (top-down) through different time scales, that can varies upon certain states that are later described in this article: (i) a daily (24 h) or shift (8h) basis for orchestrator's changes in given technical optimum criterion and constraints; (ii) an hour basis for row orchestrator outputs to lower levels (set points or overriding); (iii) a ten minutes' basis for advanced control and (iv) a one to ten seconds of sampling time for basic control. Regarding the dynamic approach of the hierarchy, depending on the mode (tracking or regulatory) and/or the variable being profiled, the three-layer hierarchy can vary it behavior. Next figures show the three layered row control hierarchy, presenting the main components. The technical optimum criteria can be biased and/or weighted according to economics.

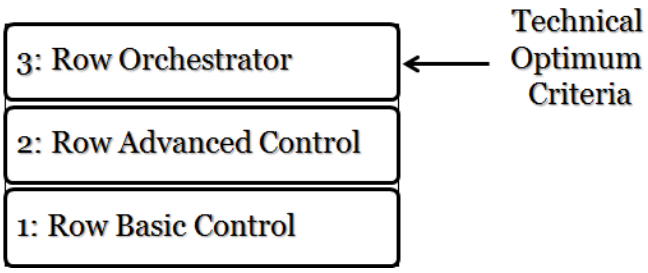

Figure 6.1: Row control hierarchy

In next figures (6.2) and (6.3) the advanced control layer is firstly presented in the form of schemes, being (6.2) the advanced control for a cell and (6.3) the advanced control schema for a row.

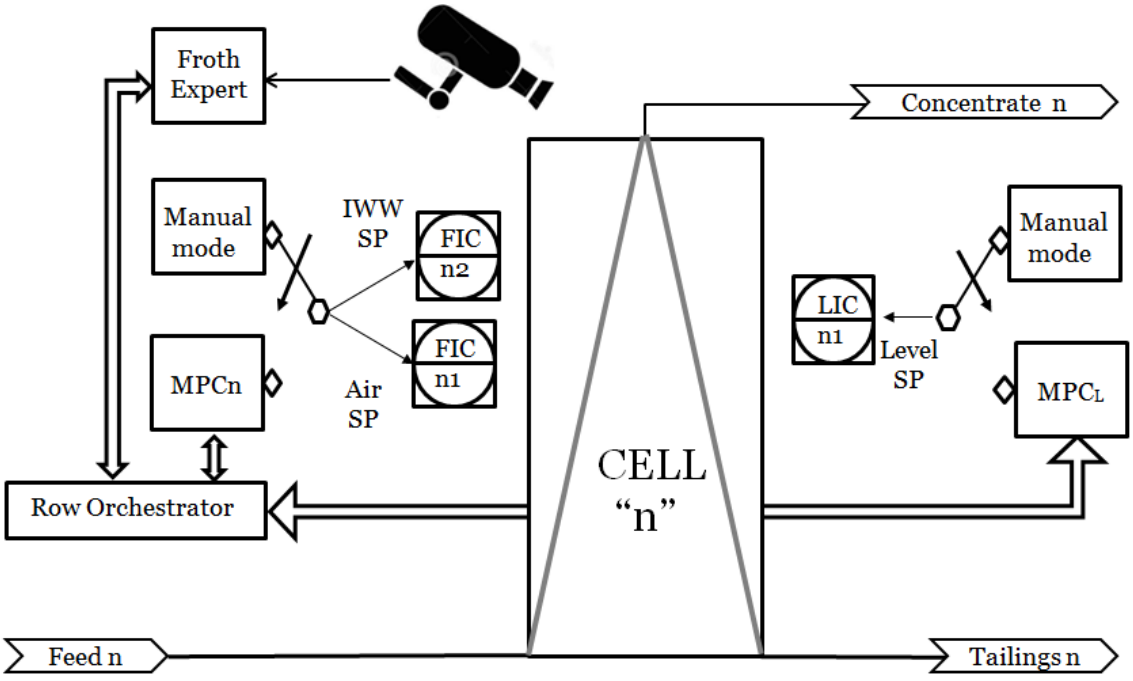

Figure 6.2: Cell-based advanced control scheme

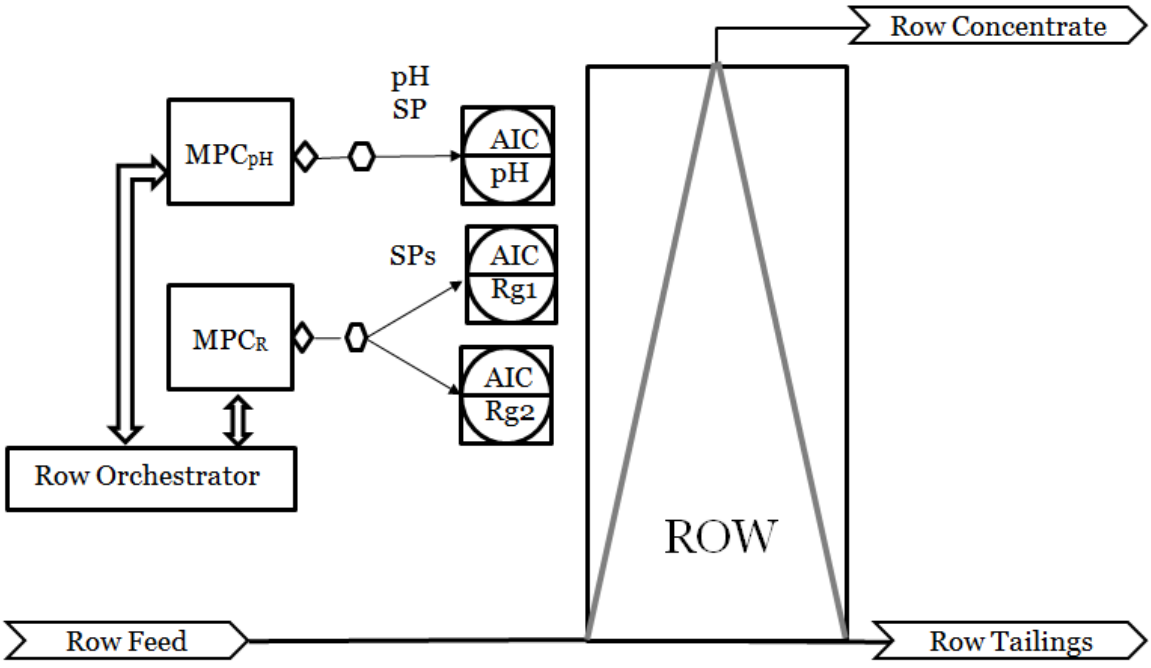

Figure 6.3: Row based advanced control scheme

As can be seen in previous figures, the advanced control layer is composed of MPC's: n cells' MPCs, MPCn; 1 MPC for all the pulp levels of a row, MPCL; 1 MPC for three reagents (Rg1, Rg2, Rg3) and; 1 MPC for ph advanced control with the capability to act as a Eh controller in addition to ph.

The hierarchical control structure considers three layers: orchestrator, advanced control and regulatory control. The orchestrator layer plays two main roles: supervision and optimization. In previous figure 6.2, the row orchestrator is shown receiving and transmitting information with MPCL, MPCn and the third party expert system.

Control Structure: Skogestad's (2004) iterative top-down/bottom-up algorithm is used as control structures' selection methodology. Nevertheless, the bottom-up approach is used to present the work because both experiments and simulations are developed in a bottom-up sequence.

Regarding measurements, state of the art, cutting edge and new instrumentation systems are used at pilot trials. Among them: (i) magnetostrictive multi-level sensor that measures both pulp level and top of froth depth level, (ii) concentrate volumetric flow by means of area-velocity instruments, (iii) image processing system, (iv) linear knife-characterized control valves, (v) mass flow meters, (vi) tomography density meters and, (viii) online metallurgical analyzers. Also in the first layer of the control structure, the manipulated variables are valves and the controlled variables are flows. The control objective of the first layer is to keep the controlled variables closer to the set points within a certain actuation effort. In other words, the performance or cost function to be minimized is a tradeoff between error and effort.

The following basic control loops and measurement systems are available for each mechanical cell (where n is the cell number): air control loop (FIC-n1), interface wash water control loop (FIC-n2) and, pulp level control loop (LIC-n1). These basic control loops are described in previous chapter 5. Each of them has their own dynamic behaviors, not considered for advanced control and optimization layers applying temporal decomposition. This seems right, as far as the time responses from the measurements to the valves are at least one order of magnitude faster than the advanced control time constants.

Row-based control loops are considered for collector, frother and milk of lime. These reagents are measured by means of Coriolis mass flowmeters and the manipulated variables are positive displacement dossing pumps.

The following indirect instrumentation is considered for each cell: froth expert system (AIC-nm, m variables per cell); froth stability sensors (two per cell); concentrate mass pull virtual sensor and; concentrate grade virtual sensor ($L_{Cu,\,C,\,b}$; one per cell).

The second layer of the control structure – advanced control – is where MPC's live (by the exception of row optimizer MPC, MPC_O). The manipulated variables considered herein are froth depth, wash water, air flow, frother, collectors and milk of lime. The controlled variables of the second layer are grades and recoveries. The technical optimum is configurable, as well as performance indices or cost functions.

The orchestrator is composed by two sub systems: optimizer and supervisor. The optimizer is MPC-based, called herein MPCO. The orchestrator's role in the optimization of a row performance is to achieve the given requirements. It determines a optimum set points for the controllers. Related to the supervisory role, the following virtual sensors are developed: (i) froth instability, (ii) sunken or pulping cells and, (iii) individual mass pulls and concentrate grades. In addition, the orchestrator monitors, maintains and set the mode of lower control layers and instrumentation; enunciating if they are not performing to expectations. Once the plant has reached stability, the orchestrator turns to be mainly an optimizer while maintaining its supervisory tasks.

Regarding both supervisor and optimizer, froth stability is a key factor for feasibility and optimality. Stable operation of flotation cells and consequent consistent metallurgical benefits can only be obtained if pulp levels and froth stability are under control. Froth flotation process depends on a carefully controlled and stable froth. In this work, two indices for froth stability are used. Next figure 6.4 shows expert system scheme together with froth stability observers and associated signals. The froth expert system is a packaged image processing system that delivers the following automatic measurements: froth velocities, bubble size distribution and concentrate grade estimation.

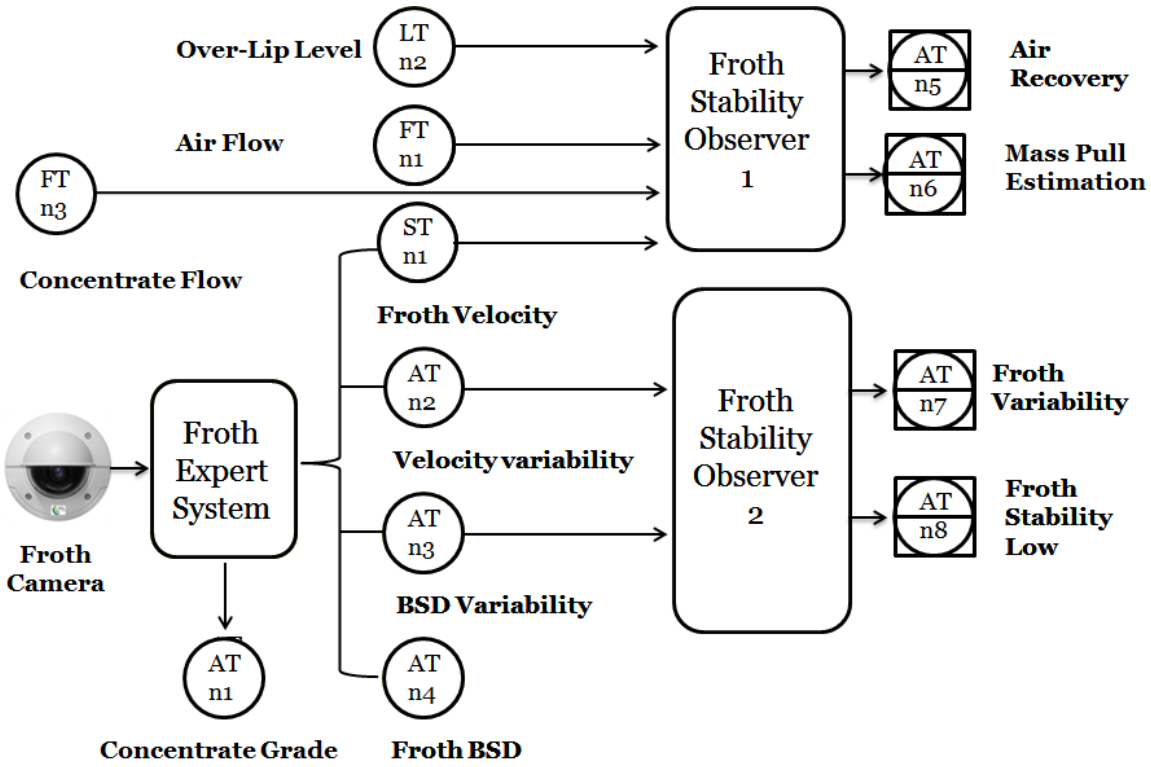

Figure 6.4: Cell n froth stability observers

Row optimizer: from a top-down perspective, Maldonado et al. (2011) find that the maximum separation efficiency is obtained when each of the cells along the row has the same recovery if entrainment is not considered. Singh and Finch (2014) confirmed that with simulations and industrial flotation. In the same article, they used mathematics and simulations to propose that, considering gangue entrainment, "a balanced mass-pull profile would be the optimal policy". Seguel et al. (2015) revisit row optimization through froth depth profiling using a genetic algorithm and the following formulation of the optimization problem: maximization of the overall Cu recovery while satisfying a minimum concentrate grade. One of their conclusions is that optimal profile also provides a balanced mass-pull profile. A balanced mass-pull profile is herein considered as base scenario, but the simulation framework allows also a balanced recovery profile and/or a biased profile. Optimal MPC (O-MPC) is considered herein as row optimizer.

The investigations referenced in previous paragraph provide simple and practical row optimization strategies for the state of the art technologies in instrumentation and control: balanced mass pull profile along the row or; balanced recovery profile along the row. As observed in the literature review, regardless the "nominal optimum", the technical optimum is achieved by means of balanced mass pull along the row and that's accomplished together with a high froth's stability. In this thesis, the stability index for optimization is the average between air recovery and the combined variability of velocity and bubble size distribution from one period to the next. In terms of abnormal situations, they are considered as redundant froth stability indices. A balanced mass pull profile along the row - with maximum froth stability - is used in this work. In next figure 6.5, the relationship between the row's mall pull Y and individual balanced mass pull y_i, considering a balanced mass pull profile (y_i=y, ∀i), is shown:

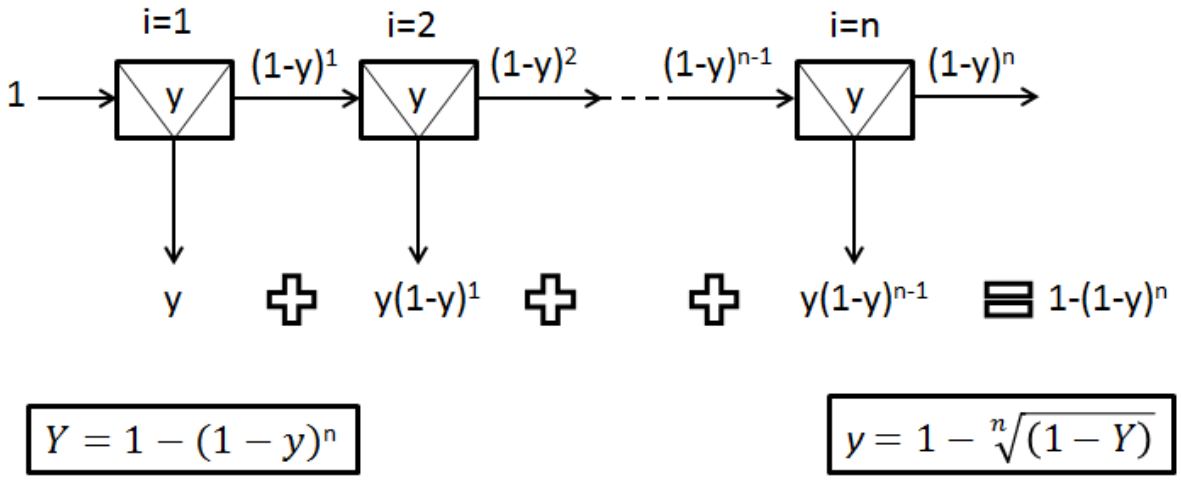

Figure 6.5: Balanced mass pull profile strategy

From figure 6.5, the individual mass pull set points are obtained. Then, the objective function for each cell is to maximize froth stability, subject to achieve the corresponding mass pull set point. Then: (i) an appropriate profiler control strategy simulation framework would contribute to support the mentioned achievements, (ii) in almost all the articles two variables are considered for profiling but only one at a time, (iii) in process control words, set point tracking is needed for the "profiled variable" while set point regulation is needed for the others.

Based on a Simulink generic adaptive MPC with a LTV Kalman Filter built-in state estimator, a set of four types of A-MPC implementations are implemented for profiling along the row: successive linearization, linear time variant system, on-line lineal parameter identification and on-line nonlinear model identification.

In next figure the entire control structure block diagram is shown:

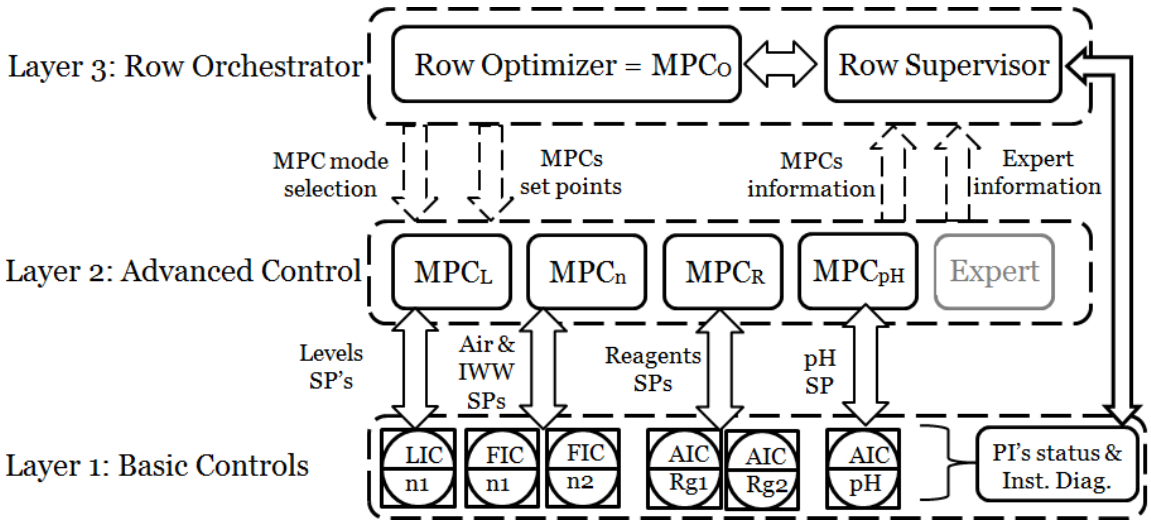

Figure 6.6: Control structure blocks diagram

If the mode of certain MPC variable (level, air flow, IWW, reagents or pH) is "profiling" then the respective MPC turns into adaptive mode; else it is "regulating".

Row Control Strategy: using the separability curves method, a match between the laboratory data of the flotation metallurgical unit block with on-line information from the metallurgical analyzers, is done. Then, the metallurgical optimum is obtained and shown to the operator by means of grade, recovery, mass pull and target separation efficiency. Row mass pull set point is therefore obtained.

According to Bergh & Yianatos (2009): "if the batch response of a sample of plant feed is intended to be used to obtain the separability curve of this material, then the operating conditions defining the batch procedure must be chosen to optimize the batch recovery". Then the best variability curve for each of the three main FGU's are selected and their operational parameters (reagents, pulp level, air and IWW flows) are used as initial set points.

6.4. CONTROL SIMULATION FRAMEWORK

The model structure used in the control simulation framework appears in the following illustration 6.7. The main reference as configurations guide is the book of Bemporad et al. (2016).

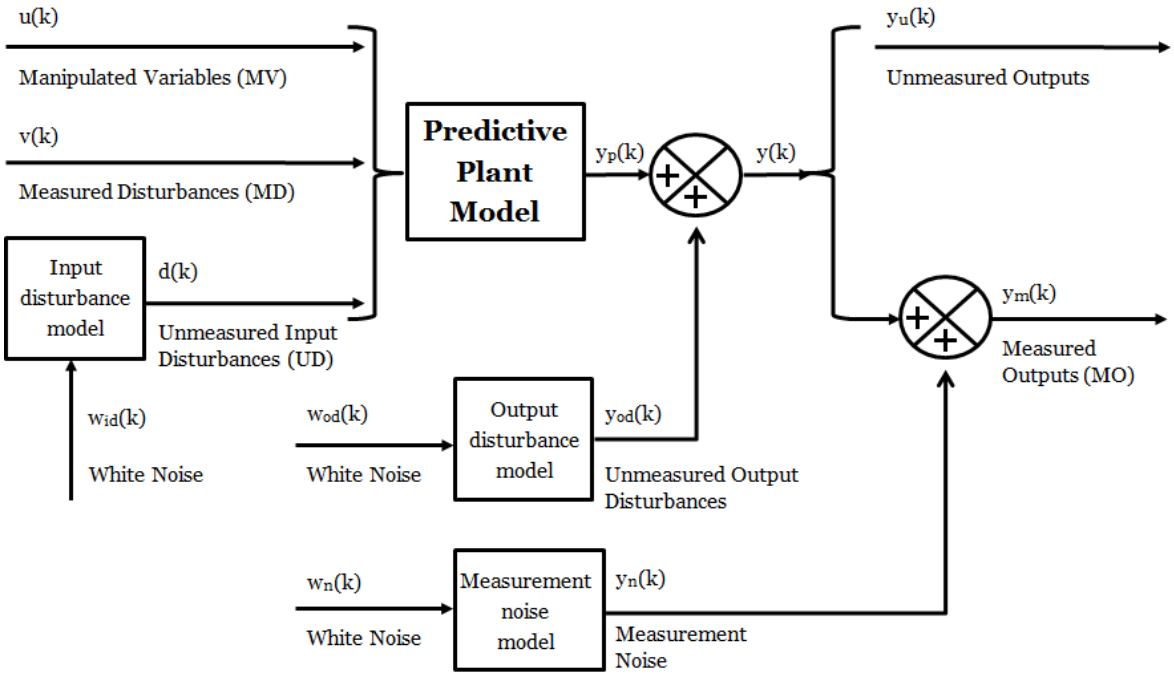

Figure 6.7: Control simulation framework diagram, from Bemporad et al., 2016

Plant predictive models: the MPC controllers implemented in this thesis perform all estimation and optimization calculations using discrete-time, delay-free, state-space systems with dimensionless input and output variables. Therefore, the following steps shall be performed: conversion to state space, discretization or resampling, delays removal and, conversion to dimensionless input and output variables. When the MPC's are in profiling mode, they mutate to adaptive MPC in which case, the models are time variant. In all the other cases, the models are time invariant. Regarding the application, three types of MPC's are developed in this thesis: (i) one row optimizer MPC, MPC_O; (iii) four individual cells MPC's, MPC_n; one row levels MPC, MPC_L; one reagents' MPC, MPC_R; and one pH MPC, MPC_{pH}. While in case of MPC_L, MPC_n and MPC_O; matrices A (t) and B (t) are symbolic; for MPC_R and MPC_{pH}; A (t) and B (t) are numerical.

While the predictive plant model must remain when the code is embedded into a commercial controller, the other models could be taken out or modified. In other words, while the models for disturbances and noise; shall be implemented for simulation purposes; predictive plant model is a must for MPC deployment.

Other difference, herein done, between predictive models and, noise and disturbance models is that, while predictive models are constructed from scratch; noise and measurements models are implemented using a tool box.

The input disturbance model is a key factor that influences the following controller performance attributes: (i) dynamic response to apparent disturbances; that is, the character of the controller response when the measured plant output deviates from its predicted trajectory, due to an unknown disturbance or modeling error; (ii) asymptotic rejection of sustained disturbances; if the disturbance model predicts a sustained disturbance, controller adjustments continue until the plant output returns to its desired trajectory, emulating a classical integral feedback controller. The input disturbance models are LTI discrete state-space, delay-free object. Then, the same steps for convert the process plant model to predictive plant model are used.

The output disturbance model is a special case of the more general input disturbance model. Its output, y_{od} (k), is directly added to the plant output rather than affecting the plant states. The output disturbance models specify the signal type and characteristics of y_{od} (k).

The measurement noise model is used to distinguish disturbances, which require a response, from measurement noise, which should be ignored. The measurement noise model specifies the expected noise type and characteristics. Using the same steps as for the plant model, the measurement noise model is herein represented as a discrete-time, delay-free, LTI state-space system.

Simulation framework strategy: For pulp levels, a symbolic model is available and therefore a symbolic-adaptive multiple input, multiple output models are implemented. For almost all the other variables, parametric models are available and therefore a “grey model” calibration approach is applied. Usually, the steady state structure is available and the dynamics are calibrated with experimental data. Finally, for reagents, data driven models are implemented. Due to the variety of model types, multiple inputs and single output models (MISO) are implemented, calibrated and then merged.

Predictive models' description: for MPC_L, the states are also the outputs and consist on pulp levels' deviations (h). The inputs are the control actions over the level valves, indirectly through the set points of individual PI controllers. The perturbations are the input flows and the interface wash water flows. Then (6.1) representation applies in profiling mode, whereas (6.2) applies in regulating mode.

$$h_{k+1}=A_L(t)\cdot h_k+B_L(t)\cdot u_k+q(t) \qquad (6.1)$$

$$h_{k+1}=A_L\cdot h_k+B_L\cdot u_k+q(t) \qquad (6.2)$$

Where h is the deviations vector of pulp levels, u is the deviations vector of pulp control valves position and, q is the volumetric feeds flows. In both cases, A_L and B_L are symbolic matrices which parameters are obtained through the realization into numerical values whenever configured. While regulating, canonical MPC is used and when profiling, successive symbolic linearization together with AMPC are utilized.

For MPC_n, the states are mass and volume variables and the outputs are individual cells' grades, recoveries and, mass pulls. The inputs are cell-based control actions over outputs: air flow and, interface wash water flow; indirectly through the set points of individual PI controllers. The perturbations are input variabilities. Then (6.3) applies in profiling mode, whereas (6.4) applies in regulating mode.

$$g_{k+1}=A_n(t)\cdot g_k+B_n(t)\cdot v_k+D_n(t) \qquad (6.3)$$

$$g_{k+1}=A_n\cdot g_k+B_n\cdot v_k+D_n(t) \qquad (6.4)$$

Where g is the deviations vector of masses and volumes, v is the deviations vector of cell-based control actions and, D weights the feed variabilities vector. In both cases, A_n and B_n are symbolic matrices which parameters are obtained through the realization into numerical values whenever configured. While regulating, canonical MPC is used and when profiling, successive symbolic linearization together with AMPC are utilized.

For row-based MPC's; MPC_R, MPC_{pH} and, MPC_O; the same description applies, by the exception that A, B, C and D; are all numerical.

Simulation framework software implementation: a modular top-down software implementation method is used. Particular attention is also paid to causality and as such, every model is created in such a way to properly represent the cause-effect correlation between inputs and outputs. Another key issue faced is the simulation backbone chosen. After assessing some of the most widely known software that looked suitable for the scope, the choice has fallen on the Matlab®/Simulink® package. Simulink® is appreciated and therefore selected for its modelling, simulation and analysis tools in the form of standard or customized blocks that allow great flexibility in model designing and are suitable for control purposes. Matlab® is selected and therefore exploited for its graphical and data analysis capabilities in addition to the capability to write specific functions which can be called during simulation. The potentialities in matrix calculation of the Matlab® language are also herein exploited. Specifically, a Simulink® simulation project is implemented considering the following main sub-systems: utilities, process and control.

Pulp level control strategy comparison: A comparison between eight different strategies for regulatory control of pulp level along a row of rougher mechanical cells. At basic cell level regulatory layer, explicit model predictive control (E-MPC) and a proportional, integral and derivative control (PID) are tested. At row regulatory control, static decoupling matrix (SDM), E-MPC and implicit model predictive control (I-MPC) are used. Also, a single layer E-MPC and I-MPC are tested without basic regulatory controllers. Regarding pulp levels control along the row, direct MPC based strategies with fast sampling (I-MPC, E-MPC), achieve the best performances in M_p, TV, IAE-Q_i, IAE-SP and τ_s. About two layered strategies, I-MPC obtains the best performance as row regulatory control, followed by E-MPC and ending with dynamic decoupling matrix (DM). Also, the MPC based couples (I-MPC + E-MPC's, E-MPC+ E-MPC's) show similar results than hybrid couples (I-MPC+PID's, E-MPC over PID's.

Nevertheless, PI controllers are finally kept at basic control layer while MPC's are used in layer 2 (advanced control) and as row optimizer in layer 3. The main reason is diachronical: metallurgical tests need to be done with certain basic controls and, the data driven adjustment needs to be done with the pilot plant on going.

7. OVERALL DISCUSSION

7.1. MODELING

Three interesting and interconnected achievements related to modelling are considered to be done in this thesis. The first one is high level: an integrated process and control design allows the validation and implementation of non-conventional machines and the adoption of cutting edge instrumentation technologies. The other two modeling achievements are related to machine technology comparison: three compartmental approach and, non-conventional machines' models.

Regarding three compartmental models applied to mechanical cells in general, it's worth noting that, in spite of the fact that the three zones are broadly mentioned in the literature, there is not a true three compartmental model working in a simulation package. One of the reasons; herein proposed for further discussion; is that, in case of conventional machines, three compartmental parameters are not directly obtained without the usage of a comprehensive set of instrumentation.

Related to the differences between conventional and RS machines, it can be noticed from (5.2) and (5.3) that; if the zone recoveries were the same, the recovery of the conventional machine would be bigger. This structural difference is due to the fact that in case of RS flotation machine, particles detached in the separator tank report to the tailings because they do not have the probability return to the RU to be collected again. Therefore, the respective recoveries are different as shall be expected for a machine that optimizes each of its sub-processes because: (i) the collection zone has a higher contacting efficiency due to its high energy density and agitation; (ii) the interface wash water has an important role in the quiescent zone and the absence of agitator improves the flow regime and; (iii) the froth zone has a better recovery due to its narrower depth and shorter average distance to the launders.

It's important to mention that model-based design methodologies are efficiently used in this thesis to support the design of high efficient flotation plants. An integrated approach supports the decision towards novel technologies.

Two future works are herein proposed for discussion: (i) further exploring three compartmental models, especially against Savassi's two compartmental one and; (ii) implementing a "commercial like" simulator.

Regarding second objective's achievement, a reactor separator type of flotation machine was selected subject to the conditions and restrictions of the referenced industrial project.

7.2. INSTRUMENTATION

As general comment, all the instrumentation for the entire row arrives at almost the same time than the first pilot cell. But, the second cell arrives almost one year later than the first one and, the third and fourth cells arrive together six months after the arrival of the second cell. This fact additional to the integrated process and control design strategy and philosophy, allows an incremental approach for models' implementation, calibration and validation.

For further contextual discussion, it's herein commented that a cold market increase the availability of instrumentation, control valves and control hardware; together with better vendor support; as demonstration packages. In other words, vendors are more interested and have more time. This fact represents an opportunity for innovation and development. As there are some difficulties regarding non-disclosure agreements, a gap of opportunity could be located in a tradeoff between commercial protection and academic diffusion together with research and development.

The main achievements in the instrumentation layer are related to integrated process and control design: it has been shown that the potential benefits of early testing of instrumentation and basic control loops are considerable. Specifically, the following instrumentation adopted and or changed during the experimental phases, proves to be more appropriate for the purposes of this work:

• Magnetostrictive double float sensors for both pulp level and froth level over the lip measurements. In case of pulp level and with respect to former technology (ultrasonic with float), the repeatability is around 25% greater, the response time is around 50% lower and the air gap is almost 100% greater, avoiding maintenance problems.

• Density electro tomography instrumentation that could eventually replace the almost always trouble-makers' nuclear density transmitters. The performance achieved is comparable. The single fact of having an alternative to nuclear technologies is an advantage by itself. The tradeoff that have to be made is related to the fact that nuclear densitometers are not invasive, but electro tomography ones are pool-pieced and need a bypass for maintenance purposes if an operational disruption is not wanted.

But, the following instrumentation needs further attention:

• Concentrate flow area velocity instruments play a good role in terms of mass pull control, it's a promising technology but need further work

• Density electro tomography instrumentation that could eventually replace the almost always trouble-makers' nuclear density transmitters, also need further work.

Regarding virtual sensors:

• Both sunken cell and pulping cell work very well and additionally point out to an important abnormal situation that needs to be fixed.

• Regarding froth stability indices, the multiplication of variabilities shows a strong non-linear behavior and seems that more data analytic work is needed. The other one, that uses Hadler & Cilliers formula is an excellent index and also behaves fairly well regarding cell optimization through peak air recovery method.

• Concentrate grade and mass pull virtual sensors behaves fairly enough in terms of regulatory control but need more work.

7.3. ADVANCED CONTROL STRATEGY AND OPTIMIZATION

Both human and artificial intelligence are used in this thesis to support the design of high efficient flotation plants. An integrated approach supports the decision towards advanced control strategies.

Related to particular objective 2**,** the overall control strategy results are promising. The control structure and its associated control strategies behave fairly well regarding disturbance rejection, especially against mineralogical and hydrodynamic variabilities in the feed. A hierarchical MPC-based control structure adds value supporting high efficient flotation processes.

In relation with specific MPC algorithms, the adaptive MPC for levels shows a great performance in profiling-tracking. The adaptive MPC using data driven and parametric models behave fairly well and better than standard non-adaptive MPC in profiling-tracking. For further discussion, the use of symbolic analytic methods as a good field for further investigation is proposed herein.

Given certain pre-defined economic assumptions, estimated results are obtained for the simulated industrial scenario: almost 40 percent reduction of capital expenditure (Capex), with almost the same operational expenditure (Opex). Almost 80% of Capex reduction is attributable to integrated process control design and model based methodologies; more than 12% comes from improvements in basic cell controls and instrumentation; 5% comes from advanced control and less than 3% comes from optimization. Although, it´s fair to note that capital expenditure for each mentioned item, are also in detrimental proportion.

The control structure provides good disturbance rejection against feed variabilities. Regarding the orchestrator, it provides smooth and logical transitions between control modes as well as good abnormal situation management.

8. CONCLUSSIONS AND FINAL REMARKS

In addition to the intrinsic value of the applications themselves, the experimental work phases are used afterwards for process simulation framework calibration and validation. Experiments are still indispensable for designing. They are not in competition with simulation methods; both approaches are ideal complements to each other. Experimental work is the main tool for all the applications: flotation cells modeling, technology selection and, advanced control and optimization strategy.

Regarding the usage of row-based instrumentation for less cells than nominal, it can be said that: in spite of the fact that currently appears to be non-affordable, this study sets the question about the further usage of instrumentation for pilot and for industrial phases. There is also a coincidence with the work of Maldonado (2011) regarding the usage of intermediate cells' measurements to increase the metallurgical performances.

The advanced control layer demonstrates an excellent performance of the symbolic based model predictive control (MPC) for levels, specifically when it turns into profiling mode where the adaptive MPC has to demonstrate its tracking capabilities. This shows an example where, having the chance, it's worth the effort an analytical model approach. The individual cells' MPC's show modal and performances differences between the two types of mechanical cells. Virtual sensors for sunken and pulping cells are successfully tested. Regarding virtual sensors for mass pulls and concentrate grades, in spite that both behave fairly well for control purposes, further future work is needed.

In order to further capture the value of the work herein done, the following future works are proposed as discussion bullets: industrial testing; evolution from "framework-like" simulator to a "commercial like" simulator; interdisciplinary work with mechanical engineers regarding impellers, using, for example, adimensional numbers and/or computer fluid dynamics; geometallurgical and geostatistics interdisciplinary work related to clays/cells interaction and data mining related to FGU's parameters; statistics interdisciplinary work related to blends' kinetic parameters distribution and, the use of a linear transformation in order to obtain a summative space to manage the variability results; software engineering interdisciplinary work to develop a user friendly simulator and, also, a license free software platform; economics interdisciplinary work in order to match economic versus technical optimality.

As final comment, it's worth to mention that together with the end of this thesis, "Ministro Hales", CODELCO's newest mine, accomplishes around one year of full remote operations across all the production chains (Tapia, 2017), from a central control room located in Santiago, about 2 thousands of kilometers far away from Santiago. This kind of achievement is only possible with an extensive usage of MPC, as far as it is almost impossible to manage remotely the huge amount of control loops with no slow dynamics, without the support of "cruise control" as they call MPCs algorithms. Therefore, industrial expectations for MPC have increased from providing superior control for multivariable systems to doing so with minimum set-up effort and ease of maintenance. In today's process industries, MPC is often considered a required solution for many applications.

BIBLIOGRAPHY

Alves dos Santos, N., Savassi, O.N., Clark, A. E., Henriquez, A., 2014: Modelling flotation with a flexible approach – integrating different models to the compartment model, Minerals Engineering 66–68, 68–76.

Araujo, A.C., Viana, P.R.M., Peres, A.E.C., 2005: Reagents in iron ores flotation Original Research Article Minerals Engineering, Volume 18, Issue 2, Pages 219-224

Arbiter, N. and Harris, C.C. 1962: Flotation kinetics. In: D.W. Fuerstenau (Editor), Froth Flotation. AIME, New York, NY, pp. 215-262.

Aske, E.M., 2009: Design of plant wide control systems with focus on maximizing throughput, Department of chemical engineering, Norwegian university of science and technology, PhD Thesis.

Bemporad, A., Morari, M., Lawrence, N, 2016: "Model Predictive Control Toolbox™ Reference Guide", The Mathworks, Inc.3 Apple Hill Drive Natick, MA 01760-2098

Bergh, L. and, Yianatos, J.B., 2009: Integrating separability curves to expert control systems of flotation plants, In: Proceedings of the VI International Mineral

Brooks, A., 1991: Intelligence without representation, Artificial Intelligence, 47, 139–159.

Buckley, P.S., 1964: Techniques of Process Control, Wiley, New York.

Camacho, E. F. and Bordons, C., 2004: Model Predictive Control, 2nd edition, New York: Springer-Verlag.

Cameron, I. and Hangos, K., 2001: Process Modelling and Model Analysis, Academic Press Dictionary of Science and Technology, Edited by Christopher G. Morris.

Chachuat B., Srinivasan, B., Bonvin, D., 2009: Adaptation strategies for real-time optimization. Computers and Chemical Engineering, 33(10), 1557–1567.

Cutting G.W. and Devinish, M., 1975: A steady-state model of flotation froth structures, Soc. Min. Eng., AIME, Annu. Meeting, New York, Feb. 16-20, 1975. Preprint 75-B.56.

Downs, J.J., Skogestad, S., 2011: An industrial and academic perspective on plant wide control, Annual Reviews in Control 35 (1), 99–110.

Edgar, T.F., 2004: Control and operations: when does controllability equal profitability? Computers and Chemical Engineering, 29 (1), 41–49.

Froisy, J.B., 1994: Model predictive control: past, present and future, ISA Transactions, 33, 235–243.

García-Zúñiga, H., 1935: Flotation recovery is an exponential of its rate, Boletín Minero de la Sociedad Nacional de Minería, Chile 47, 83–86.

Goodwin, G., Seron, M., Mayne, D., 2008: Optimization opportunities in mining, metal and mineral processing, Annual Reviews in Control 32, 17–32.

Gorain, B.K., Franzidis, J.P. and, Manlapig, E.V., 2000: Flotation cell design: Application of fundamental principles, in "Encyclopedia of Separation Science, Vol II, Academic Press, pp 1502-1512, 2000.

Hadler, K., Cilliers, J.J., 2010: The relationship between peak in air recovery and flotation bank performance, Minerals Engineering 22, 451–455.

Hanumanth, G.S., and Williams, D.J., 1992: A three-phase model of froth flotation, International Journal of Mineral Processing, 34:261-273.

Harris, C.C., Jowett, A. and, Ghosh, S.K., 1963: Analysis of data from continuous flotation testing. Trans. Amer. Inst. Min. Eng., 226: 444-447.

Harris, C.C. and Rimmer, H.W., 1966: Study of two-phase model of the flotation process. Transactions of the Institution of Mining and Metallurgy, 75: C153-162.

Jovanović, I. and Miljanović, I., 2015: Contemporary advanced control techniques for flotation plants with mechanical flotation cells – A review, Minerals Engineering 70, 228–249.

Kämpjärvi, P., Jämsä-Jounela, L.J., 2003: Level control strategies for flotation cells', Minerals Engineering, 16, 1061–1068.

Klimpel, R. 1980, Selection of chemical reagents for flotation, in Mular, A.L. and Bhappu, R. (editors), Mineral Processing Plant Design, 2nd edition 907–934 (SME, Littleton, USA).

Liu, J.J. and MacGregor, J. F., 2008: Froth-based modeling and control of flotation processes, Minerals Engineering 21, 642–651.

Ljung, L., 1990: System Identification: Theory for the User, Prentice Hall, Second Edition, ISBN: 9780136566953, Ch. 1 pp. 3-7, Ch. 3 pp. 51-65, Ch. 4 pp. 81-105.

Luyben, W. L., 1990: Process Modeling, Simulation and Control for Chemical Engineers, 2nd Ed., McGraw Hill.

Malcolm, A., Polan, J., Zhang, L., Ogunnaike, B.A. and, Linninger, A.A., 2007: Integrating systems design and control using dynamic flexibility analysis. AIChE J. 53 (8), 2048–2061.

Maldonado, M., Sbarbaro, D., Lizama, E., 2007: Optimal control of a rougher flotation process based on dynamic programming, Minerals Engineering 20, 221–232.

Maldonado, M., Araya, R., Finch, J., 2011: Optimizing bank performance by recovery profiling, Minerals Engineering 24, 939–943.

Matzopoulos, M., 2011: Dynamic Process Modeling: Combining Models and Experimental Data to Solve Industrial Problems, Process Systems Engineering, 7, 3-20, ISBN: 978-3-527-31696-0.

McKee, D.J., 1991: Automatic flotation control – a review of 20 years of effort, Minerals Engineering, 7-11, 228–249.

Meyer, B., 1997: Object-Oriented Software Construction, Prentice Hall, Second Edition, ISBN: 978-0136291558, Ch. 1 pp. 1-5, Ch. 2 pp. 21-24, Ch. 3 pp. 39-41.

Ogunnaike, B.A., Ray, W.H., 1994: Process Dynamics, Modeling and Control. Oxford University Press, New York.

Polat M., Chandler, S., 2000: First order flotation kinetics models and methods for estimation of the true distribution of flotation rate constants, International Journal of Mineral Processing 58, 145-166.

Putz, E., Cipriano, A., 2015: Hybrid model predictive control for flotation plants, Minerals Engineering 70 (2015) 26–35.

Qin, S.J., Badgwell, T.A., 2003: A survey of industrial model predictive control technology. Control Engineering Practice, 11 (7), 733–764.

Rawlings, J. B. and, Mayne, D. Q., 2015: Model Predictive Control: Theory and Design, Ed. Nob Hill Pub, ISBN-13: 978-0975937709.

Rawlings, J.B. & Stewart, B.T., 2007: Coordinating multiple optimization-based controllers: new opportunities and challenges. In DYCOPS, Cancun, Mexico, June 2007.

Rojas, D., Cipriano, A, 2011: Model based predictive control of a rougher flotation circuit considering grade estimation in intermediate cells. Dyna 78 (166), 29–37.

Rossiter, J. A., 2004: Model-Based Predictive Control: A Practical Approach, CRC Press.

Savassi, O.N., 2005: A compartment model for the mass transfer inside a conventional flotation cell, International Journal of Mineral Processing, 77:65–79.

Seguel, F., Soto, I., Krommenacker, N., Maldonado, M., Becerra, N., 2015: Optimizing flotation bank performance through froth depth profiling: Revisited, Minerals Engineering 77, 179–184.

Singh, N., Finch, J.A., 2014: Bank recovery and separation efficiency, Minerals Engineering 66–68, 191–196.

Skogestad, S., 2004: Control structure design for complete chemical plants, Computers and Chemical Engineering, 28 (1–2), 219–234.

Stephanopoulos, G., Reklaitis, G.V., 2011: Process systems engineering: from solvay to modern bio- and nanotechnology, a history of development, successes and prospects for the future, Chemical Engineering Science, 66, 4272–4306.

Schulze, H.J. (1984). Physio-chemical Elementary Processes in Flotation, Elsevier Science Publishing Co., Amsterdam.

Tao, G., 2014: Multivariable adaptive control: A survey, Automatica 50, 2737–2764.

Tapia, J., 2017: Ministro Hales avanza en su operación remota, Revista de Minería Chilena, N°428, 35-43.

Trahar W.J., Warren, L.J., 1976: The floatability of very fine particles—A review, Int. Journal of Mineral Processing, Volume 3, Issue 2, June 1976, Pages 103-131.

Wills, B. A., 2006, Mineral Processing Technology, Elsevier Science & Technology Books, 7th edition, ISBN: 0750644508, chapter 4: Particle size analysis, pp. 90-107, and chapter 12; Froth Flotation, pp. 267-352.

Yianatos J.B., 2007a: Fluid flow and kinetic modelling in Flotation related processes Columns and Mechanically Agitated Cells - A Review, Chemical Engineering, Vol 85 (A12) 1591–1603.

Yianatos, J.B. and Henriquez, F., 2007b: Boundary conditions for gas rate and bubble size at the pulp-froth interface in flotation equipment, Minerals Engineering, 20: 625–628.

Yianatos, J.B., Bergh, L.G., Tello, K., Dıaz, F and, Villanueva, A., 2007c: Residence time distribution in single big industrial flotation cells, Miner. Metal. Process J.